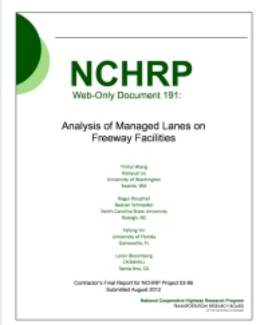

Analysis of Managed Lanes on Freeway Facilities

DETAILS

0 pages | 8.5 x 11 | PAPERBACK
ISBN 978-0-309-43473-7 | DOI 10.17226/22677

AUTHORS

Wang, Yinhai; Liu, Xiaoyue; Rouphail, Nagui; Schroeder, Bastian; Yin, Yafeng; and Bloomberg, Loren

ACKNOWLEDGMENT

This work was sponsored by the American Association of State Highway and Transportation Officials (AASHTO), in cooperation with the Federal Highway Administration, and was conducted in the National Cooperative Highway Research Program (NCHRP), which is administered by the Transportation Research Board (TRB) of the National Academies.

THE NATIONAL ACADEMIES

Advisers to the Nation on Science, Engineering, and Medicine

The **National Academy of Sciences** is a private, nonprofit, self-perpetuating society of distinguished scholars engaged in scientific and engineering research, dedicated to the furtherance of science and technology and to their use for the general welfare. On the authority of the charter granted to it by the Congress in 1863, the Academy has a mandate that requires it to advise the federal government on scientific and technical matters. Dr. Ralph J. Cicerone is president of the National Academy of Sciences.

The **National Academy of Engineering** was established in 1964, under the charter of the National Academy of Sciences, as a parallel organization of outstanding engineers. It is autonomous in its administration and in the selection of its members, sharing with the National Academy of Sciences the responsibility for advising the federal government. The National Academy of Engineering also sponsors engineering programs aimed at meeting national needs, encourages education and research, and recognizes the superior achievements of engineers. Dr. Charles M. Vest is president of the National Academy of Engineering.

The **Institute of Medicine** was established in 1970 by the National Academy of Sciences to secure the services of eminent members of appropriate professions in the examination of policy matters pertaining to the health of the public. The Institute acts under the responsibility given to the National Academy of Sciences by its congressional charter to be an adviser to the federal government and, on its own initiative, to identify issues of medical care, research, and education. Dr. Harvey V. Fineberg is president of the Institute of Medicine.

The **National Research Council** was organized by the National Academy of Sciences in 1916 to associate the broad community of science and technology with the Academy's purposes of furthering knowledge and advising the federal government. Functioning in accordance with general policies determined by the Academy, the Council has become the principal operating agency of both the National Academy of Sciences and the National Academy of Engineering in providing services to the government, the public, and the scientific and engineering communities. The Council is administered jointly by both Academies and the Institute of Medicine. Dr. Ralph J. Cicerone and Dr. Charles M. Vest are chair and vice chair, respectively, of the National Research Council.

The **Transportation Research Board** is one of six major divisions of the National Research Council. The mission of the Transportation Research Board is to provide leadership in transportation innovation and progress through research and information exchange, conducted within a setting that is objective, interdisciplinary, and multimodal. The Board's varied activities annually engage about 7,000 engineers, scientists, and other transportation researchers and practitioners from the public and private sectors and academia, all of whom contribute their expertise in the public interest. The program is supported by state transportation departments, federal agencies including the component administrations of the U.S. Department of Transportation, and other organizations and individuals interested in the development of transportation. **www.TRB.org**

www.national-academies.org

Table of Contents

List of Tables

List of Figures

Acknowledgments

The authors appreciate the following individuals who provided valuable input and perspectives on performance assessment and analysis of managed lane facilities during the course of this research effort:

The NCHRP Project Manager, Ray Derr; all of the members of the NCHRP Project Panel, Dirk B. Gross (Chair), Barbara J. Hoage, Jorge A. Laval, Marco Ruano, Virgil Y. Tillander, Shuming Yan, and Greg Jones; Transportation Research Board staff members Richard Cunard and Andrea Harrell; the research team at University of Texas, Arlington, led by Dr. James Williams; and John Rosen, Ken Lakey, and Matthew Heathscott from the Washington Department of Transportation.

Abstract

This report documents and presents the results of a study for evaluating the performance of Managed Lane (ML) facilities on freeways. A methodological framework is for analyzing freeway facilities with ML and General Purpose (GP) lanes operated in parallel. The framework acknowledges that the composition and behavior characteristics of the ML traffic stream are expected to be quite different from those for the GP lanes in terms of traffic volume, free-flow speed, capacity, vehicle type, etc. It further considers that there may still be certain levels of interactions between these two lane groups, especially for those facilities do not have physical (barrier) separations, either en route or at access points, between them. Within that framework, different modules were developed based on sensor-measured or simulation-generated data, including the characterization of ML speed-flow relationship, the frictional effect of adjacent lane traffic speed, the adjustment for cross-weave effects, and the development of side-by-side facility-wide ML and GP performance measures. Thus, the proposed methodology is sensitive to different GP and ML segment types (basic, weaving, etc.) and separation styles (none, buffer, barrier), and is capable of analyzing extended facilities across multiple time periods.

Executive Summary

The National Cooperative Highway Research Program (NCHRP) 03-96 research initiative aims at developing guidelines for performance evaluation of Managed Lane (ML) facilities on freeways. This report details the work performed in this research project. The objectives of this project are to (a) develop methods for the performance assessment and capacity analysis of freeway facilities with MLs in the United States, and (b) develop draft material on MLs capacity and quality of services for incorporation in future editions of the Highway Capacity Manual (HCM).

A methodological framework is developed in this project for analyzing freeway facilities with ML and General Purpose (GP) lanes operated in parallel. The framework acknowledges that the composition and behavior characteristics of the ML traffic stream are expected to be quite different from those for the GP lanes in terms of traffic volume, free-flow speed, capacity, vehicle type, etc. The framework further considers that there may still be some levels of interactions between these two lane groups, especially for those facilities do not have physical (barrier) separations, either en route or at access points, between them. The dichotomy of design and behavioral attributes therefore requires an updated analytical framework fitting within the HCM methodology to accommodate both ML and GP facilities, while retaining the impact of interactions between the two.

In order to develop such a framework, the research team first performed a review of state-of-the-practice and state-of-the-art on analytical methods used for assessing the performance of freeway facilities with or without MLs. The review found that there are considerable activities in the development of performance measures for ML facilities, as well as evaluation of ML operational strategies in a microscopic simulation environment. However, there is relatively little research conducted on the development of analytical framework and methodology for analyzing freeway segments with MLs in the HCM context. The research team developed such a methodological framework to evaluate performance of freeway facilities with MLs based on the concept of parallel lane groups of MLs and GP lanes. The lane group concept was borrowed from traffic signal timing analysis. A lane group in this study refers to either the set of parallel MLs or GP lanes. To use the framework, a ML group must start and end at the same point to its parallel GP lane group. However, the two lane groups do not need to be in the same segment type.

Within that framework, different modules were developed based on sensor-measured or simulation-generated data throughout the project, including the characterization of ML speed-flow relationship, the frictional effect of adjacent lane traffic speed, the adjustment for cross-weave effects, and the development of side-by-side facility-wide ML and GP performance measures. Thus, the proposed methodology is sensitive to different GP and ML segment types (basic, weaving, etc.) and separation styles (none, buffer, barrier), and is capable of analyzing extended facilities across multiple time periods. Key findings of this research are described as follows.

- Continuous access MLs are by far the most common type of implementation. They consist of a single ML separated from the neighboring GP lanes simply via pavement markings. The research team found that while the ML operates at good to excellent levels of service when

there is no significant interaction with GP lanes – this occurred up to a maximum volume of approximately 1,800 vehicle per hour per lane (vphpl) – their performance degrades significantly due to decreased maneuverability when traffic density on the GP lanes reaches or exceeds a certain level. This phenomenon is referred to as "frictional effect" in this study. The GP lane density level that starts the frictional effect was observed at approximately 35 passenger car per mile per lane (pcpmpl), which also coincides with the Level of Services (LOS) D/E threshold for basic freeway segments in the HCM 2010. Thus, for this case and all other basic segment cases where frictional effects exist, two separate speed flow models are constructed: one predicts speed under no-friction conditions, and the other for use with friction conditions. The fact that ML performance is affected by GP lane traffic requires that the GP lane analysis be done before the ML analysis. When the GP lanes operate at densities above the specified threshold, the friction-based speed prediction model should be invoked. As an example, a continuous ML that has a prevailing flow rate of 1,600 vphpl would operate at a speed of 53 mph under no friction conditions, but only at 36 mph when frictional effects from the GP lanes are considered. The research team has successfully applied this concept to both continuous and buffer separated basic ML segments.

- In the case of barrier-separated ML, no significant frictional effects were observed. However, for single-lane barrier-separated MLs, the presence of a barrier was shown to have reduced the level of maneuverability (and speed) even at low volume levels. This led to the development of new speed-flow relationships for single ML facilities, which feature a negative slope even at low volumes. Overall, none of the basic MLs observed in this study routinely operated at near capacity conditions, and none experienced breakdown on a regular basis. Thus the capacities reported in the document are derived from both limited observations and estimates of traffic flow models calibrated using field observed data. Those capacity values varied by site from 1,600 to 2,100 passenger car per hour per lane (pcphpl).

- For ML facilities that allow access only at intermittent access segments, *cross-weave* maneuvers were observed at access segments with close upstream GP lane onramps. When the upstream end of an access segment happens to be close to a GP entrance onramp, onramp vehicles targeting the MLs need to conduct cross-weave maneuvers, i.e. rush multiple lane changes over a relatively short distance, to enter the MLs. These cross-weave maneuvers could have a significant capacity-reducing impact on GP lanes. To quantify the impact through field observations, however, is very difficult because the segment lengths involved is typically beyond the range of a video camera and the lack of sensors that are placed at the right locations. Therefore, this analysis was carried out using a carefully calibrated simulation model using data collected at a cross weave site in Dallas, Texas. The framework developed in this study enables the analysis of cross-weave impacts. The research team found that the impact of cross weave on *GP lane capacity reduction* increases proportionally with the cross-weave demand entering at the onramp and the number of lanes to be crossed. It decreases proportionally with the distance between the onramp gore point and the start of the closest access segment. Additionally, intermittent-access MLs are proposed to be analyzed as regular weaving segments using the HCM 2010 procedures due to the similarities between the two segment types. This may not be an ideal solution but is certainly a feasible one given the time and budget constraints of this research project.

- The set of methods described in the previous paragraphs has been implemented in the FREEVAL-ML computational engine, which was developed in the course of this project to integrate, test, and evaluate the proposed approach. The Excel-based, Visual Basic coded tool is an extension of the FREEVAL computational engine which has been made available in the HCM 2010 Volume 4 for the analysis of extended Freeway Facilities. FREEVAL-ML is capable of analyzing both GP and ML segments on parallel facilities. FREEVAL and the freeway facilities method have been in use for more than ten years. The method has been independently validated against empirical data for congested facility, and compared very favorably to simulation-based analyses. In this project, the FREEVAL-ML tool was applied to two real-world case studies to demonstrate its applicability to current implementations of ML, and to verify that the various components work together as designed. This exercise highlighted the need for some modifications in the tool, which were subsequently implemented.

There are three key deliverables of this project. The first one is this final report, which documents literature review, ML analysis framework, data collection methodology, analysis results, case studies, and a discussion of implementation in the post-2010 HCM. The second key deliverable is the FREEVAL-ML software tool, which will allow analysts to test and evaluate the methodology. The FREEVAL-ML computational engine has been submitted to the TRB Committee on Highway Capacity and Quality of Service Committee for their consideration in updating the HCM. Information about the status of FREEVAL-ML and obtaining a copy is available at http://sites.kittelson.com/hcqs-fwy. Finally, this document resulted in draft text for inclusion in a future edition of the HCM, which is presented as an appendix to this report.

In summary, this project successfully developed an analytical methodology for evaluating freeways with parallel GP lanes and MLs in the HCM context. The methodology is supported by extensive field data collected at ML facilities in several states of the U.S., and is implemented in a computational engine for testing and application. However, this research was not able to address all the important issues. The authors have the following recommendations for future research:

- Research efforts are needed to explore congested ML facilities, with a special emphasis on queuing patterns at intermittent access points, and queue spillback allocation between ML and GP lanes.

- Future research may further investigate the beginning and end point designs of ML facilities. Variations in the design of these termini are expected to impact operations of the overall facility, and future research should explore what design aspects minimize the turbulence created at these locations.

- It is desirable to tie the operational HCM methodologies with demand-estimation procedures. Since many ML facilities in the U.S. feature a congestion-pricing component, the distribution of corridor demands between ML and GP lanes has been proven sensitive to pricing. While the HCM is traditionally not focused on demand estimation (demand is generally treated as an input), a closer scrutiny on the supply and demand tradeoffs is needed for ML design and operations.

- Investigations on special configurations of ML access points are needed. In addition to the lane-change or weaving access mentioned above, grade-separated ramp access points also warrant further scrutiny, especially ramps to and from single-lane ML facilities. The methodology for merge and diverge sections in the HCM generally assumes a ramp-influence-area (RIA) of two lanes, and it is likely that ramps on single-lane facilities have different operational attributes.

- Future research may also take a field data based approach to estimating capacity-reducing effects of ML cross-weave maneuvers on the GP lanes. The simulation-based approach taken in this research showed the hypothesized sensitivity, but this should be confirmed by field data.

- Finally, future research should focus on applying the methodology developed in this project to real-world case studies, and validating the predicted performance with field-measured performance data.

Chapter 1 Introduction

1.1 Research Problem Statement

Managed lanes (MLs) are becoming more prevalent on freeway facilities. While there is no nationally recognized definition of MLs, for the purposes of this project, MLs include High-Occupancy Vehicle (HOV) lanes, High-Occupancy/Toll (HOT) lanes, and express toll lanes. Obviously, the operational strategies and geometric characteristics of MLs may vary greatly from site to site.

Highway Capacity Manual (HCM) has been widely accepted as the guidelines for designing and analyzing freeway facilities. However, its current version, HCM 2010 (TRB, 2010), contains no methodology for MLs, although HOV facilities have been in use since 1970s and many HOT lanes facilities are in operations or under design/deployment. The current HCM freeway methodologies are not applicable to MLs due to the following reasons: (1) ML access control patterns and associated driver behaviors; (2) significant speed differentials between MLs and GP lanes; (3) interaction between tolling and traffic flow dynamics; and (4) slow vehicle constraint on single MLs. Therefore, a methodological framework dedicated to MLs is needed. Development of such a framework requires great efforts for modeling and understanding of the operational strategies and geometric characteristics of freeway facilities with MLs. Given the increasing popularity of MLs, including performance assessment and capacity analysis methods of MLs in HCM is highly desirable and would also greatly enhance its usefulness to engineers, designers, planners, and decision makers.

The NCHRP 03-96 project was launched to address this need. It has ten independent tasks described as follows:

Task 1. Conduct a literature review on the design and operation of MLs and summarize information on performance measures and operational analysis methods for MLs. Review the latest methods for determining speed-flow-density curves and capacities on freeway segments. Catalog the different types of managed lane designs (e.g., barrier-separated, buffer separated, non-separated, access point design, typical sections, single lane and multi-lane, reversible).

Task 2. Develop a performance-measurement framework for freeway facilities comprising both managed and GP lanes. The framework should include performance measures for the managed and GP lanes and consider the use of composite measures for the facility. The performance-measurement framework should provide inputs to toll demand models commonly used for MLs and allow transportation agencies to assess the facility's operation and convey system performance information to the public.

Task 3. Develop a data collection and analysis plan to support Tasks 6 and 7. Data from existing traffic management systems and transit vehicle locator systems on facilities with managed lanes should be used as practical, augmented by original data collection as project resources allow. Data collection sites should include facilities with single and multiple MLs and cover the full range of designs for separation between the GP and managed lanes. If adequate field data are not available

or feasible to collect, validated microscopic simulation models may be used to generate synthetic data if the models are properly calibrated and the results thoroughly documented.

Task 4. Prepare and submit an interim report summarizing Tasks 1 through 3. The interim report shall also contain a detailed, updated work plan and an updated budget for the remaining tasks.

Task 5. Carry out the Task 3 data collection plan as approved by the project panel.

Task 6. Assess the applicability of the HCM 2010 freeway analysis methodologies to single- and multi-lane ML operations, including the effects of cross-sectional elements. Determine whether these methodologies can be modified to properly model the operations of MLs. Discuss the results in a web conference with the panel.

Task 7. Develop methodologies for quantifying the performance measures identified in Task 2 for MLs. The methodologies should account for the effect of transit and other heavy vehicles on the managed lanes. The methodologies should also account for the effect of slower-moving traffic in an adjacent general purpose lane has on uncongested managed-lane traffic for different types of separation. The methodologies should include speed-flow-density curves based on field data and recommend maximum service flows, recognizing that managed lanes are intended to operate uncongested. Describe limitations of the methodologies and situations where alternative analysis tools should be used.

Task 8. Develop a computational engine for the Task 7 methodologies, based on HCM 2010 requirements and building upon HCM 2010 modules as applicable. The computational engine should follow the documentation requirements for the HCM 2010.

Task 9. Prepare draft text for the HCM, either as part of the Freeway Facilities chapter or as a separate chapter.

Task 10. Submit a final report that documents the entire research effort and includes the Task 9 text as an appendix.

1.2 Research Objective and Scope

The objectives of this project were to develop methods for the performance assessment and capacity analysis of MLs and to develop draft material for the post-2010 HCM.

Through NCHRP Project 3-92, the TRB Committee on Highway Capacity and Quality of Service (HCQS) has developed a new edition of the HCM, which was published in early 2011 as HCM 2010. It is expected that the results of this project will be incorporated into a subsequent edition of the HCM. The products of this research should adhere to the development standards being used for the HCM 2010 to facilitate acceptance by the Highway Capacity and Quality of Services (HCQS) Committee and publication by TRB.

1.3 Research Approach

1.3.1 User Input Requirement

Following the research objectives and aiming at developing methodologies for analyzing ML facilities, the research team proposed to introduce the *lane group* concept for the freeway facilities with MLs. The lane group concept is well-established in the signalized intersection methodology of HCM 2010. By adopting it in the context of NCHRP 03-96, the analyst will be able to ascribe separate attributes to parallel ML and GP lane facilities, while retaining the ability to model certain degrees of interaction between the two. This concept is discussed in greater detail in Chapter 4 of this report.

When using the methodological framework developed in this project to evaluate the performance of the facilities, the user is required to enter variables such as geometric characteristics (e.g. number of lanes), behavioral attributes (e.g. free-flow speed, capacity), and traffic demands separately for each lane group. The performance assessment method implemented in this project is consistent with the segmentation of a GP freeway facility in HCM 2010, except that the implementation would be represented as having either one or two lane groups, depending on whether parallel MLs are present. The methodology would then assess the operational performance of each lane group, under consideration of empirically-derived interaction effect between the two lane groups.

1.3.2 Research Findings

- **Methodological Framework**

In current practice, some ML facilities are physically separated from GP lanes through a buffer or barrier, whiles others are constructed concurrent (flow in the same direction and not physical separated) with GP lanes separated only by a painted stripe. In all cases, however, the composition and behavior of the ML traffic stream is different from those of traffic in the GP lanes. The dichotomy of geometric and behavioral attributes of parallel MLs and GP lanes, as well as the interaction between traffic operations in the two lane groups, makes it necessary to develop an updated methodological framework, suited particularly to the ML facility. The current HCM 2010 freeway methodology first establishes the input data requirements, then adjusts demands (if necessary), and computes the operational performance of each individual segment according to the updated methodologies for basic freeway segments, merge and diverge segments, or freeway weaving segments. Capacities can then be adjusted to emulate the effects of adverse weather or work-zones, before computing segment demand-to-capacity ratios (d/c). If no segment is at d/c>1.0, the methodology then aggregates the facility performance from individual segment operations. If any segment operates at d/c>1.0, an entirely different procedure applies to estimate the effects of congestion based on shockwave theory.

In the proposed ML framework, the introduction of lane group concept would affect the definition of facility geometry. While existing freeway segment types in HCM 2010 are used for GP lanes, several new ML-specific segment types are introduced. Associated capacities will these ML

segments need to be defined and calibrated. Then the segment capacities are adjusted for work zones and weather effects as in the current HCM.

In HCM 2010, either undersaturated or oversaturated performance modules are invoked depending on the prevailing traffic conditions on a freeway segment. It is assumed that the oversaturated methodology for GP lanes will remain unchanged in the new framework. For undersaturated operations, performance measures are estimated for each segment, with traffic demands considered and appropriate adjustments to segment capacity applied. While GP lane segments can mostly be handled through existing methodologies, new methods are needed for some specific ML configurations. For ML segments with stripe-separation or buffer separation from GP lanes, frictional effects need to be reflected in the speed-flow curves. Finally, facility Measures of Effectiveness (MOEs) are estimated as regular freeway segments, with the caveat that additional MOEs specific to MLs or the relative comparison of the two are needed. Since an ML facility itself typically operates at a demand to capacity (d/c) ratio less than 1.0, this methodology assumes that the operational flow range of MLs is below the breakpoint and hence no queuing algorithms are implemented for the ML lane group.

In HCM 2010, freeway segments are classified into four different categories: basic segment, on-ramp segment, off-ramp segment, and weaving segment. This research followed this segment type classification established for GP lanes. In addition to these GP lane segments, this research proposed five new ML segment types as follows:

- ML Basic: This is analogous to the general basic freeway segment, but serves for ML traffic demands. For barrier-separated ML-Basic segments, the existing GP lane procedure is applicable because frictional effect is insignificant. For stripe or buffer-separated ML-Basic segments, as well as segments with a single ML, new speed-flow models are developed and calibrated. Note that Continuous Access ML segment type, where access between the ML and GP lanes is allowed at any point, is classified into the ML Basic type. It should be distinguished from the ML Access Segment (ML-AcS) which is introduced later in this section.
- ML On-Ramp and ML Off-Ramp: These are analogous to GP Lane On-Ramp and Off-Ramp segments, but with ML traffic demands. The ML On-Ramp and Off-Ramp segments are suitable for using the existing GP lane procedures for ramps.
- ML Weave: This is analogous to the GP Weave segment, but with ML traffic demands. The operational characteristics of an ML Weave segment are reasonably close to those of a GP Weave segment and hence the existing GP lane procedure for weaving segments can be applied.
- ML Access Segment (ML-AcS): This is a new segment type and unique to the ML facilities with intermittent access. Lane changing between the GP lane group and the ML group can occur throughout the segment. Different from the Continuous Access ML Basic type, this segment type exists as the intermittent access segment where access between the ML and GP lanes is prohibited in the segments connect to it. It is treated as a weaving segment and HCM 2010 weaving methodology is applied to compute its impact.

An ML segment can take on a variety of configurations including different number of MLs and separation type from the adjacent GP lanes. Each segment type is featured with different traffic flow characteristics. Understanding the interaction between the MLs and parallel GP lanes is also

critical to properly assessing ML performance. This project investigated the performance and traffic flow characteristics of ML facilities at sites selected from different states. Traffic flow characteristics for the five ML Basic segment types were analyzed under different separation types and number of lanes. Factors such as frictional effects on the ML due to poor performance of the GP lanes and slow vehicle effects on ML facilities with passing constraints were considered in developing the speed-flow curves for each of the five ML Basic segment types. These speed flow relationships are expressed in a manner similar to those for GP basic freeway segment types in HCM 2010, and can be readily incorporated into the post-2010 HCM for determining the LOS of combined GP and ML facilities.

For the ML On-Ramp, ML Off-Ramp, and ML Weave segments, existing procedures for the corresponding GP lane segments can be applied because their configuration and traffic flow characteristics are similar to their GP lane counterparts. For ML Access Segment (ML-AcS), the ML-targeting vehicles entering the freeway from GP lane on-ramps need to *cross weave* over multiple GP lanes to access the ML. These vehicles have a negative impact on the operating performance of the parallel GP lanes due to intensive weaving. This cross-weave effect is found to be a function of different roadway geometric configurations as well as traffic conditions. A microscopic simulation model was built and calibrated using field-collected video data to explore this effect. The cross-weave intensity is consequently quantified using a Capacity Adjustment Factors (CAF) to account for its impact on the parallel GP facility. This concept is discussed in greater detail in Chapters 4 and 5 of this report. Beyond the effect of cross-weaves, an ML-AcS is analyzed as a regular weaving segment using the HCM 2010 procedures.

- **Performance Measures**

Performance measures are selected for quantitatively evaluating the effectiveness of different designs of ML facilities. The selected MOEs for the ML facilities are: 1) compatible with those used in the existing HCM 2010 freeway methodologies; and 2) capable of meeting the needs of agencies and users of the facility to describe the quality of service with and without the presence of MLs. To this end, the MOEs are applied at both the segment and facility levels. The facility-level describes the operational performance of a path through the entire facility, allowing analysts to compare the paths of GP lane and ML vehicles. For example, this project assesses the facility travel time, more precisely, the path travel time differential between the ML and GP lanes. Because travel time is not a typical HCM MOE, it is calculated after the determination of the average speed and density measures for each segment.

- **Computational Engine**

The application of the HCM 2010 freeway facilities methods relies heavily on the use of the FREEVAL computational engine, which is made available in HCM 2010 Volume 4, to apply and test the GP freeway methodology. Consequently, the research team developed an enhanced computational engine, FREEVAL-ML for analyzing both GP and ML segments in parallel facilities. FREEVAL-ML was developed on the same *Excel/Visual Basic* structure as the HCM 2010 engine, which combines a user-friendly and intuitive spreadsheet interface with a flexible coding language to execute the computations. FREEVAL and the freeway facilities method have been in use for more than ten years (Eads, *et al*., 2000). The method has been independently validated against empirical data for congested facilities, and compared very favorably to

simulation-based analyses (Hall, *et al., 2000*). Of course, the current version of computational engine developed via this research (available at http://sites.kittelson.com/hcqs-fwy) has certain limitations and future work would be needed. For example, the facility model in the FREEVAL-ML uses a spatial-temporal scope to analyze the performance of freeway across all segment and time periods for both GP and MLs. Although the GP lane module is capable of modeling both undersaturated and oversaturated conditions, the proposed ML module is only limited to the undersaturated conditions based on the ML operational requirement. Therefore, no spillback effect on ML can be modeled in the current ML module. Also, the current version cannot evaluate the performance of ML beginning and end points, at least not where they act as key bottlenecks of the facility, which was beyond the scope of this project. The computational engine is consistent with the material presented in this report, including consideration of the new ML segment types, new ML speed-flow curves, frictional and slow vehicle effects, and cross-weave effects on GP lane operations.

Chapter 2 Managed Lane Overview and Definitions

2.1 State-of-the-Practice

The focus of current highway system analyses has shifted from infrastructure expansion to better managing existing facilities for improved sustainability and efficiency. The concept of MLs has been gaining more and more popularity and is being adopted nationwide. MLs, as defined by the Federal Highway Administration (FHWA), are *"highway facilities or a set of lanes in which operational strategies are implemented and managed (in real time) in response to changing conditions"* (Obenberger, 2004). MLs include a wide range of operational and design options including HOV lanes, express toll lanes or HOT lanes, and exclusive-use lanes such as truck-only toll (TOT) lanes, etc. The ML concept encompasses a series of operational strategies to efficiently manage the traffic demand by altering pricing, vehicle eligibility, and access control. In the *Managed Lane Handbook* (Kuhn *et al*., 2005), ML facilities are defined as a "freeway within freeway" where a set of lanes are physically separated from GP lanes within a freeway cross section to allow a certain degree of operational flexibility over time in response to changing traffic conditions. The NCHRP 03-96 scope was limited to three categories of ML strategies: HOV lanes, HOT lanes, and express toll lanes. A major difference between HOT lanes and express toll lanes is that HOVs do not pay for use of HOT lanes but all kinds of vehicle need to pay to use express toll lanes. However, operation-wise express toll lanes are often considered as a special case of HOT lanes because both require tolling and access control, and express toll lanes are simpler in operations by tolling both HOV and Single Occupancy Vehicles (SOVs). The NCHRP 03-96 project, therefore, focuses on the methodology development for only on two of the three facility types, i.e. HOV and HOT lanes. Some important operating characteristics of existing ML facilities that may affect the performance of the MLs are reviewed as follows:

2.1.1 Operational Strategy

HOV lanes are by far the best documented among all the ML facilities in terms of design, implementation, and performance monitoring (TTI, 2001). The development of HOV facilities in the United States has evolved over 30 years. An HOV pooled fund study initiated by FHWA in 2002 continuously assembles information on existing HOV facilities in the United States, which by 2008 identified 345 HOV facilities in operation across the U.S. (Chang *et al*., 2008). The two longest active HOV facilities are I-95 between SR 112 and Gateway Blvd in Miami, Florida (116.0 lane-miles, 58.0 route miles) and I-405 in Los Angeles County, California (105.2 lane-miles, 52.6 route miles) with more under construction. The main intent of implementing HOV lanes is to improve person-throughput rather than vehicle-throughput on congested freeway corridors. Accessing an HOV facility often requires two or more persons (HOV 2+) per vehicle. Some agencies require three or more occupants per vehicle to assure reliable travel conditions in those lanes. Of the HOV facilities listed by the FHWA compendium (Chang *et al.*, 2008), 185 (54 percent) are purely HOV 2+. Fourteen facilities (4 percent) are purely HOV 3+. Two facilities, the I-10 HOV facility in Los Angeles, California and the Nimitz Highway in Honolulu, Hawaii, are HOV 3+ during certain time periods of the day and HOV 2+ otherwise.

In locations where HOV lanes are underutilized, a conversion to HOT lanes is considered an effective way to increase the overall throughput by providing single-occupancy vehicles (SOVs)

or low-occupancy vehicles (LOVs) the ability to choose the MLs as an alternative to the GP lanes. Pricing constitutes a core element of this practice. SOVs are allowed to use the HOT lanes by paying a toll in exchange for travel time savings or improved trip reliability. The toll is either dynamically-changed based on real-time traffic conditions or scheduled by time of day. There are ten HOT facilities in operation at the time of this report (Liu *et al.,* 2011), including I-10 and US 290 in Houston, Texas, I-394 MnPass and I-35 in Minneapolis, Minnesota, I-95 in Miami, Florida, I-15 in San Diego, California, SR 91 in Orange County, California, SR 167 in Seattle, Washington, I-25 in Denver, Colorado, and I-15 in Salt Lake City, Utah. Tolling policy may be customized for different facilities to achieve their specific objectives, whether it is to reduce emissions, to collect revenue, or to increase overall throughput. This will greatly affect how the users respond to the pricing. However, in general HOT lanes are operated as a reliability control valve for the overall system. When the GP lane is experiencing congestion, some SOV drivers may opt to pay to use the HOT lane in exchange for travel time savings. As those SOVs divert to the HOT lane, the level of GP lane congestion is expected to decrease as a result of the drop in demand. Thus theoretically the HOT strategy can improve the overall throughput and operations of the freeway facilities with MLs.

The increasing number of ML projects across the U.S. demonstrates the strong need of a robust and consistent analysis methodology to quantify the operational performance of these types of facilities.

2.1.2 Separation Type

Most concurrent-flow MLs are separated from GP lanes by painted stripe or narrow buffer (at least 2 feet or 0.6m wide). According to Chang *et al*. (2008), 118 (34 percent) of U.S. HOV facilities are stripe-separated. Sixty HOV facilities (17 percent) use buffers. Forty-five HOV facilities (13 percent) have barrier separations. The remaining facilities do not have their separation type specified. Because of this proximity of GP and ML traffic, increasing congestion levels on GP lanes may have an adverse effect on ML operations, well before the ML demand reaches breakdown levels. This adverse effect on ML operations is referred to as frictional effect in this study. The reason for frictional effect is that drivers in the stripe or buffer separated MLs can readily observe the slow traffic on the adjacent lanes, and feel uncomfortable passing congested GP traffic at a high speed differential. While the effect of narrow lanes and freeway shoulders are documented to result in a reduction in free-flow speed according to HCM 2010 (TRB, 2010), this ML-GP frictional effect has not been well documented to date. To increase the capacity of the ML facility by avoiding this potential friction effect, many two-lane or reversible ML facilities chose to use concrete barrier separations. Some facilities use soft barriers (plastic pylon) for separation and frictional effect can be reduced. Intuitively, a wider and more permanent separation between the GP lanes and MLs is hypothesized to reduce the interaction between the two parallel lane groups.

2.1.3 Number of Lanes

Most ML facilities in operation or being planned in the United States are one-lane facilities, which means that they have a single ML in each direction. Two-lane ML facilities can be found only in California, Northern Virginia, Minnesota, Florida, Texas, and Washington. Similar to the

GP lane facilities, the number of lanes within an ML facility affects its performance. For a single ML facility, a slow-moving vehicle drags down the speed of vehicles following it, much like it would on a two-lane highway or a single-lane tunnel. On the contrary, multi-lane ML facilities allow opportunities for passing, and the impact of slow-moving vehicles is expected to be lower, at least until higher flow levels are reached.

2.1.4 Access Points

The designs of termini and access points of ML facilities tie directly to ML performance, capacity, and safety (Wang *et al.*, 2009). According to the *Managed Lanes Handbook* (Kuhn *et al.*, 2005), MLs are often accessed through three types of access points: direct access ramp, slip ramp, and at-grade access (continuous or limited access). Chang *et al*. (2008) reported that the most common type of ML facility is left-concurrent (e.g. the HOV lane is on the left side of GP lanes), where at-grade access is the treatment commonly used. Of the HOV facilities identified in the compendium (Chang *et al.*, 2008), 41 (12 percent) allow continuous access, using either painted stripe or narrow buffer to separate the facilities from GP lanes. This type of HOV lanes are sporadically distributed in Northern California, Texas, and Washington. In contrast to the continuous access, limited access allows several intermediate accesses along the HOV facilities, typically by changing the pavement marking (e.g. from narrow buffer to dashed line). There are 180 HOV facilities (52 percent) with limited access nationwide. No intermediate access is allowed on 26 facilities (8 percent) located in Arizona, Southern California, Connecticut, Hawaii, Massachusetts, New York, and Texas. The access designs for the remaining HOV facilities in Chang *et al*. (2008) are unknown. For limited access, the opening area length and access point density are expected to affect the ML lane performance.

This limited access configuration is illustrated in Figure 1. For a facility with limited access, vehicles are allowed to enter or exit the MLs in certain designated locations only. This type of access is often preferred by agencies as a cost-effective design when compared with direct grade-separated access. However, it requires GP on-ramp traffic that desires to enter the MLs to weave across multiple GP lanes. It is hypothesized that these “cross-weave” actions may cause significant frictions on GP lane traffic depending on cross-weave demand, the distance available to complete the cross-weave maneuvers, and the GP lane density (Liu *et al.*, 2012).

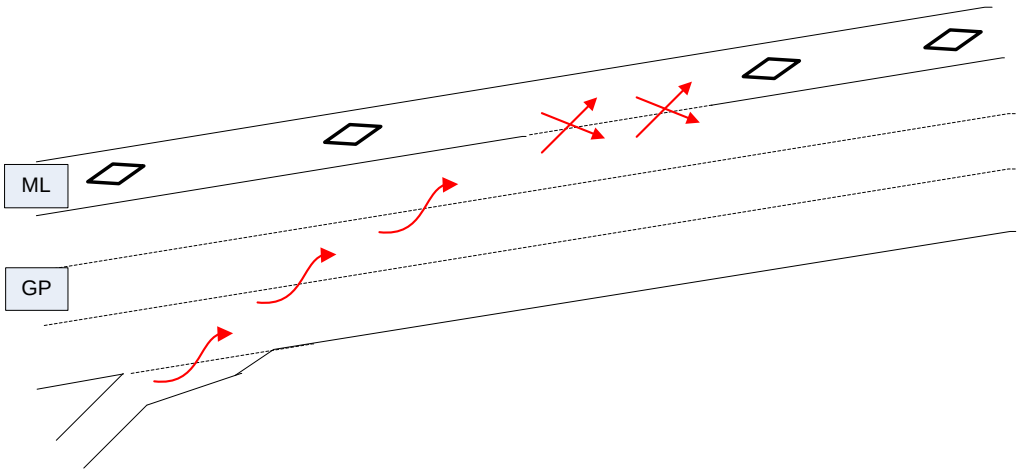

FIGURE 1 Schematic of At-Grade Access with Limited Access Point

2.2 Analysis Methods

2.2.1 Methodological Framework for ML Performance Analysis

In practice, most ML facility analyses are performed in a micro-simulation context (e.g. Zhang *et al.*, 2009; Gomes *et al.*, 2004; and Bloomberg and Dale, 2000). Micro-simulation tools are appealing for analyzing ML facilities because there are no standard methods for such analyses in HCM 2010 and they allow analysts to code and evaluate various design alternatives and operational strategies for the facility in question. Simulation tools are also capable of dealing with oversaturated or congested operations, as queuing patterns are being tracked over time and space. However, micro-simulation-based analyses are limited due to the fact that the build-in driver behavior models have severe constraints and intensive resources are needed to code and configure a network and calibrate the model to fit local conditions (Park and Qi, 2005). One of the most challenging aspects of a simulation analysis is the calibration of the actual maximum throughput or capacity of a road segment, which has been found to vary significantly with changes in calibration parameters (Tian *et al.*, 2002). Simulation tools therefore must be used with caution and require significant time and monetary investments that may exceed the available resources for an agency.

In addition to the modeling challenges associated with simulation, there is presently limited guidance on performance evaluation of ML facilities, which is confirmed by a recent report entitled *Monitoring and Evaluating Managed Lane Facility Performance* (Carson, 2005). While several states continuously monitor the performance of their ML systems (e.g. OCTA, 2007), comprehensive guidance is missing. Among the electronic tools developed specifically for assisting agencies for analyzing MLs, majority are geared at analyzing policies (not traffic operations) related to HOV lanes or HOV lane conversion to HOT lanes. For example, POET-ML (POET-ML, 2008) is a tool for demand modeling and evaluation of HOV policies.

One deterministic freeway analysis tool that does include a feature to evaluate HOV lanes is FREQ (Rodrigues *et al.*, 2008). FREQ was originally developed at the University of California at

Berkeley's Institute of Transportation Studies in 1970. One of the weaknesses of the FREQ tool is its analytical approach for weaving sections, which is still based on the method in HCM 1965 (Rodrigues *et al.*, 2008). Also, a new version of FREQ may not be expected as the software is no longer supported. Other than FREQ, no analytical analysis methodologies for ML facilities could be identified by the literature review.

2.2.2 Traffic Flow Characteristics on ML Facilities

A limited number of studies have examined the traffic flow characteristics of ML facilities including capacity and driver behavior characteristics (see for example Varaiya, 2005 and Guin *et al.*, 2008). ML traffic flows were found behaving differently from those of GP lane facilities. Nee *et al.* (1999) observed that concurrent HOV lane traffic moves slower than expected when GP lanes get congested in Washington State. The two reasons for the slowing HOV traffic were attributed to HOV motorists' lack of comfort traveling at a large speed differential to GP lanes, and to the fact that vehicles merging from the uncongested HOV lane to the congested GP lane were forced to reduce their speeds. Martin *et al.* (2002) observed a similar phenomenon on HOV lanes in Utah. HOV lanes did not operate at expected speeds relative to volume. HOV lanes adjacent to congested GP lanes operated at a speed well below the speed associated with the flow level that is significantly under the capacity.

Varaiya (2005) investigated a drop in capacity of HOV lanes on I-880 in San Francisco. The HOV facility on I-880 is the leftmost lane and is separated by skip-stripe painting. As the HOV facility restrictions on I-880 are only in effect during peak travel periods, the difference between the same facility operating as an HOV lane and a GP lane was observed. Operating as a GP lane, the capacity and speed of the lane were higher than during the times it was operating as an HOV lane. Kwon and Varaiya (2008) also observed this phenomenon as HOV's observed capacity was around 1600 vphpl. This indicated a reduction in lane capacity of at least 20% on California HOV lanes. It was also noted that the operating speed at capacity was lower than the expected speed of 45 mph. Since the studied HOV site was a single HOV lane facility, the HOV speed reduction was contributed to a "snail" effect, meaning that the speed on the HOV lane was governed by the slowest moving vehicle. Since passing was constrained on the single HOV lane, vehicles were trapped behind the "snail" when GP lanes are heavily congested. As the traffic flow increased, so did the number of slow drivers.

Guin *et al.* (2008) then took an in-depth look into the traffic behavior associated with the interaction of parallel, buffer-separated HOV and GP lanes along I-85 in Atlanta, Georgia. Their results indicated that the speed differential between the HOV lane and the adjacent GP lane is affected by the level of congestion in each lane. When the GP lane is uncongested, there is no speed differential between the two systems. When the GP lane is congested, the HOV lane's speed is higher than the GP lane's speed. The maximum speed differential between the facilities was between 20-30 mph. The speed differential gradually decreased until both facilities reached a state of equal congestion. The capacity of the HOV lane in the study was 1,600 vphpl, similar to the results from other studies mentioned earlier.

Liu *et al*. (2011) confirmed Guin *et al.*'s (2008) breakdown process of HOV facilities and described the GP facility as stochastically dominant over the HOV facility. They observed HOV

speed reductions due to HOV lane's own breakdown, in addition to those caused by the slow moving traffic on the adjacent GP lane. They termed the ML speed reduction caused by adjacent GP lane congestion "frictional effect" and investigated the frictional effect between GP lanes and MLs across different separation types. The frictional effect of buffer-separated facilities appeared to be the biggest, followed in turn by soft barrier (plastic pylon) and concrete barrier separations. Concrete barrier separation appeared to have no statistically significant frictional effect. Loudon (2007) proposed a transportation modeling method accounting for the frictional interaction between the HOV lane and the parallel GP lane based on the standard Bureau of Public Roads (BPR) equations used in many transportation models. A mathematical relationship was established estimating HOV lane speed based on the volume/ capacity (v/c) ratio of the HOV lane and the parallel GP lanes. The model accounted for the reduction in HOV speed caused by poor GP lane performance. This model, however, considered only data from a single freeway facility with a buffer-separated, limited access HOV lane.

Loudon's research (2007) was found the only attempt to model ML performance prior to NCHRP 03-96. No other literature was found attempting to use the observed traffic flow characteristics to develop speed-flow relationships for MLs. Of course, there have been extensive efforts to develop speed-flow curves for freeway and highway facilities. Perhaps the most widely used speed-flow curves are those contained in HCM 2010 (TRB, 2010). The HCM-type speed-flow curves first appeared in the 1965 version of the HCM and have evolved over several decades. It began as purely theoretical relationships in the 1965 HCM, as the relationships were created without the use of any supporting empirical data. However, even the curves created for HCM 2010 based on regression techniques were still partly adjusted following engineering judgment (TRB, 2010).

Other methods of forming speed-flow relationships for freeways include Van Aerde and Rakha's (1995) multivariate approach for automatically fitting speed-flow relationship and Brilon and Ponzlet's (1995) continuous single curve. Van Aerde and Rakha's (1995) method allows speed flow curves to be fitted to loop detector output, providing a unique curve for each detector location. This method easily allows users to observe the shape of the speed-flow relationship for the specific location and provides information such as the capacity at the location. Brilon and Ponzlet's method was considered by Roess in developing the speed-curves for freeway in the 2010 version of the HCM (Roess, 2011). Roess also tested a three-segment linear approach and a parabolic speed flow curve. Based on Roess's results, a modified version of the HCM 2000 approach was used in HCM 2010.

2.2.3 Existing Method for Weaving Analysis for ML

Weaving is considered as one of the most important elements in the freeway capacity and Level-of-Services (LOS) analysis in HCM 2010. There are three key geometric characteristics that affect the performance of a weaving segment: width (number of lanes), length, and configuration. The HCM 2010 methodology utilizes a series of predictive algorithms to evaluate the weaving segment characteristics, all of which were based on theoretical or regression models (TRB, 2010).

Chapter 1 of this report defined new segment types for ML facilities, which will be discussed in greater detail in Chapter 3. The segments involving weaving movement, such as ML On-ramp, ML Off-ramp and ML Weave, all follow similar operational concepts to what is currently

included in the 2010 version of HCM for corresponding GP segment types. However, ML-AcS is a new segment type and unique to ML facilities with intermittent access. The segment design of ML-AcS is quite similar to the two-sided weave described in HCM 2010. This type of access is often preferred by agencies as a cost-effective design when compared with direct grade-separated access. However, it requires GP on-ramp traffic that desires to enter the MLs to weave across multiple GP lanes. The resulting cross-weaving maneuvers impose disturbances on the GP lane traffic flow movements.

Some research has been done to provide recommended distances for cross-weaving from operational perspective. A simulation study by Venglar *et al.* (2002) concluded that for general ML planning purposes, the recommended minimum distance between a freeway entrance/exit ramp and an ML access point should be 2,500 ft. The recommended desirable distance between the two is 4,000 ft. The recommendation was based on the GP lane volume as well as the average speed reduction that the GP lane would experience due to the cross-weave flows. Williams *et al.* (2010) used a calibrated VISSIM simulation model to determine the distance that can maximize the capacity of the cross-weave. It was concluded that maximum capacity was guaranteed for distances of 4,000 ft. However, no sensitivity analysis was conducted to quantitatively analyze the cross-weave impact on the GP lane capacity. There are several design guidelines providing a range of answers on the recommended cross-weave distance between a GP on/off ramp and a ML access point. According to the Caltrans HOV Design Guidelines (2003), a minimum distance of 500 ft per lane change, with a desired distance of 1,000 ft per lane change is needed.

Several other efforts have used micro-simulation to determine the capacity of the weaving segment (similar to two-sided weave) on a ML facility. Vo (2008) used the VISSIM microscopic simulation package to develop a capacity model for a two-sided Type C (TRB, 2010) weaving segment as a function of mainline flow, exit ramp flow, and ramp-to-ramp flow. The simulation model was calibrated based on field observations in San Antonio (SB IH 35/410 between the Rittiman on-ramp and the SB IH 410 left exit). Williams *et al.* (2010) investigated the spacing requirements for at-grade access points to ML with respect to the location of entrance and exit ramps on the GP lanes. Again using a calibrated VISSIM simulation model, capacity was estimated by changing the GP input flows, ramp flows, length of weave, etc. It was found that under the four GP-lanes scenario, the principal determinant for spacing was the weaving flow (ramp to ML flow), with a minimum weaving distance of 2,000 to 3,500 ft for flows from 200 to 400 pcph. However, none of the research has established a quantitative relationship between the cross-weave impact and roadway geometric and traffic conditions.

While using the HCM 2010 weaving methodology (two-sided weave) may be feasible from a procedural standpoint, this approach constrains the cross-weaving effect to a single (weaving) analysis segment in the HCM context. It is however desirable to be able to apply the cross-weave demand over multiple segments if other segment types are present between the GP on-ramp and the ML access points.

Chapter 3 Analysis Methodology

3.1 Methodological Framework for ML Facilities

The proposed methodology for evaluating MLs in a deterministic analysis context is based on the freeway facilities method in HCM 2010. Figure 2 shows the current methodology for analyzing a GP-only freeway facility in HCM 2010.

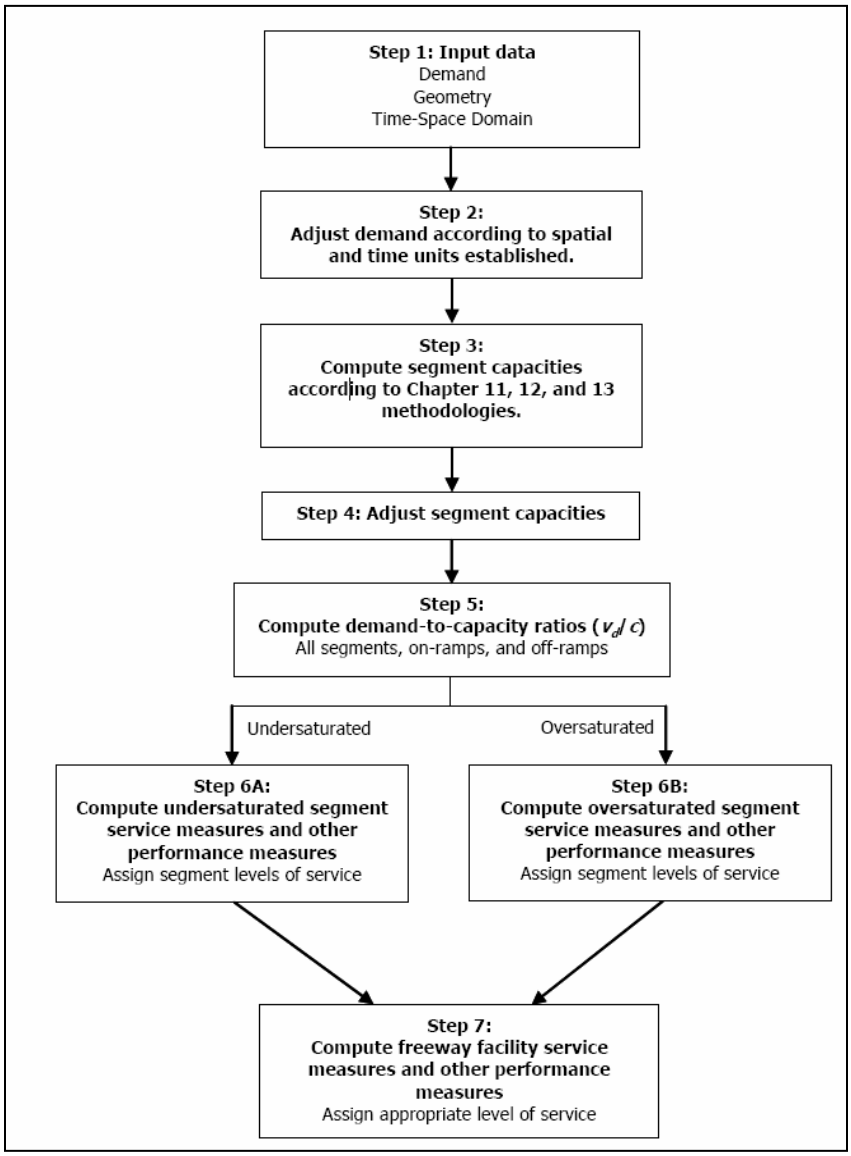

FIGURE 2 Existing Methodology Flow Chart based on Chapter 10 in HCM 2010

The current methodology first establishes the input data requirements, then adjusts demands (if necessary), and computes the operational performance of each individual segment according to the updated methodologies for basic freeway segments, merge and diverge segments, or freeway weaving segments. Capacities can then be adjusted to emulate the effects of adverse weather or

work-zones, before computing segment demand-to-capacity ratios (d/c). If no segment is at d/c>1.0, the methodology then aggregates the facility performance from individual segment operations. If any segment operates at d/c>1.0, an entirely different procedure applies to estimate the effects of congestion based on shockwave theory.

A revised methodological flowchart that incorporates ML facilities is depicted in Figure 3. While both undersaturated and oversaturated scenarios are shown, the proposed enhancements to the method are limited to the undersaturated conditions. By design, majority of ML facilities operate below capacity, especially when they include a pricing component (HOT lanes). It is therefore difficult to obtain ML performance data at or above its critical density, making the development of an empirical relationship impractical. It will therefore be assumed in this method that the operations of congested ML facilities are beyond the scope of the current HCM method, and will be reserved for a simulation-based analysis if necessary (Schroeder *et al.*, 2012). This approach is consistent with the reference to alternative tools that is a theme throughout the HCM 2010.

A significant difference between the existing and the proposed methodologies is the introduction of the new lane group concept, which affects the definition of facility geometry in Step 1. With the introduction of MLs, the time-varying demand volumes needed in Step 1 will require additional analysis to estimate. In Step 3, capacity estimation for the GP segments is computed without considering the impact from the introduction of MLs. Several new ML-specific segment types and associated segment capacities need to be defined and calibrated in this step. Then segment capacities are adjusted for work zones and weather effects in Step 4a as in the current HCM. Adjustment to GP lane capacity is needed for those segments affected by cross-weave maneuvers in Step 4b. As this research did not see a need to specifically explore the impacts of work zones and weather on ML facilities, and the existing methods in the HCM 2010 are adopted.

Depending on the prevailing congestion levels, either undersaturated or oversaturated performance modules are invoked. It is assumed that the oversaturated methodology for GP lanes (Step 6b) will remain unchanged. For undersaturated operations (Step 6a), performance measures are estimated for each segment, under the consideration of traffic demands and appropriate adjustments to segment capacity. GP lane groups are handled through existing methodologies, and some new methods will be needed for specific ML configurations. Readers may have known that current HCM 2010 assigns a segment LOS at the end of Step 6 (a or b), but that the LOS assignment with MLs is now moved after the completion of assignment of adjacent friction effects (Step 7). Finally, facility MOEs are estimated as before, with the caveat that additional MOEs specific to MLs or the relative comparison between the two are needed.

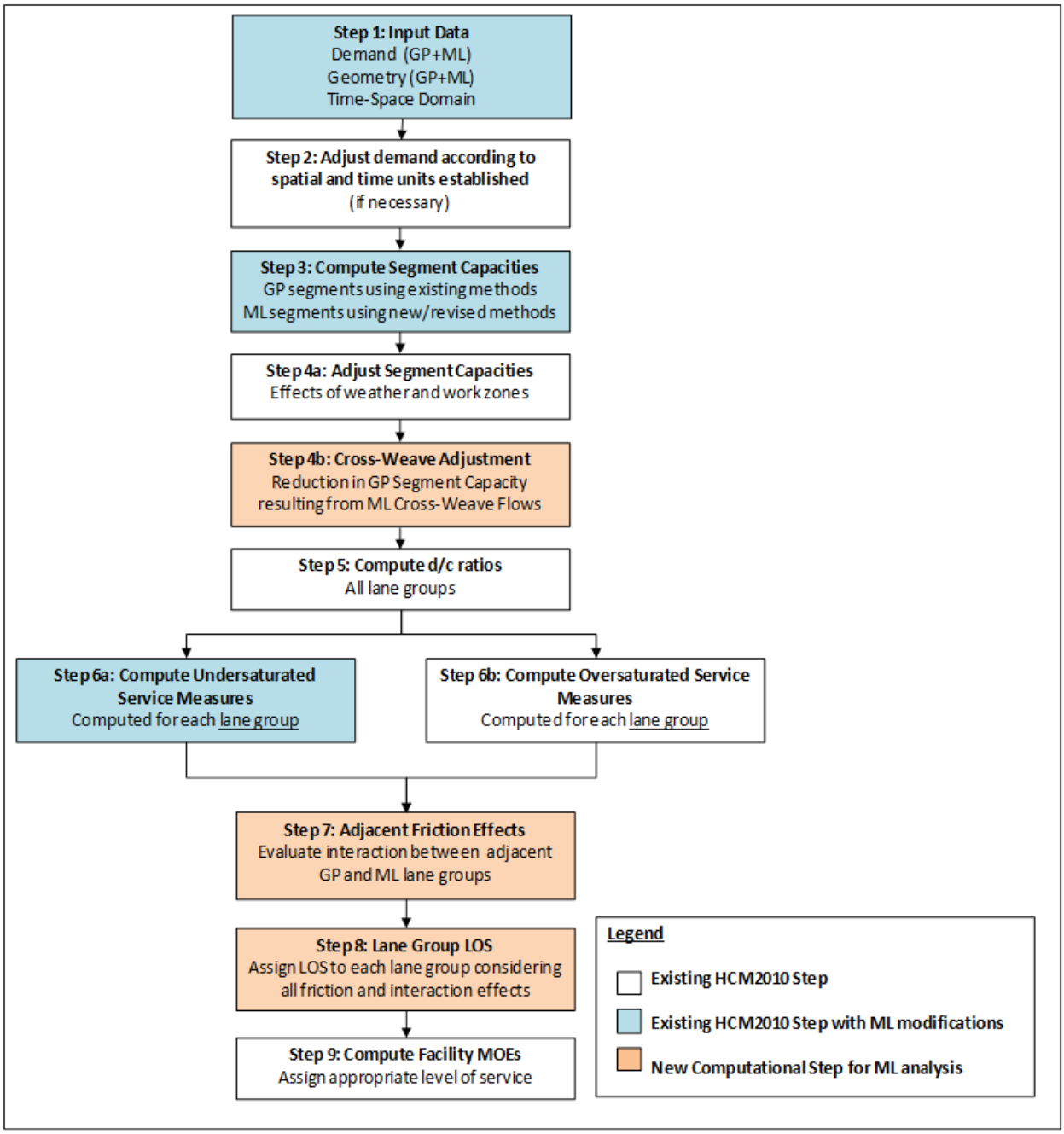

FIGURE 3 Revised Methodological Flow Chart Incorporating MLs

3.2 Defining ML Analysis Segments

The framework introduced in Section 3.1 assumes that all GP freeway facilities are defined in consistence with HCM 2010, including the segment type classification (basic freeway segment, merge segment, diverge segment, and freeway weaving segment). In addition to these GP segments, five new ML segment types need to be defined.

The proposed five new ML segment types are presented in Figure 4. These five new ML segments described as follows:

- ML Basic: This is analogous to the general basic freeway segment, but serves for ML traffic demands. Five different ML Basic segment types are identified and the traffic flow characteristics for these five ML segment types are analyzed in Section 3.3 considering separation types and number of lanes. For barrier-separated ML-Basic segments, the existing GP lane procedure is applicable because frictional effect is insignificant. For stripe or buffer-separated ML-Basic segments, as well as segments with a single ML, new speed-flow models are developed and calibrated. Note that Continuous Access ML segment type, where access between the ML and GP lanes is allowed at any point, is classified into the ML Basic type. It should be distinguished from the ML Access Segment (ML-AcS) which is introduced later in this section.
- ML On-Ramp and ML Off-Ramp: These are analogous to GP Lane On-Ramp and Off-Ramp segments, but with ML traffic demands. The ML On-Ramp and Off-Ramp segments are suitable for using the existing GP lane procedures for ramps.
- ML Weave: This is analogous to the GP Weave segment, but with ML traffic demands. The operational characteristics of an ML Weave segment are reasonably close to those of a GP Weave segment and hence the existing GP lane procedure for weaving segments can be applied.
- ML Access Segment (ML-AcS): This is a new segment type and unique to the ML facilities with intermittent access. Lane changing between the GP lane group and the ML group can occur throughout the segment. Different from the Continuous Access ML Basic type, this segment type exists as the intermittent access segment where access between the ML and GP lanes is prohibited in the segments connect to it. It is treated as a weaving segment and the HCM 2010 weaving methodology is applied to compute its impact. By definition, an ML-AcS segment is always parallel to a GP Access Segment (GP-AcS) which is also shown in Figure 4. In the methodology, it is assumed that the operational performance of the ML/GP Access segment is only estimated once, and results are applied to both ML and GP lane groups.

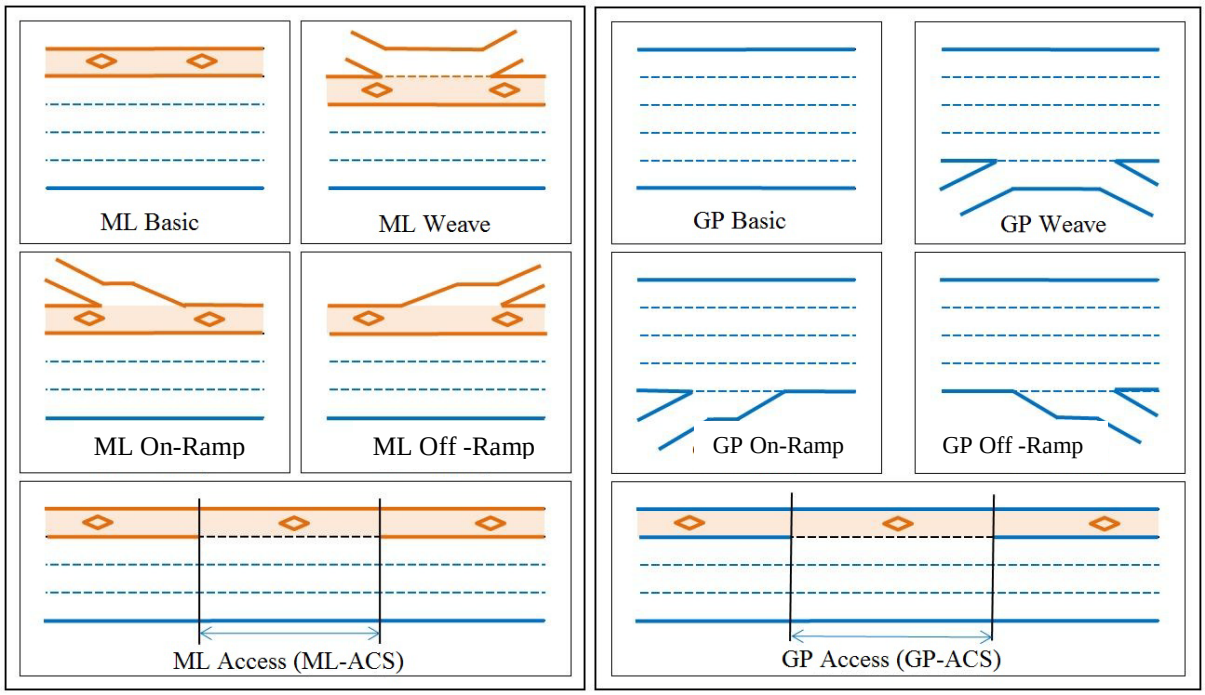

FIGURE 4 Different Segment Types for ML and GP Lanes

3.3 Speed-Flow Models Developed for ML Basic Segments

As a major component of the NCHRP 03-96 project, speed-flow models for the basic ML segments were developed based on empirical data collected through this study. To this end, traffic behavior characteristics of various ML strategies were carefully identified and studied. Data from the ML and the adjacent GP lanes were gathered from each ML site to allow for the interaction of parallel facilities to be investigated. An extensive database was created to house the large amount of data. Fifteen-minute speed and volume data were archived at each location to be consistent with the HCM 2010 procedure requirements. Heavy vehicle volumes were collected to convert vehicle volumes to units of Passenger Car Equivalents (PCE). Heavy vehicle adjustments and PCE conversions were made in accordance with the coefficient values used in HCM 2010.

For MLs that impose restrictions only during certain hours of the day or days of the week, only data from the periods of time where restrictions were in place were used. Data from each location were then grouped into one of the following five configuration types based on separation type and number of MLs:

1) **Continuous Access** – Skip-stripe or solid single line separated, single lane, continuous access
2) **Buffer 1** – Buffer-separated, single lane
3) **Buffer 2** – Buffer-separated, multiple lane
4) **Barrier 1** – Barrier-separated, single lane
5) **Barrier 2** – Barrier-separated, multiple lane

More details of the five configuration types are discussed in Chapter 4.

3.3.1 Form of the Speed-Flow Curve

Each ML Basic segment type does not follow the same speed flow characteristics as determined from empirical observations. Therefore, each of the five ML Basic segment types will have a unique form of the speed-flow curve. The formation procedure will follow the HCM 2010 speed-flow methodology for basic highway segments to ensure consistency and compatibility. The methodology used in this study is similar to that described by Roess (2011).

Each speed-flow curve comprises of two parts: 1) a linear segment starting from the Free Flow Speed (FFS) at a volume of zero and ending at the breakpoint, and 2) a curvilinear segment from the breakpoint to the capacity of the ML system. Breakpoint, as defined in HCM 2010, is the point separating the linear-speed portion of the curve from the rest of it.

Linear Portion

For ML types Continuous Access, Buffer 2, and Barrier 2, where passing is allowed and the slow car following effect is not significant, the linear portion is basically flat, indicating that traffic travels constantly at the FFS. For types Buffer 1 and Barrier 1, the two ML types where vehicles are unable to perform passing maneuvers, the linear portion of the curve is sloped slightly downward.

The linear coefficient is estimated by anchoring the curve to the FFS at zero flow and determining the slope from zero flow to the breakpoint. Linear regression was used to determine the linear coefficient describing the slope of the curve. The linear portion takes the form:

$$S = FFS - C_1 v \quad (3.1)$$

Where:

S=Speed (mph)
FFS = Free flow speed (mph)
C_1= Linear coefficient (or slope)
v=Flow rate (pcphpl)

Curvilinear Portion

This curvilinear portion takes the form:

$$S = SBP - \frac{(SBP-CS)(v-BP)^{C_2}}{(c-BP)^{C_2}} \quad (3.2)$$

where:

S = Speed (mph)
c = Capacity (pcphpl) – This value was obtained from field observations or estimation of traffic flow models calibrated using the collected data. The FFS for each facility type was assigned a maximum observed speed based on the empirical data.
SBP = Speed at breakpoint (mph) – For ML types Continuous Access, Buffer 2, and Barrier 2, this value is equal to the FFS. For ML types Buffer 1 and Barrier 1, this value should be the speed at breakpoint determined by the linear portion of the curve.
CS = Speed at capacity (mph) – For ML types that do not experience a frictional effect (Buffer 2, Barrier 1, and Barrier 2), the speed at capacity is determined by dividing the capacity by a density of 45 pcpmpl. A density of 45 pcpmpl was chosen as the end point of the speed flow relationship to conform to HCM 2010's current breakdown point for freeway facilities. For ML Basic segment types Continuous Access and Buffer 1, where a frictional effect can be observed, the speed at capacity was determined by dividing the maximum observed flow by a density of 30 pcphpl.
v= Flow rate (pcphpl) – This is the input value to determine speed.
BP = Flow at the breakpoint (pcphpl) – Breakpoints were estimated by calculating the standard deviation of speed for each volume range of 100 pcphpl. The breakpoints are determined at the volume where the speed standard deviation begins to increase abruptly. The breakpoint signifies the point in the speed flow relationship where the linear portion ends and the curvilinear portion begins, separating the two parts of the curve.
C_2 = Calibration constant – The calibration constant is the variable used to fit the curve to the data.

Frictional Curve

The performance of the Continuous Access and Buffer 1 facilities is dependent not only on the characteristics of the ML, but also the performance of the adjacent GP lanes. For these two ML types, a second frictional curve has been produced showing the speed-flow relationship for periods of time when GP lanes are congested.

The frictional curve is a function of both the non-friction curve and the flow rate. During the periods of low flow where a frictional effect is not observed, the frictional curve takes the value of

the non-frictional curve from zero flow to the breakpoint (BP). Based on regression work using the filed-collected data, after the break point, the friction curve takes the form:

$$S_f = S_{nf} - C_f(v - BP)^2 \quad (3.3)$$

where:

S_f =ML speed during GP congestion (adjacent GP lane has density > 35 pcpmpl)
S_{nf} =Speed of the corresponding non-friction curve for the same flow rate
C_f = Frictional curve constant – While this constant was originally intended to be formed from regression, it was ultimately determined from anchoring the right end of the friction curve along the density line of 45 pcpmpl and the capacity. This method was chosen so that the speed flow curves are consistent not only among the five basic types of MLs but also with the freeway speed-flow curves.

3.4 Access Point Analysis

It is determined from this project that ML On-Ramp, ML Off-Ramp, as well as ML Weave segments have similar operational models that generally match the ones developed for the GP lanes in HCM 2010. Therefore, no duplicate effort would be performed in this project.

For the ML Access Segment (ML-AcS), the vehicles entering the freeway from GP lane on-ramps need to *cross weave* over multiple GP lanes to access the ML. These weaving vehicles will have a negative impact on the operating performance of the parallel GP lanes. This cross-weave effect is found to be a function of different roadway geometric configurations as well as traffic conditions. A microscopic simulation model was built and calibrated using empirically-collected video data to explore this effect. The cross-weave intensity is consequently quantified using CAF to account for its impact on the parallel GP facility. This concept is discussed in greater detail in Section Chapter 4 of this report. Beyond the effect of cross-weaves, the ML-AcS is analyzed as regular weaving segments using the HCM 2010 procedures.

Chapter 4 Operational Concepts and Traffic Flow Principles in Managed Lanes

4.1 Segment Types

In practice, some ML facilities are physically separated from GP lanes (e.g. with a barrier), while others are constructed concurrent with GP lanes with only narrowly painted lane markers or buffers in separation. In all cases, the composition and behavior of the ML traffic stream is expected to be very different from traffic in the GP lanes. Most notably, traffic volumes, FFS, driver type (commuter vs. casual), and potential per-lane capacity, are expected to differ between ML and GP lanes. This dichotomy of geometric and behavioral attributes of parallel ML and GP facilities poses a major challenge for a deterministic analysis framework. Further, despite this difference in attributes, it is postulated that there is at least some degree of interaction between traffic operations in the ML and GP lanes. This is especially true for concurrent ML facilities, as ML and GP traffic is oftentimes only separated by narrow unobtrusive striping as documented by Liu *et al.* (2011). Interaction may even apply to barrier-separated facilities, where congestion in the GP lanes may have a "rubbernecking" effect on the parallel MLs.

4.1.1 The Lane Group Concept

To capture interaction effects between ML and GP lanes, while allowing varying demand, capacity, and speed inputs, it is proposed to introduce the concept of *lane groups* into the analytical framework for freeway MLs. The lane group concept is well-established in the signalized intersection methodology of the HCM 2010 (TRB, 2011), where it is recognized that exclusive left turn lanes have different geometric and/or behavioral characteristics from the adjacent through lanes, or from shared lanes. By adopting the lane group concept in the ML context, the analyst will be able to ascribe separate attributes to parallel ML and GP facilities, while retaining the ability to model some degree of interaction between the two.

Each segment of a freeway facility in the proposed implementation would therefore be represented as having either one or two lane groups, depending on whether parallel MLs are present. The analyst codes input variables such as geometric characteristic (e.g. number of lanes), behavioral attributes (e.g. free-flow speed, capacity), and traffic demands separately for each lane group, but still within the same computational engine environment. The methodology would then assess the operational performance of each lane group, under consideration of empirically-derived interaction effects between the two lane groups. Any portion of the facility where no ML is present would simply be coded as a single lane-group that serves all traffic demand.

The following assumptions apply to the proposed framework:

- A freeway GP segment with a parallel ML segment is coded as two adjacent lane groups in the methodology.
- Adjacent lane groups (one GP and one ML segment) must share the same segment lengths.
- Adjacent lane groups can be of different segment types for example, a basic ML segment may be concurrent with a GP segment with an on-ramp.

- Each lane group may have different geometric characteristics, including number of lanes, lane widths, shoulder clearance, etc.
- Each lane group can have unique behavioral attributes, including free flow speed, segment capacity, or various capacity- or speed-reducing friction factors. The attributes are represented by GP speed-flow relationships available in HCM 2010, as well as ML-specific relationships presented in this report.
- Each lane group can have unique traffic demand parameters, which are input by the user, and which are obtained through an external process. As an operational methodology, the HCM is not intended to make predictions about traffic demands.
- The operational performance of adjacent ML and GP lane groups is interdependent in that congestion in one lane group may have a frictional effect on operations in the adjacent lane group depending on the type of separation. This friction effect was empirically-derived in this project, can be user-calibrated, and is sensitive to the type of physical separation between lane groups (i.e. striping vs. buffer vs. barrier).

The method assumes that all ML segments should have a demand-to-capacity ratio less than 1 (d/c<1), which means that no congestion would occur on ML segments. Congested ML facilities are relatively rare in practice, as one of the underlying principles for ML operations (especially for HOT lanes) is to assure that ML traffic density is below the critical density level even in peak periods, which in turn guarantees satisfactory service to ML customers. Congestion on GP lanes can and should be considered by the method, as systems of congested GP lanes with below-capacity ML conditions are very common.

4.2 Speed-Flow Model Development for Basic ML Segments

This section presents the operational performance and speed-flow relationships for the basic segments of ML facilities. Data collection sites selected for this study were located at least 1,500 ft from merging and diverging segments to minimize possible weaving impacts. That distance threshold was selected because it corresponds to the length of the ramp influence area in HCM 2010 (TRB, 2010).

For the development of the speed-flow relationship for basic segments of ML facilities, HOV, HOT, and express toll lane facilities were combined. While it is recognized that differences in operations between facilities affect the demand, it was assumed that traffic behavior on basic segments was independent of the management practice on the facilities. Only the separation type and number of lanes were hypothesized to affect the traffic flow behavior of the ML facility (Thomson *et al.*, 2012).

4.2.1 Different Separation Type Characteristics

4.2.1.1 Continuous Access

Continuous Access separation type refers to single lane, concurrent ML facilities in which access between the ML and GP lanes is allowed at any point. Entrances and exits to the ML lane are unrestricted. These facilities are typically located on the leftmost lane on freeways parallel to the GP lanes. Figure 5 shows the schematic of this configuration. The solid single line separating the

ML from the GP lanes can also be skip-striped. Either way, vehicles can cross between the ML and GP lanes at any time. A section of I-5 in Seattle, Washington, provides an example of the solid-line separated Continuous Access facility, and a section of I-95 in Broward County, Florida, provides an another example for skip-strip separated Continuous Access facility, as shown in Figure 5. Although these types of facilities are very common, they are not favorable for HOT lane operations as continuous access is more difficult to manage for most tolling schemes. No dual-lane ML facilities with continuous access were identified by the team across the U.S.

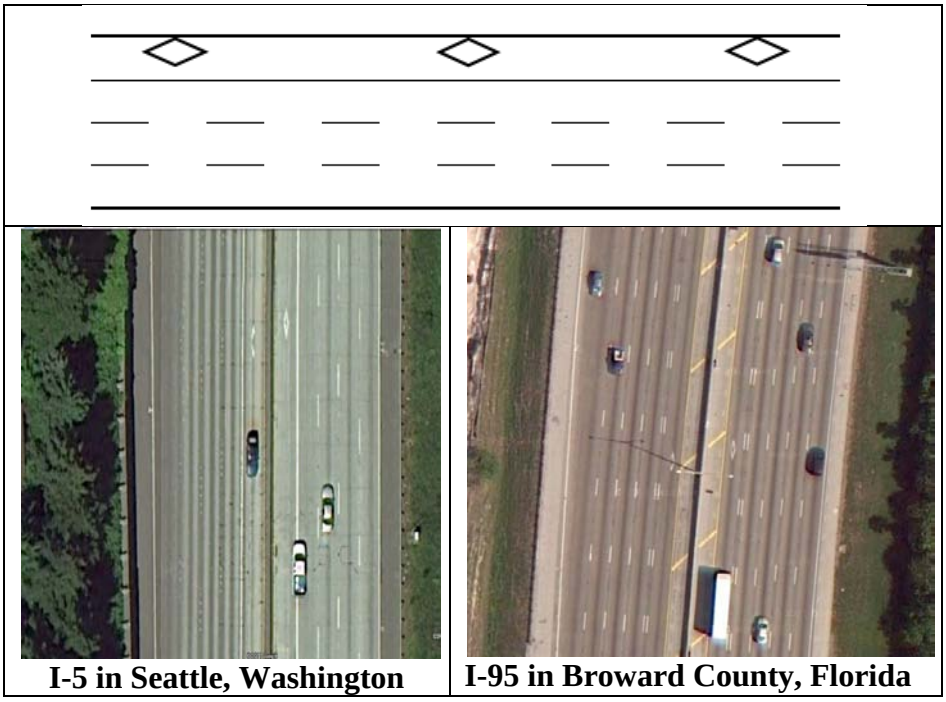

FIGURE 5 Schematic of Continuous Access and Examples at I-5 Seattle, Washington and I-95 in Broward County, Florida (Source: Google Earth)

4.2.1.2 Buffer 1

Buffer 1 refers to the single, concurrent lane ML facilities with intermittent access. Similar to Continuous Access, these facilities are located in the leftmost lane of the freeway cross section. They are separated from the GP lane with a two- to four-foot striped buffer. The striping techniques for Buffer 1 also vary by location, and can feature a double white line, a double yellow line, or two yellow stripes and one white stripe (as is typical in California). Access to and from the ML is limited to occasional buffer opening areas designated by dashed line separation. This geometry is commonly used for both HOV and HOT facilities. Figure 6 shows the basic schematic of a Buffer 1 facility along with an example at I-394 in Minneapolis, Minnesota.

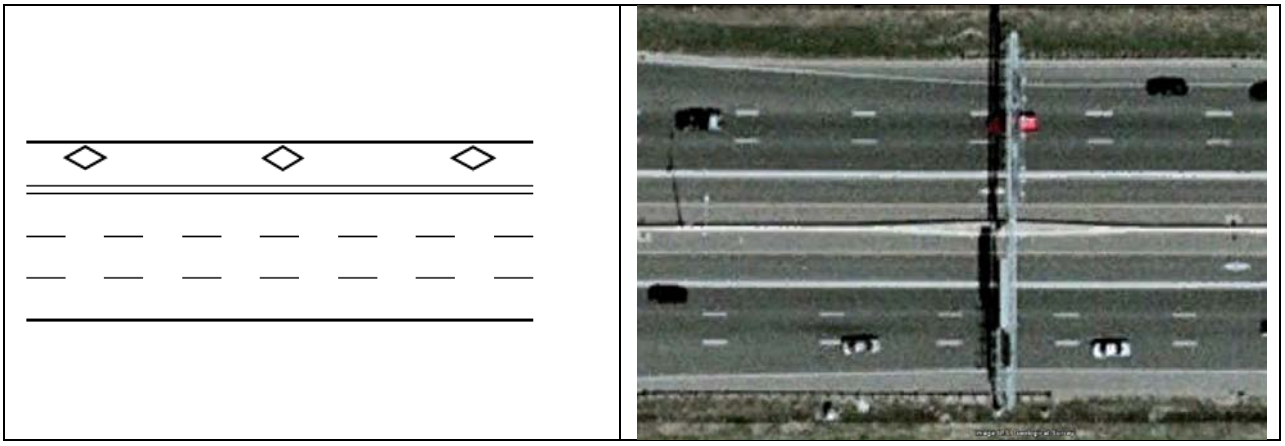

FIGURE 6 Schematic of Buffer 1 and Example at I-394 Minneapolis, Minnesota (Source: Google Earth)

4.2.1.3 Buffer 2

Segment type Buffer 2 is similar to type Buffer 1 but with multiple MLs. It is generally separated from the GP lanes with a two- to four-foot buffer consisting of various painting schemes. This type of facility is the rarest of the five facility types studied, although it may become more popular in future deployments. I-110 in Los Angeles, California was the only location with data available for this type of configuration. Figure 7 displays a schematic of the facility type and an aerial view of I-110 in Los Angeles, California.

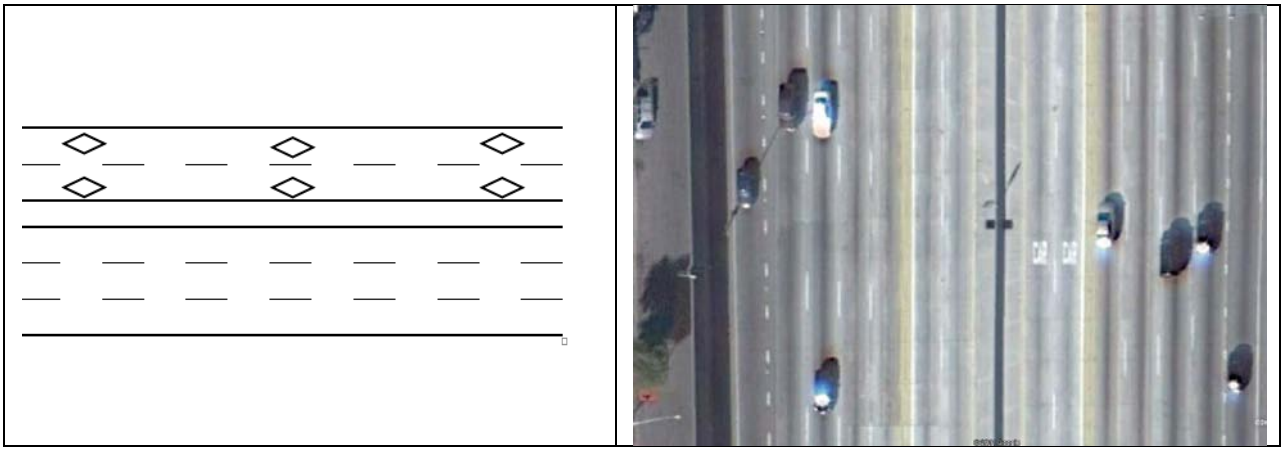

FIGURE 7 Schematic of Buffer 2 and Example at I-110 Los Angeles, California (Source: Google Earth)

4.2.1.4 Barrier 1

Barrier 1 refers to single lane barrier separated MLs. The barrier in all facilities used in this study was concrete barrier. Other physically separating schemes such as landscaping could also be considered barrier-separated. This facility type is suitable for HOV, HOT, and express toll lanes. Figure 8 shows the schematic of Barrier 1 separation and an example of Barrier 1 with an aerial view of I-5 in Orange County, California.

FIGURE 8 Schematic of Barrier 1 and Example at I-5 Orange County, California (Source: Google Earth)

4.2.1.5 Barrier 2

Barrier 2 refers to barrier-separated facilities with multiple lanes. The barrier can consist of a concrete barrier or wide landscaped separation. Access between the MLs and GP lane are limited and can be in the form of either a weave access, or direct ramp access. This type of facility is commonly used for HOV, HOT, and express toll lanes. Note that pylon separated facilities were not considered in this study and should not be compared to barrier separation. Figure 9 shows a sample schematic of the Barrier 2 configuration and an image of I-5 in Seattle, Washington, is shown as an example of a Barrier 2 facility.

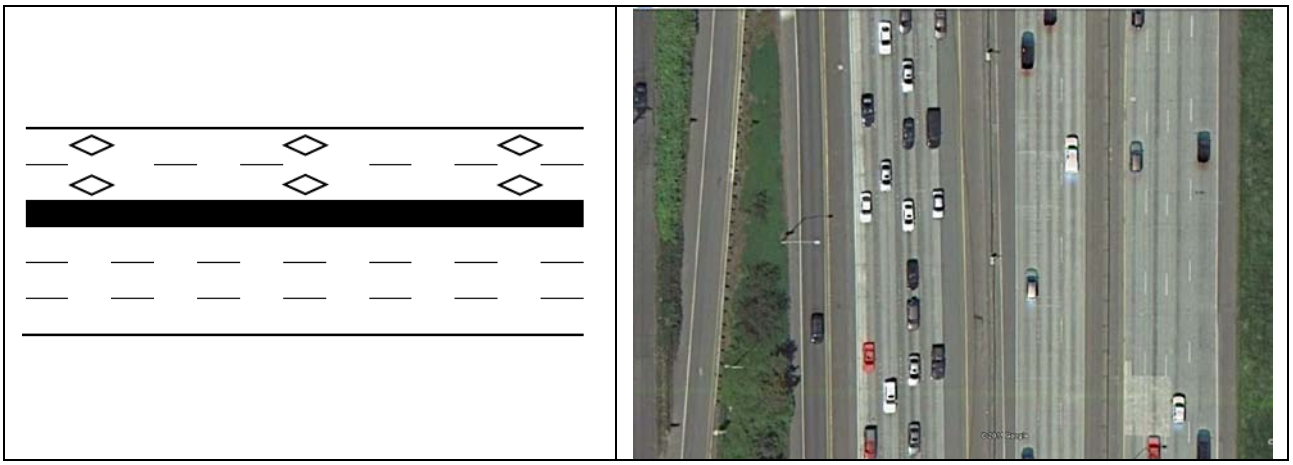

FIGURE 9 Schematic of Barrier 2 and Example at I-5 Seattle, Washington (Source: Google Earth)

4.2.2 Data Acquisition

Data were collected at different sites across the country for each of the five segment types.

4.2.2.1 Continuous Access Sites

I-5 Seattle, Washington, and I-405 King County, Washington

Two facilities from the Puget Sound region in Washington were used in the continuous access data set. I-5 in Seattle, Washington and I-405 in King County, Washington contain continuous access HOV facilities located in the leftmost lane in both the northbound and southbound directions. The HOV lane is separated from the GP facility by a single solid striped line. The HOV restriction of 2+ occupants is enforced at all times on I-5, and every day from 5:00am to 7:00pm on I-405. Data from the two facilities was collected from the Washington State Department of Transportation's (WSDOT) Compact-disc Data Retrieval (CDR) system. Data for the entire month of August 2010 was gathered. August was chosen for data collection because it is a dry month and the weather impacts on driver behavior can be minimized. The locations from each of the facilities are summarized in Table 1.

TABLE 1 Continuous Access Data Site, I-5 & I-405 Washington State

Facility	Direction	Milepost	Cross-Street
I-5	Northbound	172.89	NE Northgate Way
I-5	Northbound	176.74	NE 185th St
I-5	Northbound	179.76	NE 213th St
I-5	Northbound	193.03	SW 36th St
I-5	Southbound	173.75	NE 130th St
I-5	Southbound	174.60	NE 145th St
I-405	Northbound	6.08	SE 24th St
I-405	Northbound	18.07	NE 97th St
I-405	Southbound	3.59	SE 3rd St
I-405	Southbound	7.00	SE 37th St
I-405	Southbound	18.07	NE 97th St

I-95 Broward County, Florida

Two locations along I-95 in Broward County, Florida were used as part of the dataset for continuous access MLs. The HOV lanes operate both northbound and southbound parallel to the GP lanes on the leftmost side of the traffic stream for each direction. They are separated from the GP lanes by a double dashed line. The HOV lane restrictions are only active during peak travel times, limiting use to vehicles with 2+ persons during the periods of 7:00-9:00 AM and 4:00 to 6:00 PM, Monday through Friday.

Data were gathered from Florida's Statewide Transportation Engineering Warehouse for Archived Regional Data (STEWARD). It is a central database program sponsored by Florida Department of Transportation (FDOT) and maintained by University of Florida Transportation Research Center.

TABLE 2 Continuous Access Data Sites, I-95 Florida

Facility	Direction	Milepost	Cross-Street
I-95	Northbound	29.6	NW 19th St
I-95	Northbound	20.4	Johnson St

4.2.2.2 Buffer 1 Sites

I-405 Los Angeles, California

Four sites along I-405 in Los Angeles, California were used as part of the data set for Buffer 1 separation. These sites are listed in Table 3. This facility has intermittent access to the HOV lane on the leftmost side of both the northbound and southbound directions. The HOV lane is separated from the GP lanes by a double yellow line buffer. Data from each of the sites was taken from California's Performance Measurement System (PeMS).

TABLE 3 Buffer 1 sites at I-405 California

Facility	Direction	Milepost	Cross-Street
I-405	Northbound	39.20	Crenshaw
I-405	Southbound	39.28	Crenshaw
I-405	Northbound	32.46	Alameda
I-405	Southbound	31.82	Santa Fe

SR-167 King County, Washington

Four sites along SR-167's HOT lane in King County, Washington were used as part of the Buffer 1 dataset. SR-167's HOT lane was introduced in May 2008 as an underutilized HOV lane was converted to a HOT lane. A single HOT lane and two GP lanes run in each direction along the corridor. The HOT lane is separated from the GP lanes by a double white line buffer. Movement into and out of the HOT lane is restricted to specific access points. Dynamic pricing is used to optimize the performance of the corridor, maintaining a speed above 45 mph. The HOT lane's restrictions are in effect from 5:00am to 7:00pm daily. Data from SR-167 was collected from the WSDOT CDR system. Data for the entire month of August 2010 was gathered. The locations from which the data were gathered are summarized in Table 4.

TABLE 4 Buffer 1 Data Sites, SR-167 Washington State

Facility	Direction	Milepost	Cross-Street
SR-167	Northbound	24.61	SW 41st St
SR-167	Northbound	23.90	S 187th St
SR-167	Northbound	22.93	S 202nd St
SR-167	Southbound	22.93	S 202nd St

I-394 Minneapolis, Minnesota

Three sites from I-394's HOT lanes in Minneapolis, Minnesota were used in the Buffer 1 dataset. The buffer-separated section on this facility stretches eight miles west from downtown Minneapolis. The HOT lane is located on the leftmost side of the traffic stream in both the eastbound and westbound directions. Access to the HOT lane is restricted to specific locations. The HOT lane is separated from the GP lanes by a double white line buffer. The toll rate along the corridor is dynamically adjusted to ensure the system operates above 50 mph at all times. Data for the corridor was obtained through the Minnesota Department of Transportation's online Data Extract Tool.

TABLE 5 Buffer 1 Data Sites, I-394 Minnesota

Facility	Direction	Cross-Street
I-394	Eastbound	General Mills Blvd
I-394	Eastbound	US 169
I-394	Eastbound	Co Rd 73

4.2.2.3 Buffer 2 Site

I-110 Los Angeles, California

I-110 in Los Angeles, California is the only ML facility identified in the United States with a buffer-separated multilane configuration. Both the northbound and southbound directions have two HOV lanes located on the inside lanes. The HOV lanes are separated from the GP lanes by a double yellow line buffer for part of the freeway (other sections have barrier-separation). While this facility is over ten miles in length, data from only two locations can be used. This is due to the fact that the high density of ingress and egress points' deployment caused many of the sensor locations to fall outside of the required 1,500 ft for basic segment consideration. Data was gathered from Caltrans' PeMS database.

TABLE 6 Buffer 2 Data Site, I-110, Los Angeles, California

Facility	Direction	Cross-Street
I-110	Northbound	N/o Florence Ave
I-110	Southbound	S/o Florence Ave

4.2.2.4 Barrier 1 Site

I-5 Orange County, California

Barrier 1 sites were located all along I-5 in Orange County, California. The location information is shown in Table 7.

TABLE 7 Barrier 1 Data Site, I-5 Orange County, California

Facility	Direction	Cross-Street
I-5	Northbound	W Santa Clara Ave
I-5	Southbound	N/o 17th Ave
I-5	Southbound	S/o 17th Ave
I-5	Southbound	W Santa Clara Ave

4.2.2.5 Barrier 2 Sites

I-5 Seattle, Washington

I-5 in Seattle, Washington has reversible express lanes that run through the center of the facility. These lanes serve traffic heading inbound to the City during the morning commute and outbound during the evening commute. Data from only one site could be used as part of the Barrier 2 dataset. The site is located at the cross of 63rd Street. Both northbound and southbound traffic was gathered.

I-394 Minneapolis, Minnesota

A three-mile portion of I-394's HOT lane system is a two lane, concrete barrier-separated facility. SOV users pay an electronic toll upon entering the facility. Data were gathered from the Minnesota Department of Transportation's online Data Extract Tool from the locations shown in Table 8.

TABLE 8 Barrier 2 Sites, I-394 Minneaplois, Minnesota

Facility	Direction	Cross-Street
I-394	Eastbound	W/o Wirth Pkwy
I-394	Eastbound	E/o Wirth Pkwy
I-394	Eastbound	Penn Avenue

4.2.2.6 Site Summary

Table 9 displays the summary of the data used for each segment type including the total number of 15-min sample points. As Continuous Access and Buffer 1 are the two most common facility types, a greater amount of data could easily be collected from these sites. Buffer 2, Barrier 1, and Barrier 2 are less common configurations. Data collection sites were therefore limited and the total number of data points was less than those for the Continuous Access and Buffer 1.

After data had been gathered, it was classified into different FFS categories. FFS categories of 55, 60, 65, 70, and 75 mph were considered. FFS was determined based on the average speed of the facility at a flow rate less than 100 pcphpl. Based on this average speed, sites were assigned to the closest FFS category. For example, any average FFS that fell between 62.5 mph and 67.5 mph fell

into the category of 65mph. The rounding to the nearest 5 mph is consistent with guidance in the HCM 2010 (TRB, 2011). Table 10 summarizes the number of fifteen-minute data points in each FFS category for each segment type. Although an extensive amount of data was collected, not every FFS could be covered for each segment type.

As data were collected from a variety of sources, filtering of erroneous data was imperative. Data points outside of the normal distribution pattern, or outliers, were removed from the dataset. This included many data points with unreasonably high speeds, such as over 100 mph. Data points with very low speeds under low flow conditions were also removed as these were likely attributed to queue spillback from downstream congestion, or may be associated with detector error.

TABLE 9 Data Site Summary

Segment Type	Facility	No. of Sites	Span of Data Collected	No. of Points
Continuous Access	I-405, King County, Washington	5	1 month, All days, 5:00am to 7:00pm	30,617
	I-5, Seattle, Washington	6	1 month, All days, all hours	
	I-95, Broward County, Florida	2	1 month, TWTh, 7:00 am-9:00am and 4:00pm-6:00pm	
Buffer 1	I-405, Los Angeles, California	4	1 month, Wednesdays only, all hours	17,683
	SR-167, King County, Washington	4	1 month, all days, 5:00am-7:00pm	
	I-394, Minneapolis, Minnesota	3	1 month, TWTh, 6:00am - 10:00am	
Buffer 2	I-110, Los Angeles, California	2	2 months, TWTh, all hours	4,981
Barrier 1	I-5, Orange County, California	4	1 month, TWTh, all hours	5,263
Barrier 2	I-5, Seattle, Washington	1	1 month, Mon-Fri, 5:00am-11:15am, noon-11:00pm (Reversible lanes in operation)	5,112
	I-394, Minneapolis, Minnesota	3	1 month, TWTh, 6:00am - 1:00pm	

TABLE 10 Number of Sample Points for FFSs by Separation Type

	Number of Points				
FFS (mph)	**Continuous Access**	**Buffer 1**	**Buffer 2**	**Barrier 1**	**Barrier 2**
55	-	-	-	-	-
60	2,794	-	-	1,321	2,170
65	16,267	13,154	2,485	3,942	1,646
70	1,118	4,529	2,496	-	1,296
75	438	-	-	-	-

Note: "-" denotes not available

4.2.3 Observed Traffic Flow Characteristics of Basic ML Segments

As mentioned in Chapter 2, previous efforts have indicated that traffic behavior on ML facilities differs from that on GP lanes. The differences established in previous research can be summarized into three categories:

1) Lower Capacity –The capacity of ML is lower than it would be expected on GP lanes under the same demand.
2) Sensitive to congestion in GP lanes – Vehicles in the ML will slow down to reduce the discomfort of traveling at high speed differentials.
3) Affected by the inability to pass slow moving vehicles (single-lane facilities only) – The inability for passing slow moving vehicles in the single ML can result in slower than expected facility speeds.

This project explores these three differences for each of the five segment types.

4.2.3.1 Examining ML Capacity

Although previous studies have indicated that the capacity of MLs is less than that of GP lanes, researchers have not explored the differences between capacities of various ML facility types. This project investigated the approximate capacities of each facility type for an FFS of 65 mph. Rather than showing individual sites, all sites with an FFS of 65 were combined for each facility type. All data points with a density of over 45 pcpmpl were removed from the database to avoid including periods of time where the facility had already reached a congested state (TRB, 2010). The 99.5th percentile flow from each of the five data sets was calculated to provide an approximate value for capacity for each separation type. Because it is difficult to specify a single capacity value, the 99.5th percentile flow was used as a guide for establishing the capacity value. Engineering judgment was used to ensure that the 99.5th percentile flow corresponds to the facility capacity rather than simply the maximum observed flow rate. The observed capacity was also rounded to the nearest 50 pcphpl. Figure 10 shows speed-flow plots for the FFS of 65 mph for each of the five facility types.

Figure 10 (a) clearly shows some flow values in excess of 1,800 pcphpl for the Continuous Access facilities. However, the capacity for Continuous Access segment with FFS 65 mph was determined to be 1,700 pcphpl, using the 99.5th percentile flow method, as well as adjusting based

on empirical data from adjacent FFS curves of 60 mph and 70 mph. The capacity for the other types was determined using the same method. For Barrier 2, no sites with an FFS of 65 mph, or any other FFS's, appeared to reach capacity. Therefore, a capacity for Barrier 2 could not be determined. The several points that fall below 50 mph at lower flow rate can be seen as outliers as no breakdown trend appears.

The results from the capacity analysis show that there are differences in capacity between ML facility types. Detailed capacity values of each ML basic segment type are described in Section 5.2. The facility with the highest observed flow was the Buffer 2 facility. The Barrier 2 facility, although not reaching capacity, showed higher flow rates as well. The highest observed volume for Barrier 2 approached 1,800 pcphpl. One reason for the higher capacity in the multiple lane facilities is that there is no slow car following effect. Slower vehicles can be passed on multi-ML facilities. Also, for Barrier 2 facilities, the presence of the barrier removes the frictional effect from the congested GP lanes. Compared with the capacity of GP lane for FFS = 65 mph, all the ML types have a lower capacity than that of GP lanes, as GP lane capacity is generally observed between 2200 and 2400 pcphpl (TRB, 2010).

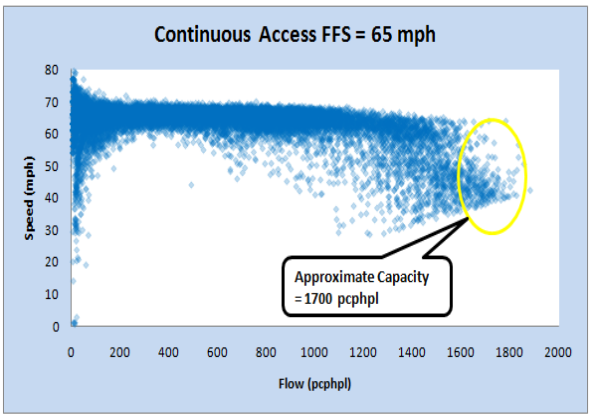

(a) Continuous Access

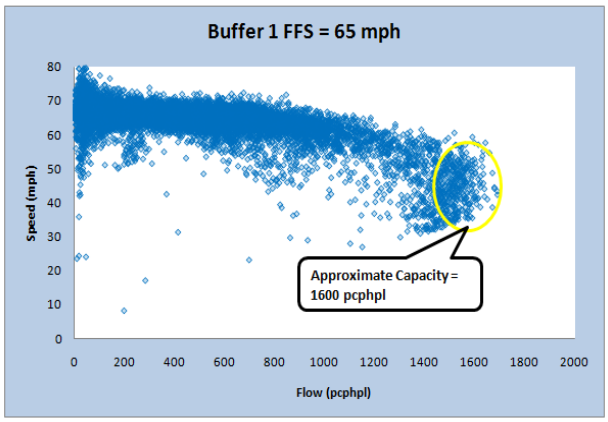

(b) Buffer

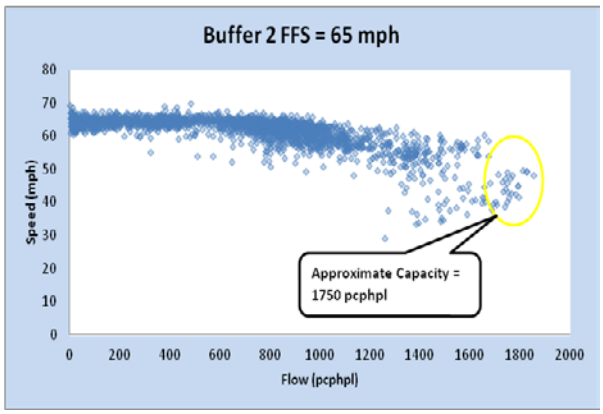

(c) Buffer 2

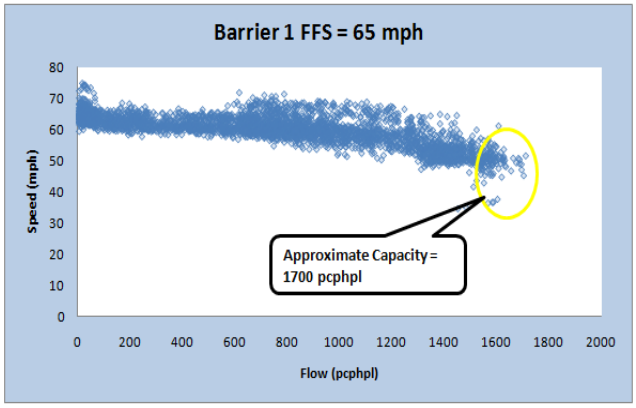

(d) Barrier 1

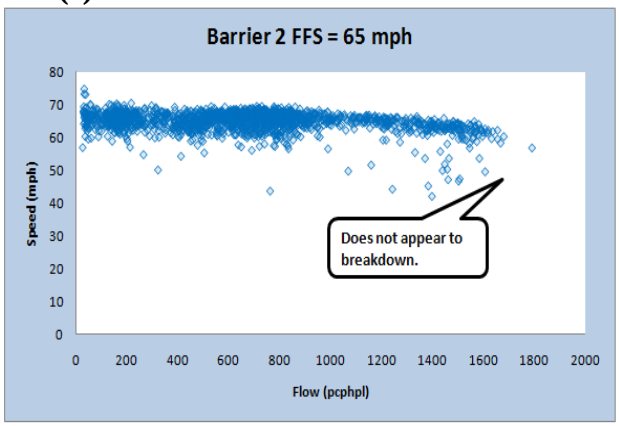

(e) Barrier 2

FIGURE 10 Speed Flow Plots for FFS=65 mph for the Five Facility Types

4.2.3.2. Slow Car Following Effect

The slow car following effect for ML facilities can be defined as the degradation in speed in a single lane ML facility, due to the inability for passing slower vehicles. As passing is allowed on multiple lane facilities, they are not subject to this effect. Although previous research indicates the

presence of this slow car following effect as a motivation for different traffic flow behavior on ML facilities, its effect was never quantified.

Figure 11 (a) provides an example of the speed-flow plot for a Buffer 1 separated facility. Figure 11 (b) shows an example of the speed flow plot for a Buffer 2 separated facility. The major difference between the two shapes of the curves can be seen on the left side of the data plot under low flow conditions. The Buffer 1 facility shows a negative slope for this low flow section of the curve while the Buffer 2 facility shows a flat line with no slope. Under low flow demand, the Buffer 2 separation type maintains its free flow speed while the Buffer 1 speed decreases with an increase in flow. Figure 11 (c) shows an example plot of speed-flow data from a facility with Continuous Access. Although the Continuous Access facility consists of only one lane, under low flow scenarios, passing can occur on the facility. As long as there is an acceptable gap in the adjacent GP lane and speeds in the GP lane are not below that of the vehicle in the HOV lane, a passing maneuver can be completed through the GP lane. Therefore, the speed-flow curve of Continuous Access facilities remains at FFS at lower flow rates.

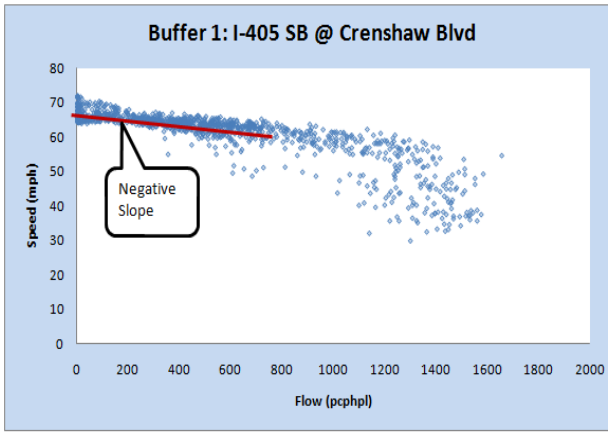

(a) Buffer 1 Facility

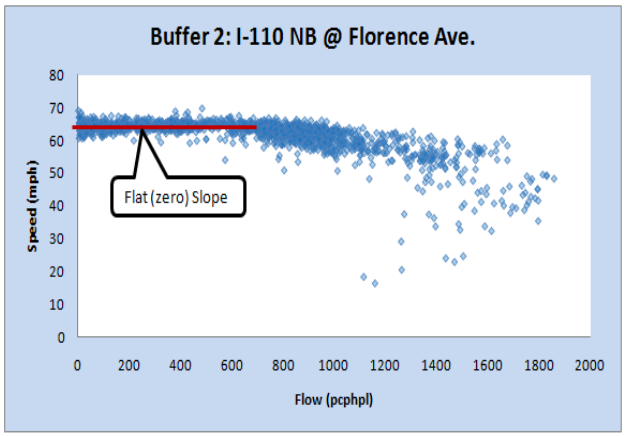

(b) Buffer 2 Facility

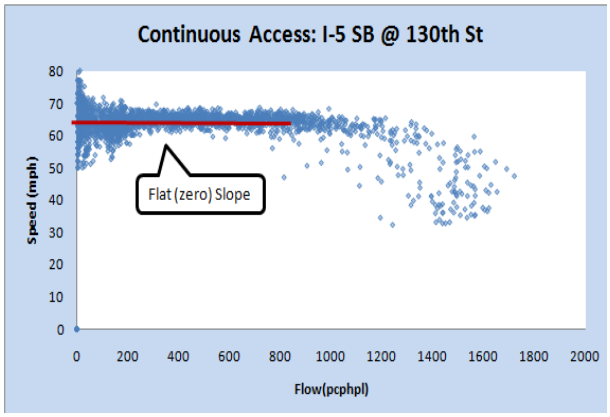

(c) Continuous Access Facility

FIGURE 11 Slow Car Following Effect Observations

To determine whether the slow car following effect could be observed on the facility, video data were collected at one of the single lane ML facilities in Dallas, Texas. The presence of platoons on the HOV facility was analyzed. The details of the validation result are presented in Chapter 5.

4.2.3.3 Frictional Impact from GP Lanes

Previous research suggests that poor performance of the GP lane causes degradation in speed on the adjacent ML. Research has also indicated that this frictional effect is stronger on facilities with less physical separation such as Continuous Access and Buffer 1 (Liu *et al.*, 2011). The frictional effect can first be observed by viewing speed-flow plots for a Continuous Access facility in Figure 12. In Figure 12 (a), all the speed-flow data points are shown. There is a wide dispersion of points from a flow of 600 pcphpl to 1700 pcphpl. This trend is atypical for what is usually seen in GP lane speed flow curves, which normally has little variance in speed between windows of equal flows.

When the data are segregated based on the operations in the GP lanes as shown in Figure 12 (b), the reason for the dispersion of speed can be observed. A density of 35 pcpmpl is used as a threshold for the drop in performance of the GP facility. This particular threshold was selected as it serves as the transition point from LOS D to LOS E in the HCM 2010. During periods of time where the GP lane has a density greater than 35 pcpmpl, lower speeds can be observed on the ML. The lack of continuity to the curve can be seen as breakdown appears to occur at different levels of flow depending on the GP lane's performance.

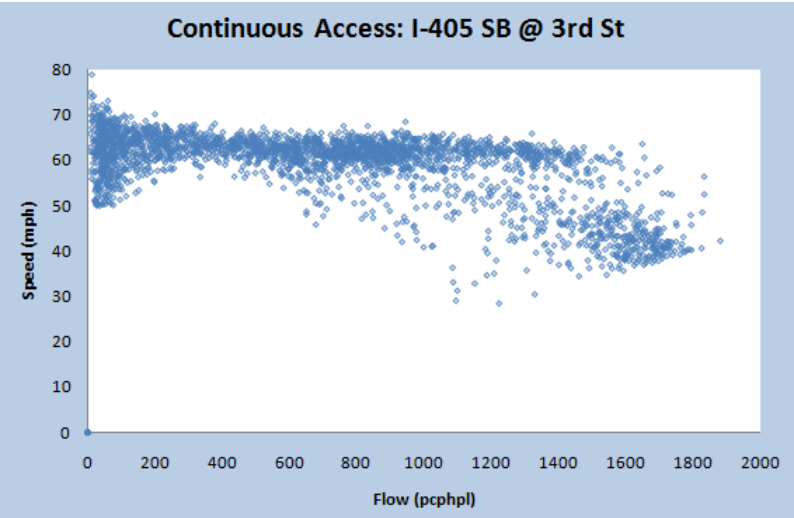

(a) All ML Data Points

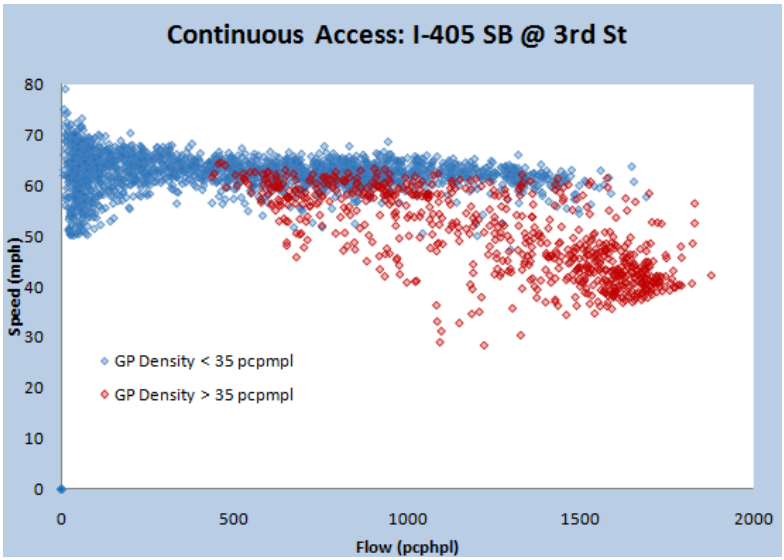

(b) Paired ML Data Points by GP Density

FIGURE 12 Continuous Access Facility at I-405 SB @ 3rd St, King County, Washington

To determine if the difference speeds during these time periods are statistically significant, a t-test was performed on the data sets. Data from each category were selected between the flows of 500 pcphpl and 1,500 pcphpl when conducting the t-test. Table 11 displays the results. As the p value is well below 0.01, the two data sets can be considered significantly different at 99% confidence level.

TABLE 11 Continuous Access Frictional Effect, t-test Results

	Speed with GP Density < 35 pcphpl	Speed with GP Density > 35 pcphpl
Mean (mph)	62.1	49.7
Variance	5.4	66.4
Observations	1095	702
t Stat	39.15	
P-value	0.00	

A similar process can be used to verify the frictional effect for Buffer 1 facilities. Figure 13 shows speed-flow data points at the same location. Again, if they are separated by the density threshold of GP lane of 35 pcpmpl, the frictional impact can be observed. Figure 13 (b) clearly shows lower speeds on the ML during periods of congestion on GP lanes.

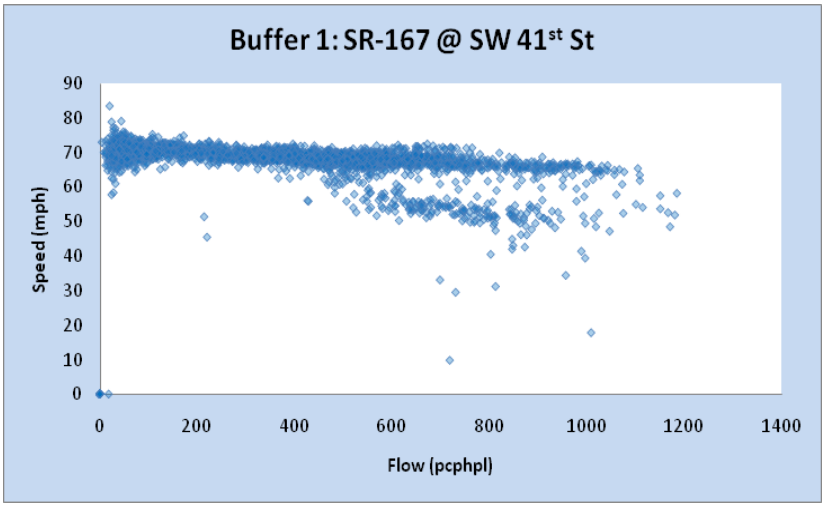

(a) All ML Data Points

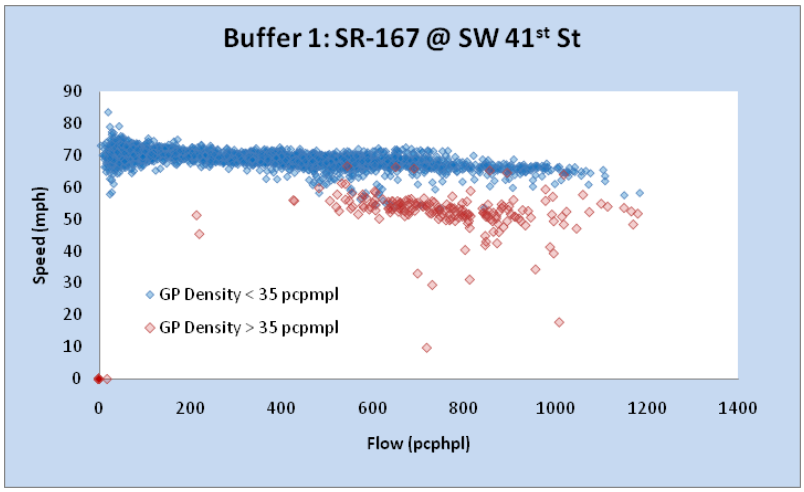

(b) Paired ML Data Points by GP Density

FIGURE 13 Buffer 1 Facility at SR-167 SB @ SW 41st St, King County, Washington

A t-test was performed to validate the statistical difference between the two data sets. The results are shown in Table 12. The results of the t-test show a P value of 0.00, validating that the difference between the two data sets are statistically significant at 99% confidence level.

TABLE 12 Buffer 1 Frictional Effect, t-test Results

	Speed with GP Density < 35 pcphpl	Speed with GP Density >35 pcphpl
Mean (mph)	67.5	52.4
Variance	5.10	42.55
Observations	1405	187
t Stat	31.49	
P value	0.00	

The result from the frictional effect analysis shows that the performance of the adjacent GP lane affects the performance of the ML for Continuous Access and Buffer 1 types. During the periods where the GP lane is experiencing congestion, the ML facility experiences degradation in speed. The operational concepts presented in Section 4.2.3 serve as the reasoning behind the methodology used in the development of the speed-flow curves for ML basic segments.

4.3 ML Access Points

4.3.1 Access Point Configurations for ML facilities

Clearly, one of the significant sources of potential congestion for an ML facility is the treatment at the access points to the ML lanes, in addition to any direct cross-flows between the ML and GP lanes. The three ML principal types of access configurations are described below and illustrated in Figure 14.

A. **At-Grade Lane-change Access (Type A)** occurs where ML traffic enters the GP lanes through a conventional on-ramp roadway (from the right), weaves across multiple GP lanes, and then enters the ML facility. The configuration is also a form of a weaving movement. This access strategy is common for concurrent ML facilities. Access between ML and GP is sometimes constrained to specific locations or openings, which affect the weaving intensity at these access points, as well as the intensity of the two-sided weaving maneuver across the GP lanes. The Type A access configuration requires a *cross-weaving* movement across GP lanes for drivers to position themselves prior to the access point, and a *lane-change movement* to get from GP into the managed lane.

B. **At-Grade Ramp Access (Type B)** occurs where arterial traffic weaves across multiple GP lanes (similar to Case A above), but where the entrance to (or exit from) the ML facility is confined to an at-grade on-ramp (off-ramp). Operationally, the GP lanes are affected by the cross-weaving flow, as well as friction caused by the on and off-ramps. The ML lane operations are in turn impacted by the cross-weaving maneuvers from and/or to the access points at the ramps. The Type B access configuration requires a *cross-weaving* movement across GP lanes for drivers to position themselves prior to the access point, and a *ramp movement* to get from GP into the managed lane.

C. **Grade-Separated Ramp Access (Type C)** occurs where access to the MLs occurs on a grade-separated structure (i.e. flyover, bridge, or underpass). The operational impact to the GP lanes is minimal in this case, since the cross-weaving movement is eliminated entirely. The MLs are affected by friction from the entering or exiting ramp flows in the normal fashion as GP lanes. The Type C access configuration does not require any cross-weaving across GP lanes due to a grade separated ramp, and the ML access is handled by a *ramp movement*.

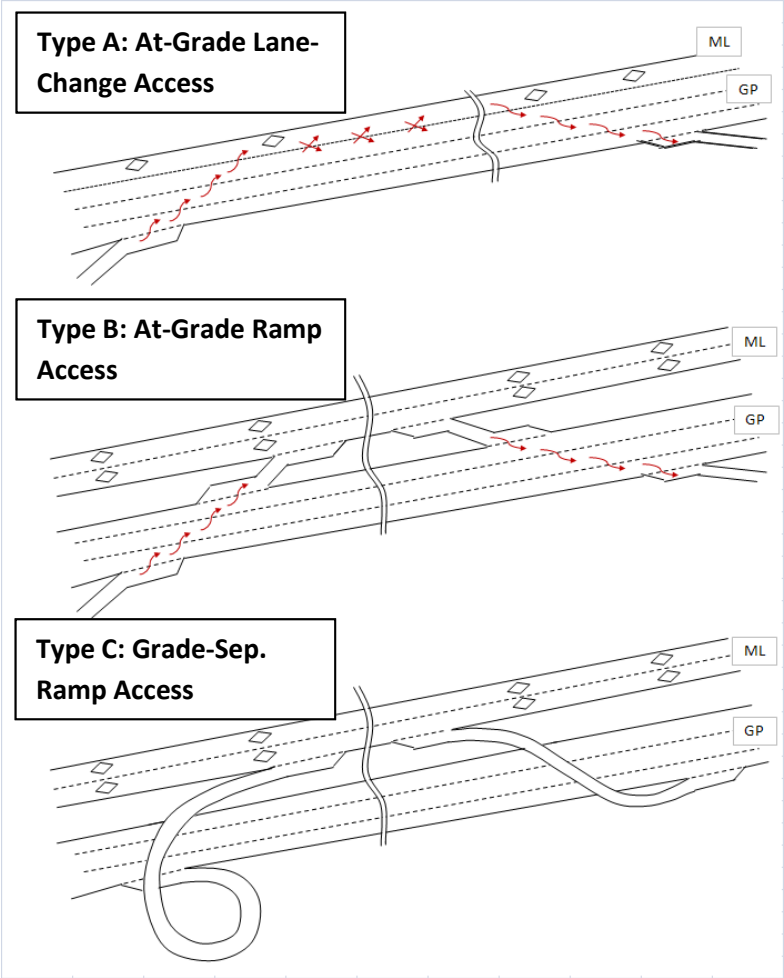

FIGURE 14 Illustrated of Access Point Designs

Incorporating these various access types into the lane group analysis framework is straightforward for Type C, since the spatial extent of the *Access-Point Influence Area* (APIA) is already defined in HCM 2010 ramp junction methodologies. The ramp influence area for GP facilities is defined as 1,500 feet from the ramp gore for both on-ramps (measured downstream) and off-ramps (measured upstream). The APIA for Type-C ML access points is assumed to follow the same convention.

For Types A and B access points, the challenge lies in predicting the intensity and impact of the *cross-weaving (CW) flows* between a GP ramp and the access region between the GP lanes and MLs. The minimum cross-weave length ($L_{CW\text{-}Min}$) is defined as the distance between the closest upstream GP on-ramp gore point to the start of the ML access opening. The maximum cross-weave length ($L_{CW\text{-}Max}$) is defined as the distance from the ramp gore point to the end of the access opening. Figure 15 illustrates this concept for a concurrent single ML next to three GP lanes with stripe-separation. In this case, on-ramp vehicles desiring to enter the ML will complete all three lane-change maneuvers (not counting the merge from the acceleration lane), resulting in a cross-weave friction on the GP lanes. It is assumed that most drivers will strive towards completing the lane change maneuver as early as possible, possibly resulting in a disturbance on

the GP lanes operating speed and capacity before the ML access point. The overall cross-weave intensity profile is postulated to be correlated to the number of lane change maneuvers as a function of the minimum and maximum available distances to complete all lane changes ($L_{CW\text{-}Min}$ and $L_{CW\text{-}Max}$). The Buffer Opening Area (BOA) is defined by the difference of these two distances.

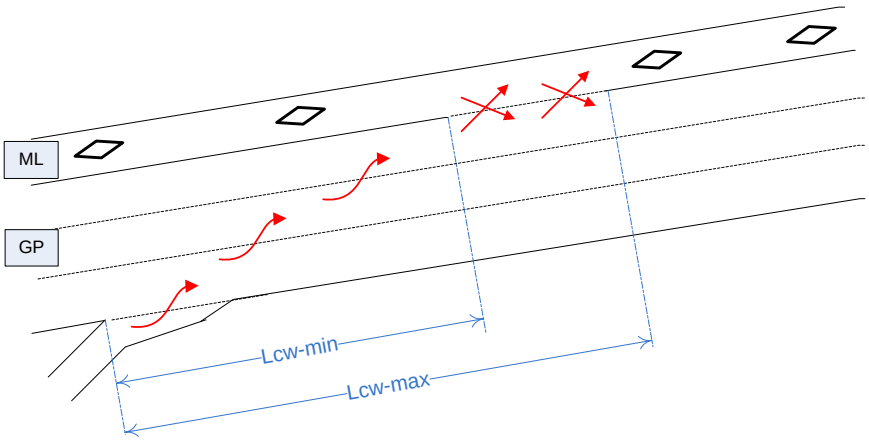

FIGURE 15 Defining Dimensions of APIA through Minimum and Maximum Cross-Weave Lengths

Methodologically, the cross-weave friction may result in a reduction in GP segment capacity and operating speeds, similar to the way a weaving segment with significant weaving traffic has a lower capacity than a basic freeway segment. Due to the technical difficulties in estimating this capacity reduction effect in the field, the NCHRP 03-96 research team relied mostly on calibrated micro-simulation models to estimate this effect. Field measurements of this effect are very challenging, because the $L_{CW\text{-}Max}$ distance can cover a length of up to one mile of freeway or more, at which point roadside (human observer) or overhead observations (surveillance cameras) are not very useful. Through a well-calibrated simulation model, various scenarios with different number of GP lanes, cross-weave demand, $L_{CW\text{-}Min}$ length can be tested. The research team proposed to use a Capacity Reduction Factor (CRF) and/or Capacity Adjustment Factor (CAF) feature to account for the capacity reducing impacts of cross-weave traffic on one or more GP segments. Lane change intensity information can also be collected from the simulation model to be applied to the overall estimates of cross-weave friction.

4.3.2 Simulation Test Scenario

A calibrated simulation model was used to simulate freeway operations as entering vehicles weave across multiple GP lanes to enter the ML. Capacity estimates for a variety of scenarios encompassing different number of lanes, $L_{CW\text{-}Min}$, GP demand, and cross-weave demand were tested in the model. CRF/CAF was subsequently estimated corresponding to various configurations. The details about the simulation model configuration are presented in Chapter 5.

4.3.2.1 Capacity Estimation from Simulation Output

After each simulation run, a speed-flow diagram was developed using the simulated data collected at virtual sensor locations. Heuristic and analytic methods were considered for capacity estimation from the diagram. The team used the analytical approach developed by Van-Aerde to calibrate the speed-flow relationship from the simulated data. Van Aerde's steady-state speed-flow model is a multivariate estimation procedure that provides better fits than other single-regime models (Van Aerde and Rakha, 1995). The capacity estimated is independent of the speed or density threshold between congested and non-congested states, which is needed in two-regime traffic flow models. The functional form of Van Aerde's model is expressed as:

$$d = \frac{1}{c_1 + \frac{c_2}{s_f - s} + c_3 s} \tag{4.1}$$

where d is the density (veh/km) or the inverse of the vehicle headway, s is speed (km/h), s_f is the free flow speed (km/h), c_1 is the fixed distance headway constant (km), c_2 is the first variable distance headway constant (km^2/h) and c_3 is the second variable distance headway constant (h^{-1}).

In this project, SPD_Cal software developed by Rakha (1995) is used for regressing the speed-flow curves from empirical data. The software uses an iterative numerical search technique proposed in Van Aerde and Rakha (1995) to determine capacity, free-flow speed, speed at capacity, and jam-density. The parameters in Equation (4.1) can then be determined by the following equations:

$$k = \frac{2s_c - s_f}{(s_c - s_f)^2} \tag{4.2}$$

$$c_2 = \frac{1}{d_j(k + 1/s_f)} \tag{4.3}$$

$$c_1 = kc_2 \tag{4.4}$$

$$c_3 = \frac{-c_1 + \frac{s_c}{v_c} - \frac{c_2}{s_f - s_c}}{s_c} \tag{4.5}$$

where s_c is speed at capacity (km/h), v_c is capacity (vph), and d_j is jam density.

4.3.2.2 Lane Change Intensity Calculation

In the simulation model, virtual sensors were configured on each GP lane starting from the ramp gore point all the way to the end of BOA. The sensors recorded aggregated volume by vehicle type, as well as speed within the designated time interval. Each set of sensors was set 200ft apart to collect aggregated data for the entire simulation period (one hour). Since the cross-weave flows were set as "ramp" vehicle type, sensors at each location could report the number of cross-weave vehicles present at that location. Using the algorithm described below, the number of lane changes conducted within each 200 ft segment was determined:

$$LCI_m = \sum_{i=1}^{n} i * (Vol_{m,i} - Vol_{m-1,i}) \qquad n = 2, 3 \text{ or } 4 \tag{4.6}$$

where LCI_m is the cross-weave lane change intensity of the m^{th} segment. Since each set of sensors is 200 ft apart, Vol_{m-1} represents the cross weave volume collected at the upstream 200ft away. i

is the lane index, labeled 1 for the right-most lane. For different lane configuration scenario (two-GP lane, three-GP lane or four-GP lane), the maximum lane index is different.

The profile of lane change intensity vs. distance can therefore describe within the specific distance, how many cross-weave lane changes have happened. The higher the *LCI*, the more disturbance will be generated to the GP segment.

Chapter 5 Empirical Study Results

This chapter presents the empirical analysis results for ML operational data gathered in this project. The data were obtained from sensors along instrumented ML facilities of several states in the U.S. Additionally, the team used calibrated micro-simulation models to supplement the data needed but were scarce or impractical to gather from field.

5.1 Slow Car Following Effect Validation

Video data were used to validate the presence of the slow car following effect on single lane ML facilities. The video data used in this process were from eastbound I-635 in Dallas, Texas. This ML facility is buffer-separated with a single HOV lane, or type Buffer 1. One hour of data were used from the hours 10:40 am to 11:40 am on March 21st, 2008. This time period represented light traffic conditions in both the GP lanes and the HOV lane. Under this situation, the assumption that no frictional effect from the GP lane was significantly degrading the speed of the HOV facility was valid.

To determine whether the slow car following effect could be observed on the facility, the presence of platoons on the HOV facility was analyzed. Platoons on the HOV facility were defined as a group of vehicles traveling closely together with car-following headways. These platoons were seen as the natural response of the traffic stream to a slow-moving vehicle. The first vehicle in the platoon would represent a slow-moving vehicle while the trailing vehicles were all vehicles that had been traveling at higher speeds until catching up to the slower-moving platoon.

The speed and number of vehicles in the platoon were recorded throughout the study period. Figure 16 below shows the study location on I-635. In Figure 16, a platoon of four vehicles can be observed in the HOV lane. The speed of the platoon was then calculated using time measurements and distance between light posts along the facility. Google Earth was used in determining the distance between light posts. Ninety-six (96) data samples were collected throughout the hour. Each sample consisted of the number of vehicles in the platoon and the corresponding speed.

FIGURE 16 Snap Shot of Platoon Effect from Video Data at I-635, Dallas, Texas (Source: University of Texas at Arlington)

To determine whether there is a significant difference in speeds between vehicles traveling in the platoons and those traveling alone, a t-test was conducted (Table 13). The speed of the group with solo vehicles was compared to the speed of the vehicles in a platoon. The number of vehicles in the platoon was not considered for the t-test, as platoons of all sizes were grouped together. It is shown that the speed of single vehicles is significantly greater than that of the platoon vehicles at 99% confidence level. This verifies that slow-moving lead vehicles affect the speed of the platoon they inherently create. In addition to verifying that single lane facilities experience a slow car-following phenomenon, the speed for platoons of different sizes can also be examined. Figure 17 shows a clear relationship between platoon size and speed. The R^2 for the linear regression is 0.7203, which indicates that it is reasonable to use the linear relationship to describe the correlation between them. The linear fit shows that the greater the number of vehicles in the platoon, the lower the speed of the platoon.

TABLE 13 t-Test Results for Slow Car Following Effect

	Single Vehicles	Platooned Vehicles
Observations	39	57
Mean (mph)	70.83	67.43
Variance	15.76	9.18
t-Statistic	4.76	
P value	0.00	

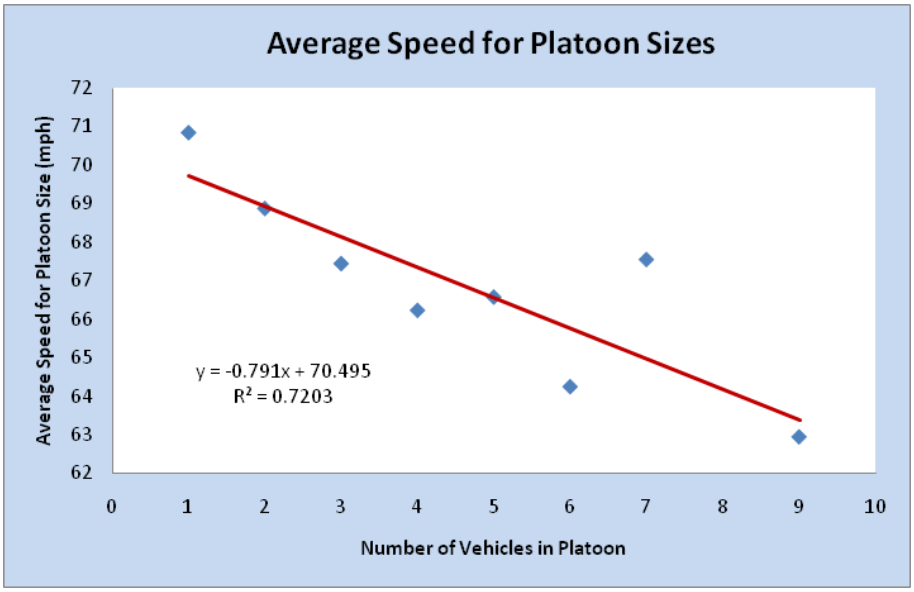

FIGURE 17 Relationship Between Average Speed vs. Platoon Size

Two conclusions can then be drawn from this relationship. First, the slower the leading vehicle is traveling, the greater the effect it will have on the single-lane ML system. More vehicles will experience a reduction in speed when the platoon is traveling at lower speeds. This also leads to the second point. There is a greater drop in the speed of the system as volume increases. With volumes increase, the chance that more vehicles will be experiencing the effects of the slow moving vehicles increases. These observations verify that the degradation in speed on single lane ML facilities can be a direct consequence of the slow car following effect. As the flow rate of the HOV lane increases, both the number of slow-moving vehicles and the number of vehicles got affected by the slow-moving vehicle increase. This slow car-following effect needs to be implemented into the formation of the speed flow curves for MLs.

5.2 Results and Discussion of Speed-Flow Curves

5.2.1 Continuous Access

Unlike any other separation type, in Continuous Access, ML users are able to move freely between the ML and GP lanes. Although Continuous Access separation may consist of only one ML, users are not subject to the same effects of slower drivers as in other single-lane ML facilities. Continuous Access users have some ability to change into the adjacent GP lane and pass slower vehicles. The ML user's ability to make this maneuver is, however, dependent on the performance of the adjacent GP lane. When the GP facility is congested, ML users are unable to pass slower moving vehicles. Slower speeds and fewer lane changing opportunities prevent ML vehicles from overtaking the slow moving vehicles.

During this congested period on the GP lanes, a frictional effect can be observed. ML users drive at slower speeds when adjacent GP traffic is congested. Drivers tend to drive more cautiously due

to their proximity to a dense stream of slowly moving vehicles. ML drivers are also aware that GP vehicles can enter the ML at any point at relatively low speeds, increasing their tendency to operate the vehicles at a slower speed. Figure 18 shows the speed-flow relationships for each FFS for the continuous access type for each FFS. Non-friction curves are shown as solid lines, while the corresponding friction curves are shown as dashed lines.

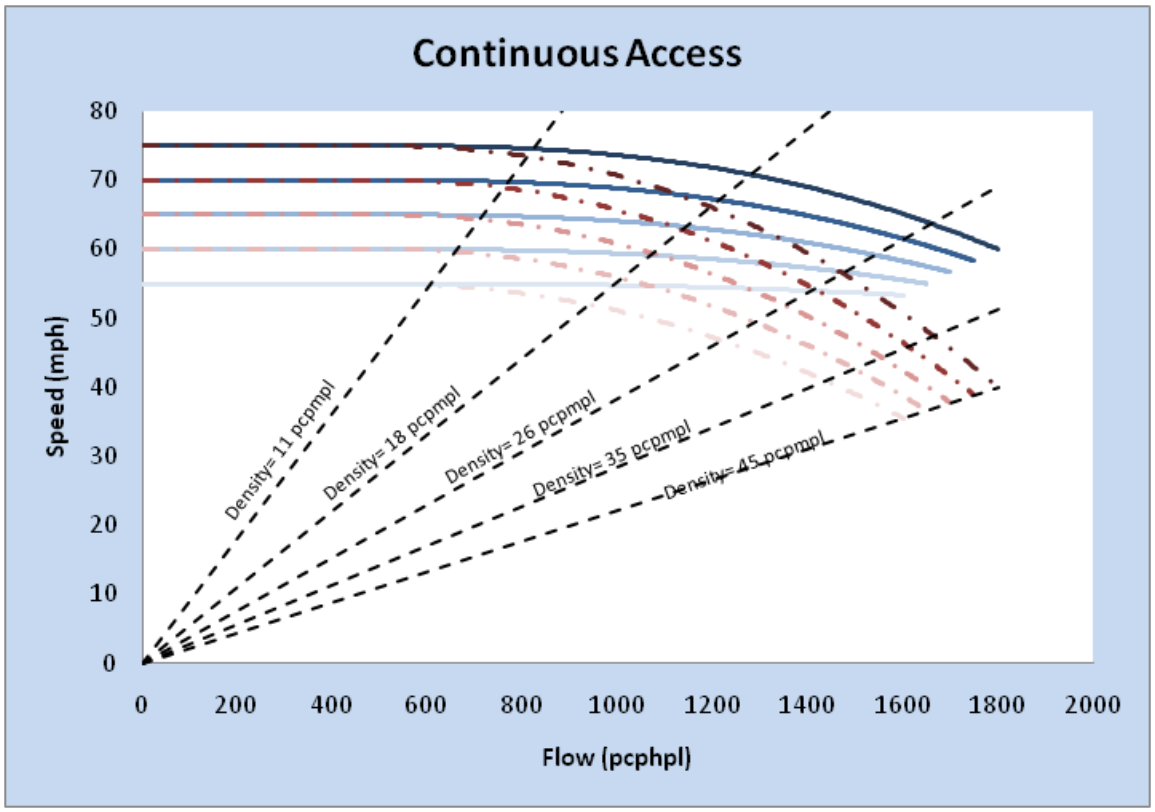

FIGURE 18 Continuous Access Speed-Flow Curves

Table 14 provides the variables used for the formation of the non-friction and friction speed-flow curves, respectively. Table 15 provides the speed-flow equations for the Continuous Access segments. It should be noted here that the friction curves terminate at a density of 45 pcpmpl, which is consistent with the methodology used in HCM 2010. The range of observed data for the non-friction curves never reached such high density levels, probably attributable to a low likelihood of observing non-friction cases in combination with high flow rates. As a result, the terminal density of the non-friction curves is 30 pcpmpl. Consequently, the points corresponding to maximum observed flow rates in Table 14 (a) occur at a density of 30 pcpmpl, while the Table 14 (b) flow rates occur at the higher HCM LOS=F density of 45 pcpmpl. The common density principle was upheld also for all other speed-flow curves in accordance with HCM 2010.

TABLE 14 (a) Continuous Access Non-Friction Curve Values

FFS (mph)	Capacity (pcphpl)	Speed @ Capacity (mph)	Breakpoint (pcphpl)	C_2	R^2
55	1600	53.33	500	2.5	-
60	1650	55.00	500	2.5	0.1856
65	1700	56.67	500	2.5	0.0624
70	1750	58.33	500	2.5	0.0967
75	1800	60	500	2.5	0.0176

Note: Refers to Equations (3.1) and (3.2)

TABLE 14 (b) Continuous Access Friction Curve Values

FFS (mph)	Capacity (pcphpl)	Speed @ Capacity (mph)	C_f	R^2
55	1600	35.56	1.47×10^{-5}	-
60	1650	36.67	1.39×10^{-5}	0.2224
65	1700	37.78	1.31×10^{-5}	0.3388
70	1750	38.89	1.24×10^{-5}	0.3515
75	1800	40.00	1.18×10^{-5}	0.3698

Note: Refers to Equations (3.3)

TABLE 15 Speed-Flow Equations for Continuous Access

	Flow Rate Range	
FFS (mph)	**0 - 500 pc/hr/ln**	**500 pc/hr/ln - Max. Flow***
75	75	$75 - (2.46 \times 10^{-7}(v_p\text{-}500)^{2.5}) - (0/1)(1.18 \times 10^{-5}\ (v_p\text{-}500)^2)$
70	70	$70 - (2.12 \times 10^{-7}(v_p\text{-}500)^{2.5}) - (0/1))1.24 \times 10^{-5}\ (v_p\text{-}500)^2)$
65	65	$65 - (1.67\times 10^{-7}(v_p\text{-}500)^{2.5}) - (0/1)(1.31 \times 10^{-5}\ (v_p\text{-}500)^2)$
60	60	$60 - (1.12\times 10^{-7}(v_p\text{-}500)^{2.5}) - (0/1)(1.39 \times 10^{-5}\ (v_p\text{-}500)^2)$
55	55	$55 - (4.15\times 10^{-8}(v_p\text{-}500)^{2.5}) - (0/1)(1.47 \times 10^{-5}\ (v_p\text{-}500)^2)$

*(0/1) represents values for non-friction (0) and friction (1) curves, respectively

5.2.2 Buffer 1

Users of Buffer 1 ML facilities are subject to slow vehicle following and also the frictional effect from the adjacent congested GP facility. In being subject to a slow car following effect, the flat section of the left side of the curve is replaced with a tilt line sloping down slightly.

The data sites used for the formation of Buffer 1 come from three different facilities: I-405 in Los Angeles, California, SR-167 in King County, Washington, and I-394 in Minneapolis, Minnesota. Of the eleven sites used, three held an FFS of 70 mph and eight held an FFS of 65 mph. FFS's of 55, 60, and 75 mph were not represented. The curves for the three unrepresented FFS's were determined from extrapolation.

Figure 19 shows an example of the regressed curves over the data corresponding to an FFS of 65 mph. Figure 20 shows the set of curves.

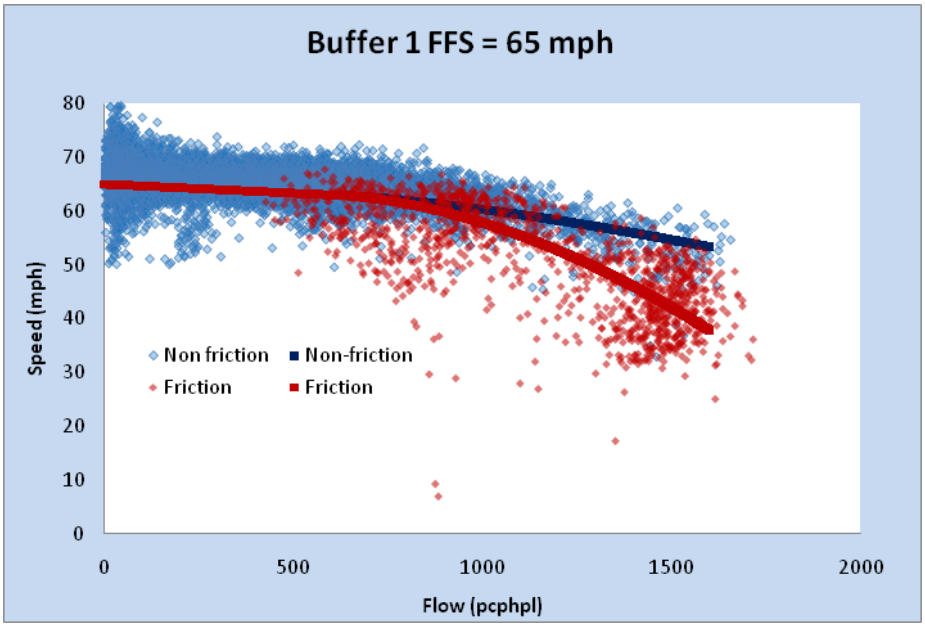

FIGURE 19 Buffer 1 Data for FFS=65 mph

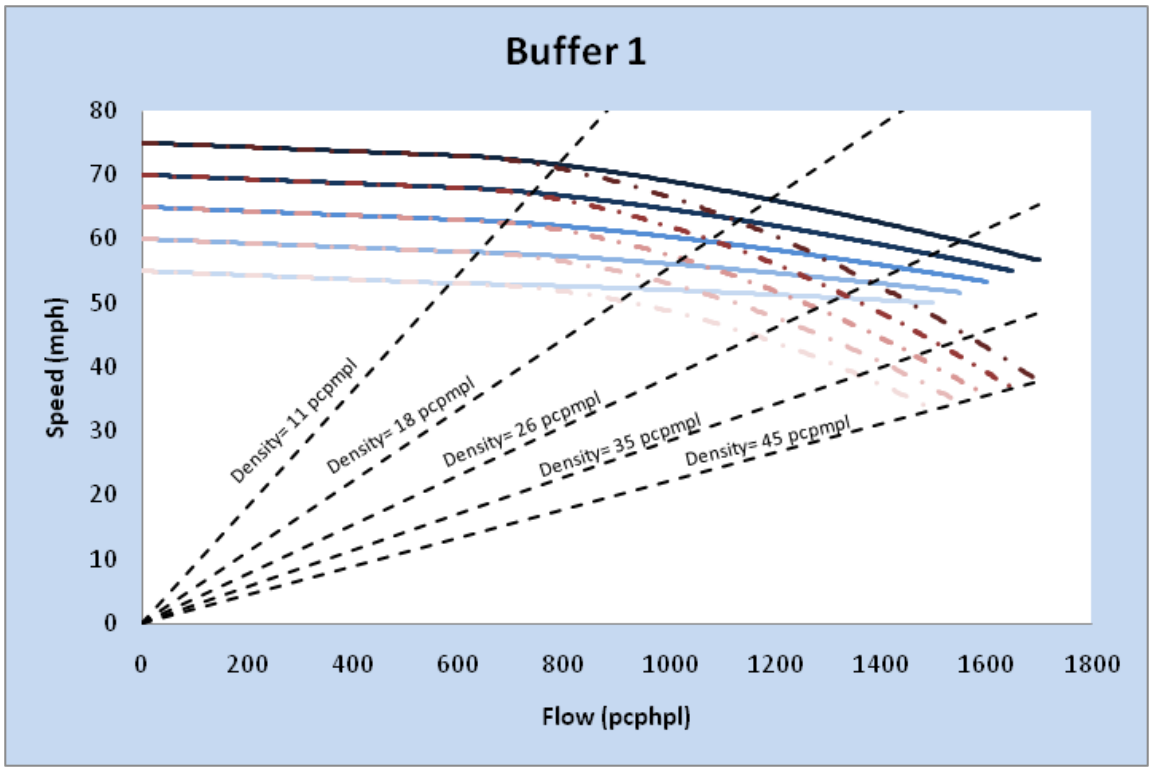

FIGURE 20 Buffer 1 Speed-Flow Curves

Tables 16 (a) and 16 (b) provide the variables used for the forming of the non-frictional and frictional speed-flow curves, respectively. Table 17 provides the speed-flow equations for the Buffer 1 segments. As with the Continuous Access curves, the non-friction curves terminate at a density of 30 pcpmpl as higher densities were not observed during periods of time where the GP lane was not congested. The set of friction curves terminates at a density of 45 pcpmpl.

TABLE 16 (a) Buffer 1 Non-Friction Speed-Flow Values

FFS (mph)	Capacity (pcphpl)	Speed @ Capacity (mph)	C_1	Breakpoint (pcphpl)	Speed @ BP_1	C_2	R^2
55	1500	50.00	0.0033	600	53	1.4	-
60	1550	51.67	0.0033	600	58	1.4	-
65	1600	53.33	0.0033	600	63	1.4	0.349
70	1650	55.00	0.0033	600	68	1.4	0.143
75	1700	56.67	0.0033	600	73	1.4	-

Note: Refers to Equations (3.1) and (3.2)

TABLE 16 (b) Buffer 1 Friction Speed Flow Values

FFS (mph)	Capacity (pcphpl)	Speed @ Capacity (mph)	C_f	R^2
55	1500	36.67	1.65×10^{-5}	-
60	1550	36.67	1.66×10^{-5}	-
65	1600	37.78	1.56×10^{-5}	0.5129
70	1650	38.89	1.46×10^{-5}	0.2294
75	1700	40.00	1.38×10^{-5}	-

Note: Refers to Equations (3.3)

TABLE 17 Buffer 1 Speed-Flow Equations

	Flow Rate Range	
FFS (mph)	**0 - 600 pc/hr/ln**	**600 pc/hr/ln – Max. Flow***
75	$75 - .00333(v_p)$	$73 - 0.00090(v_p\text{-}600)^{1.4} - (0/1)(1.38 \times 10^{-5} (v_p\text{-}600)^2)$
70	$70 - .00333(v_p)$	$68 - 0.00077(v_p\text{-}600)^{1.4} - (0/1)(1.46 \times 10^{-5} (v_p\text{-}600)^2)$
65	$65 - .00333(v_p)$	$63 - 0.00061(v_p\text{-}600)^{1.4} - (0/1)(1.56 \times 10^{-5} (v_p\text{-}600)^2)$
60	$60 - .00333(v_p)$	$58 - 0.00043(v_p\text{-}600)^{1.4} - (0/1)(1.66 \times 10^{-5} (v_p\text{-}600)^2)$
55	$55 - .00333(v_p)$	$53 - 0.00022(v_p\text{-}600)^{1.4} - (0/1)(1.65 \times 10^{-5} (v_p\text{-}600)^2)$

*(0/1) represents values for non-friction (0) and friction (1) curves, respectively

5.2.3 Buffer 2

As a slow car following effect and frictional effect were not observed in Buffer 2's small data set, only one curve is produced for each FFS. While it is somewhat intuitive to believe the buffer

separated nature of the facility is susceptible to some influence from the GP lanes, none was observed in the two study sites used in this project.

Figure 21 shows the FFS 65 mph speed flow curve overlapping the corresponding data. Figure 22 shows the family of speed-flow curves for Buffer 2.

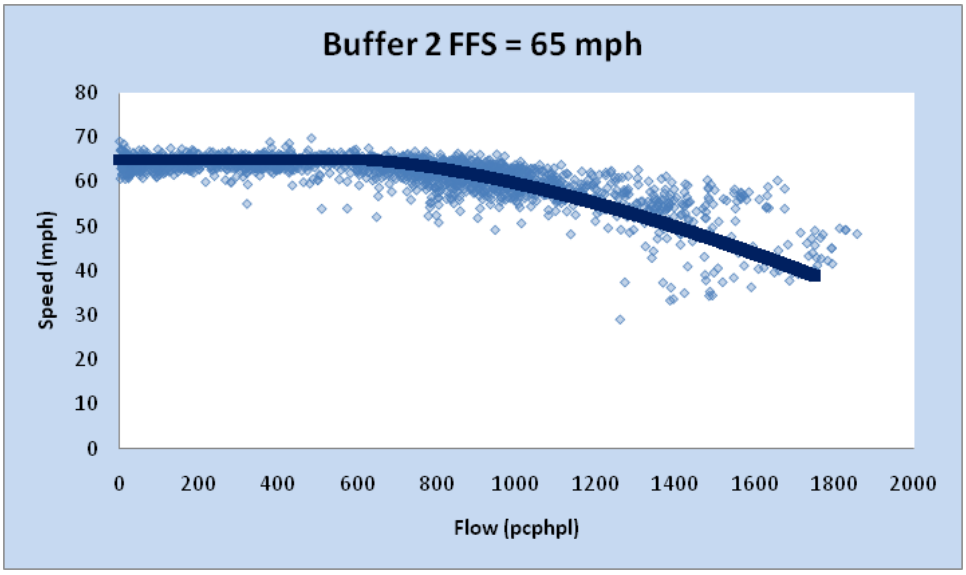

FIGURE 21 Buffer 2 Data with Speed-Flow Curve for FFS = 65 mph

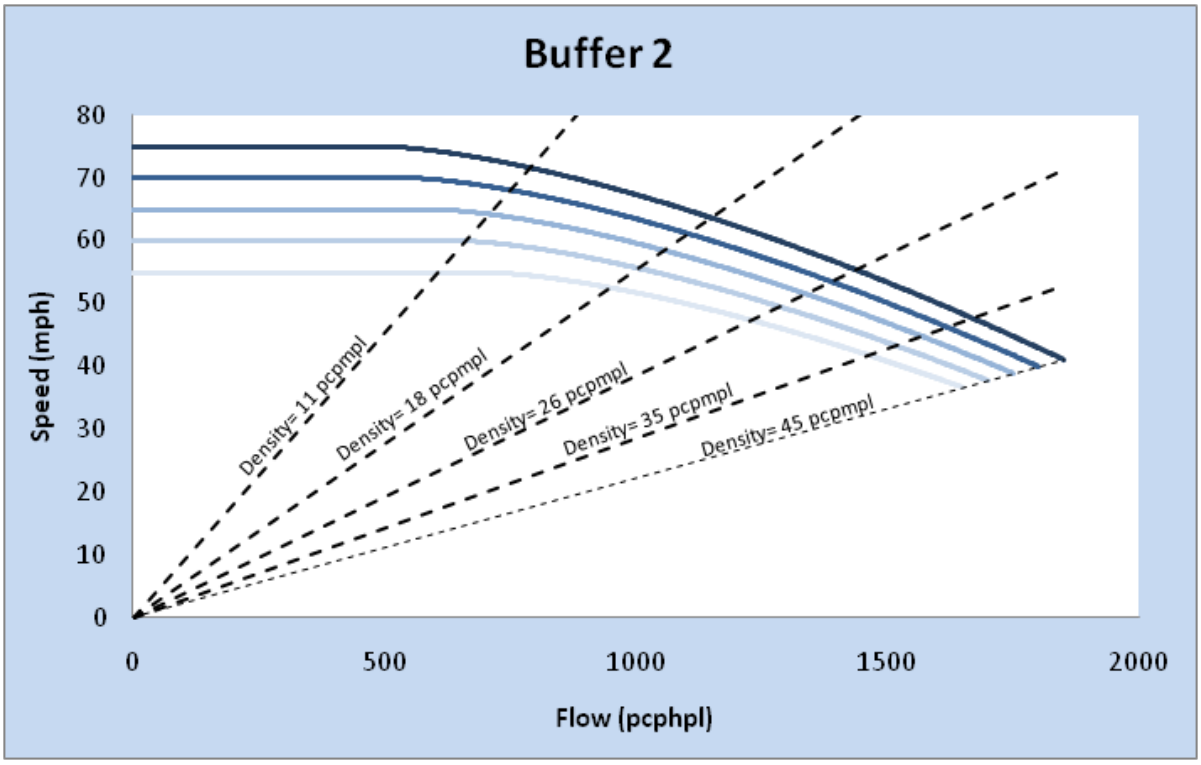

FIGURE 22 Buffer 2 Speed Flow Curves

Table 18 provides the variables used for the forming of the Buffer 2 speed-flow curves. Table 19 shows the speed-flow equations for the Buffer 2 segments. With only one site's worth of data for the 65 mph FFS curve and 70 mph FFS curve, these curves must be considered preliminary and used with caution. As no frictional impact was observed and the multiple lanes of the facility should prevent or minimize the effects of slow car following, the early drop in speed and lower capacity is difficult to understand. If possible more sites with this geometry should be investigated.

TABLE 18 Buffer 2 Speed-Flow Curve Variable Values

FFS (mph)	Capacity (pcphpl)	Speed @ Capacity (mph)	Breakpoint (pcphpl)	C_2	R^2
55	1650	36.67	700	1.5	-
60	1700	37.78	650	1.5	-
65	1750	38.89	600	1.5	0.6655
70	1800	40.00	550	1.5	0.2930
75	1850	41.11	500	1.5	-

Note: Refers to Equations (3.1) and (3.2)

TABLE 19 Buffer 2 Speed-Flow Equations

	Flow Rate Range	
FFS (mph)	**0 – Breakpoint pc/hr/ln**	**Breakpoint – Max Flow pc/hr/ln**
75	75	$75 - 0.000683(v_p-500)^{1.5}$
70	70	$70 - 0.000679(v_p-550)^{1.5}$
65	65	$65 - 0.000670(v_p-600)^{1.5}$
60	60	$60 - 0.000653(v_p-650)^{1.5}$
55	55	$55 - 0.000626(v_p-700)^{1.5}$

5.2.4 Barrier 1

The slow car following effect can be observed in Barrier 1 separation type. Therefore, the left side of the speed-flow relationship is sloped from a flow rate of 0 to that of the breakpoint. The presence of the barrier eliminates the frictional impact from the GP lanes, so only a single curve is used for each FFS.

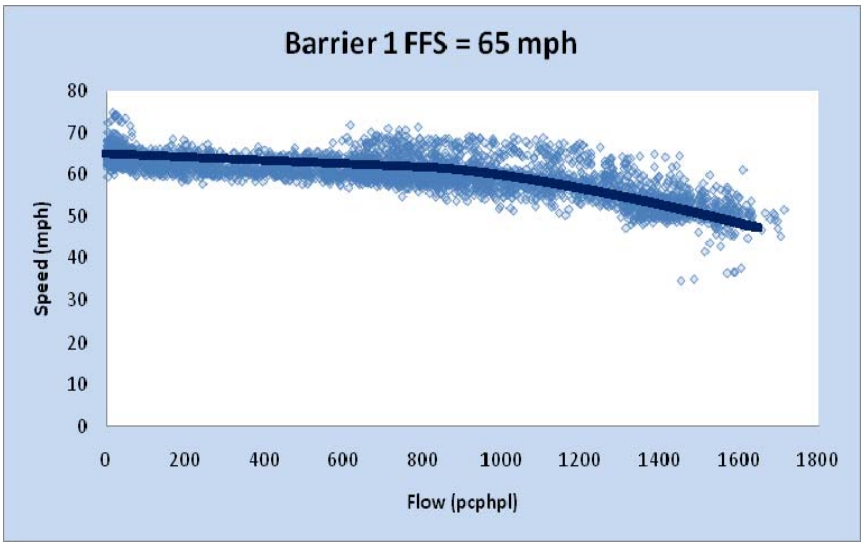

FIGURE 23 Barrier 1 Data and Speed-Flow Curve for FFS = 65 mph

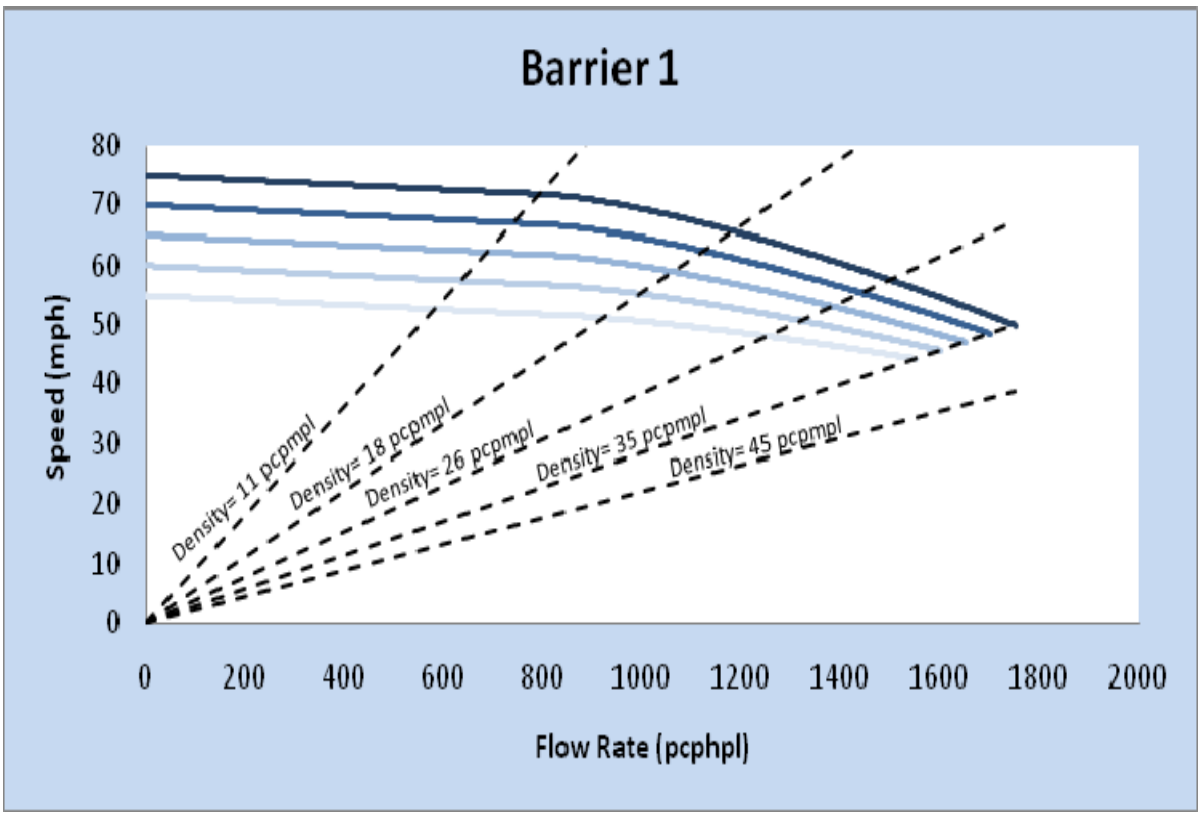

FIGURE 24 Barrier 1 Speed-Flow Curve

Table 20 provides the variables used for the formation of Barrier 1 speed-flow curves. Table 21 shows the speed-flow equations for the Barrier 1 segments. While the curves for other facility types terminate at a density of 45 pcpmpl, the breakdown for Barrier 1 facilities was observed to occur at a lower density. The termination point for the Barrier 1 speed-flow curves was

determined to be 35 pcpmpl. This lower density at the point of flow breakdown could be attributed to barrier impact of this type of facility. As barriers are present on one or both sides of the facility, there is little room for a following vehicle driver to maneuver. Should a vehicle brake, the trailing vehicle that follows the leading vehicle closely has to brake harder to avoid a possible rear-end collision because the driver does not have the option of swerving to the right or left. The reduction in headway would cause breakdown at a lower density.

TABLE 20 Barrier 1 Speed-flow Curve Variable Values

FFS (mph)	Capacity (pcphpl)	Speed @ Capacity (mph)	C_1	Breakpoint (pcphpl)	Speed @ Breakpoint (mph)	C_2	R^2
55	1550	44.29	0.004	800	51.8	1.4	-
60	1600	45.71	0.004	800	56.8	1.4	0.619
65	1650	47.14	0.004	800	61.8	1.4	0.625
70	1700	48.57	0.004	800	66.8	1.4	-
75	1750	50	0.004	800	71.8	1.4	-

Note: Refers to Equations (3.1) and (3.2)

TABLE 21 Barrier 1 Speed-Flow Equations

	Flow Rate Range	
FFS (mph)	**0 - Breakpoint pc/hr/ln**	**Breakpoint – Max. Flow (pc/hr/ln)**
75	$75-(0.004v_p)$	$71.8 - 00148(v_p-800)^{1.4}$
70	$70-(0.004v_p)$	$66.8 - 0.00133(v_p-800)^{1.4}$
65	$65-(0.004v_p)$	$61.8 - 0.00116(v_p-800)^{1.4}$
60	$60-(0.004v_p)$	$56.8 - 0.00096(v_p-800)^{1.4}$
55	$55-(0.004v_p)$	$51.8 - 0.00071(v_p-800)^{1.4}$

5.2.5 Barrier 2

The Barrier 2 speed-flow curve is more similar to that of a basic freeway segment than any other ML types. It can essentially be thought of as its own independent facility as there is no slow car following or frictional effect. All Barrier 2 study sites were found operating well below capacity. As shown in Figure 25, the maximum observed volume was about 1,500 pcphpl. This makes it challenging to determine the capacity of this segment type. Engineering judgment was ultimately used in determining the maximum flow rate for the development of the speed-flow curves based on the experience of basic freeway segments.

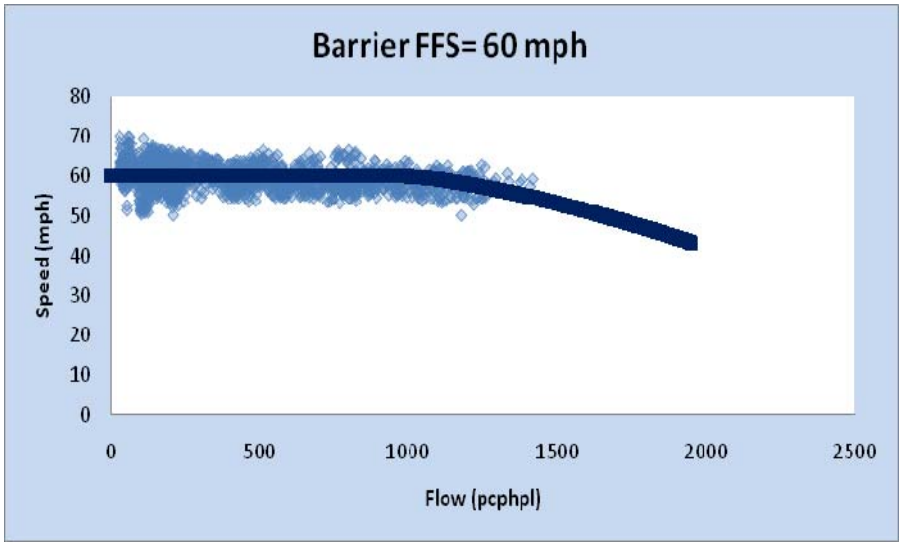

FIGURE 25 Barrier 2 Data and Speed-Flow Curve for FFS = 60 mph

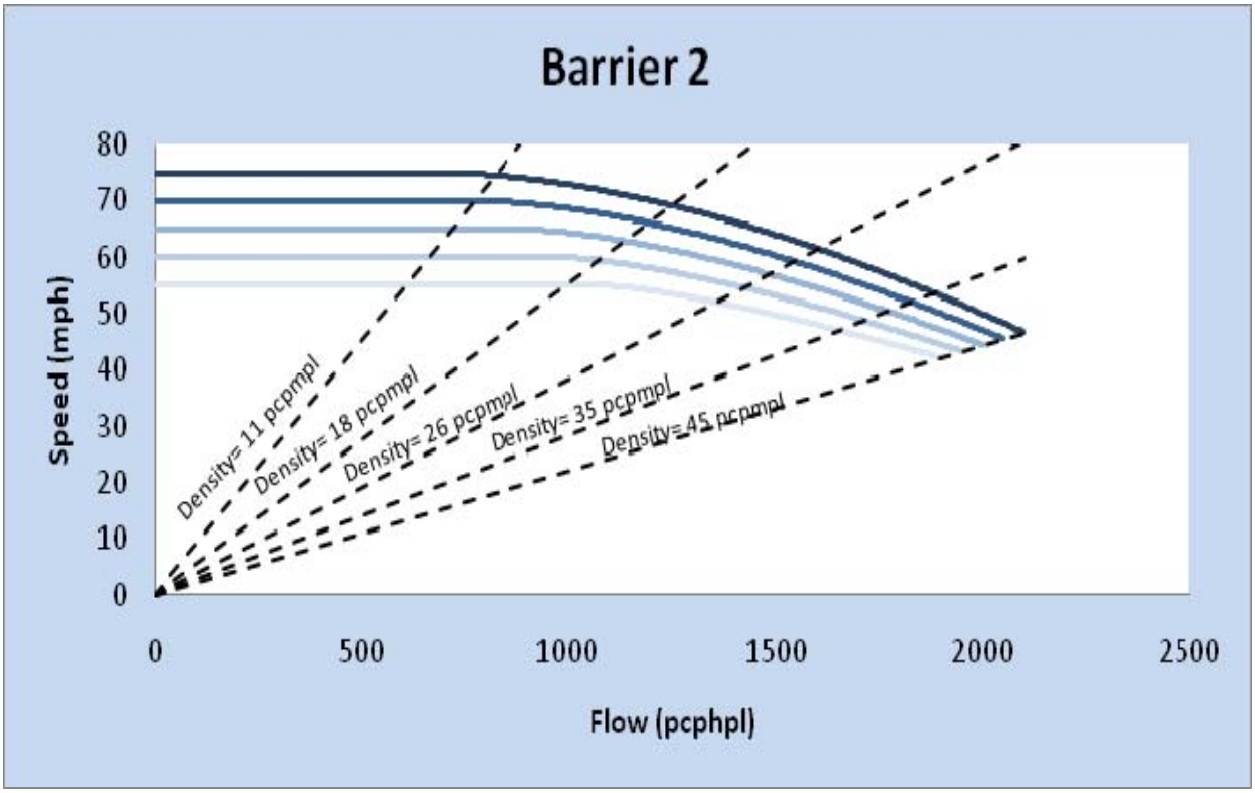

FIGURE 26 Barrier 2 Speed-Flow Curves

Table 22 lists the variables used for the formation of Barrier 2 speed-flow curves. Table 23 provides the speed-flow equations for the Barrier 2 segments.

TABLE 22 Barrier 2 Speed-Flow Curve Variable Values

FFS (mph)	Capacity (pcphpl)	Speed @ Capacity (mph)	Breakpoint (pcphpl)	C^2	R^2
55	1900	42.22	1100	1.3	-
60	1950	43.33	1000	1.4	0.0273
65	2000	44.44	900	1.5	0.1461
70	2050	45.56	800	1.6	0.0541
75	2100	46.67	700	1.7	-

Note: Refers to Equations (3.1) and (3.2)

TABLE 23 Barrier 2 Speed Flow Equations

	Flow Rate Range	
FFS (mph)	**0 - BP pc/hr/ln**	**BP pc/hr/ln - Max. Flow**
75	75	$75 - (0.000127(v_p-700)^{1.7})$
70	70	$70 - (0.000271(v_p-800)^{1.6})$
65	65	$65 - (0.000563(v_p-900)^{1.5})$
60	60	$60 - (0.00113(v_p-1000)^{1.4})$
55	55	$55 - (0.00215(v_p-1100)^{1.3})$

5.2.6 Comparison of Speed-Flow Models amongst Different Basic ML Types

Figure 27 uses FFS =60 mph as an example across the five segment types. For those segment types where frictional effect would be present, two sets of curves were developed for each FFS under friction and non-friction scenarios. Each curve consisted of two parts: a linear portion stretching from zero flow to the breakpoint, and a curvilinear portion from the breakpoint to the maximum observed flow. For single lane facilities where passing is prohibited, the linear portion was sloped downward due to the slow moving vehicle effect. For other segment types, the linear portion had a slope of zero remaining at the FFS until the breakpoint. Breakpoints were estimated by calculating the standard deviation of speed for each volume range of 100 pcphpl. The breakpoints were then determined at the volume where the speed standard deviation begins to increase abruptly.

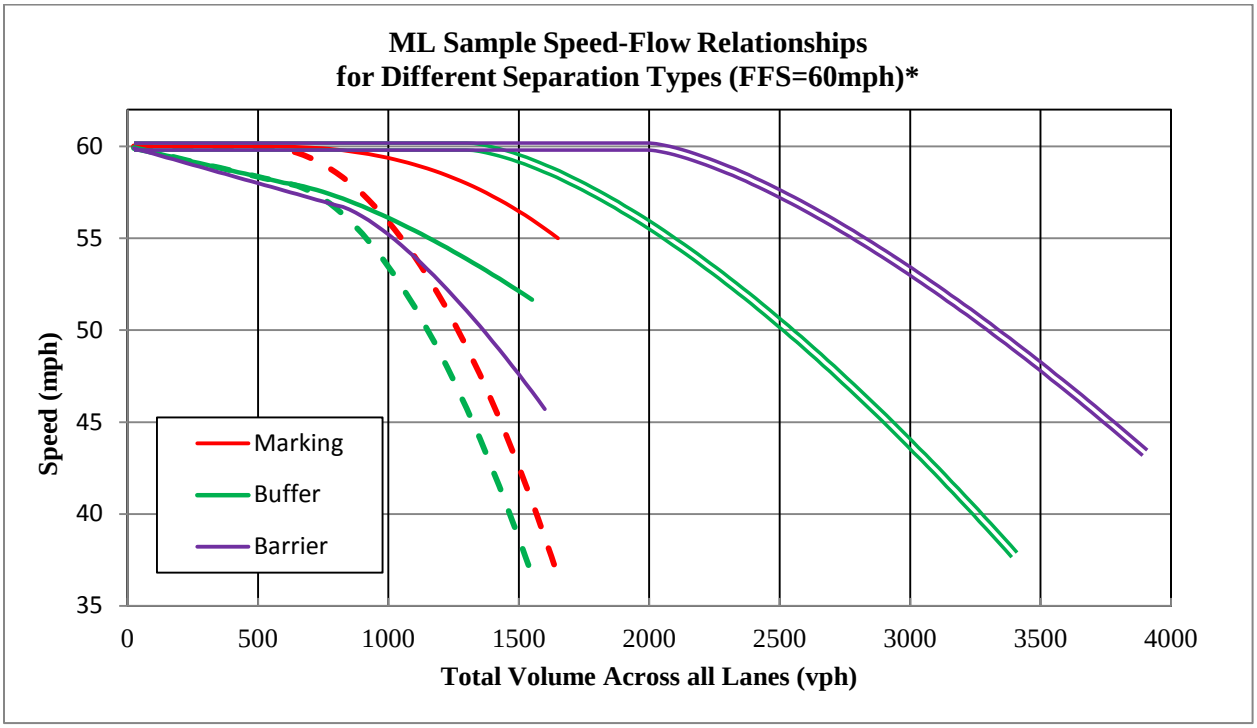

* Single lines refer to one-lane ML facilities, double lines to two-lane ML facilities; dashed lines correspond to the speed-flow relationship under *friction effect* conditions

FIGURE 27 Sample ML Speed-Flow Relationships for FFS=60mph

For single lane ML facilities separated by buffer or barrier, vehicles are unable to perform passing maneuvers. As a result, the linear portion of the curve has a negative slope even at a low volume. This initial slope of the curve can be attributed to the fact that slow-moving vehicles cannot be passed as they would have been able to in facilities with multiple lanes. The overall speed of a platoon on such a facility is then dictated by the speed of the slower vehicle.

As described earlier, the performance of the Continuous Access and Buffer 1 facilities is dependent not only on the characteristics of the ML but also on the performance of the adjacent GP facility. For these two ML strategies, a second, frictional curve (dashed line) has been produced showing the speed-flow relationship for periods of time during GP congestion. The frictional curve is a function of both the non-friction curve and the flow rate. For two-lane ML facilities, the buffer-separated facility shows an earlier drop in the speed-flow curve compared to the barrier-separated facility. No stripe-separated two-lane ML facilities were field observable.

5.3 Simulation Results and Analysis for the Cross-Weave Effect

5.3.1 Simulation Model Calibration

Simulation model calibration is crucial for realistic representations of simulated scenarios as well as reliable outputs. Calibration efforts are therefore required to ensure that the model output can replicate the observed field data. Driving behavior parameters need to be adjusted during the

process to match the outputs with field conditions. Field data were collected at one access point along IH 635 in Dallas, Texas. The lane configuration sketch is shown in Figure 28. There are four GP lanes and one buffer-separated ML in the westbound direction of the IH 635. The data collection site is located just west of Midway Road entrance ramp. The ML is an HOV-2 lane. The ML is separated from the GP lanes by a double white line buffer, and it is illegal to cross the line. At the BOA (shown in Figure 28), the separation marking changes to dashed lines, and vehicles can ingress/egress to the ML. The BOA is 1,160 ft at this site and $L_{CW\text{-}Min}$ is 0 ft, which indicates that the opening starts immediately at the GP on-ramp. Cross-weave movements occur at this location as well, with ML-targeting vehicles coming from the Midway on-ramp needing to weave across multiple GP lanes to access the ML. In most designs, $L_{CW\text{-}Min}$ is often too long to be completely covered by one freeway surveillance camera. This makes it very difficult to observe lane changing behaviors of the cross-weave vehicles, although they are essential for simulation model calibration. However, the IH 635 site shown in Figure 28 has an unusual on-ramp position which is very close to the beginning point of the BOA. This configuration made it possible to capture the entire freeway segment with one video camera placed on a downstream overpass (Figure 29 shows a snapshot from the camera). Cross-weave maneuvers were therefore extracted from the data for calibrating the model.

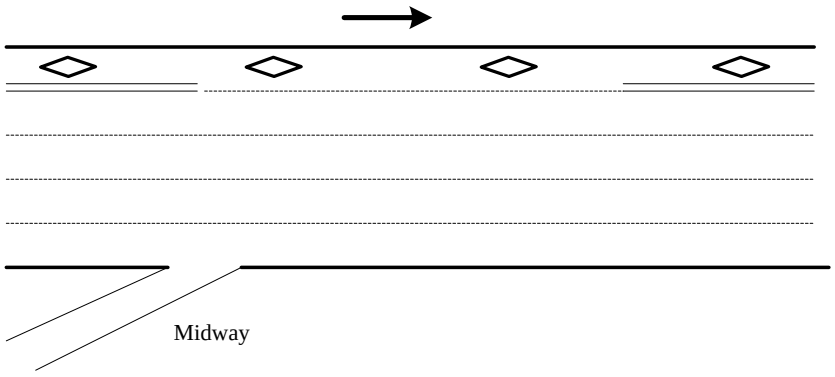

FIGURE 28 Lane Configuration of the ML Access Point at IH 635 Dallas, Texas

FIGURE 29 Video Image for IH 635 ML Access Point

Two 1-hour video recordings were evaluated for this location. The first dataset was during moderate traffic conditions on March 14, 2008 between 10:20 to 11:20 AM. The second dataset was collected during the high-volume afternoon peak period between 3:25 to 4:25 PM. For each dataset, origin-destination flows were extracted as well as the actual speed and the spatial distribution of lane changes. A VISSIM simulation model was developed for this site with many virtual sensors deployed across lanes and over the entire segment for data collection and comparison purposes. The model was carefully calibrated based on the field observed speed and total lane changing activities. The spatial distribution of lane changes in the field was collected by a research team at the University of Texas at Arlington and was used for model calibration. The data consisted of the longitudinal location of each lane change from the GP lanes to the ML. The BOA was divided into 100-foot zones. The number of vehicles that changed lanes to the ML within each zone was collected for comparing with the simulated data for calibration. The detailed field data processing is described in Williams *et al.* (2010). Driver behavior parameters were adjusted through an iterative process until the difference from the reference data is relatively small (less than 10%). Several major parameters are adjusted according to the observed field data, including standstill distance, time headway, and maximum deceleration for lane changing. Also, other parameters, such as look back distance are modified individually for weaving areas. The detailed calibration process is described in Appendix A of this report.

5.3.2 Simulation Scenario Setup

Different simulation scenarios were designed to test the cross-weave effect. The simulation network consists of a one-lane on-ramp and a multi-lane GP section. A BOA was set in the downstream section of the GP lane on-ramp to allow vehicle ingress/egress to the ML. To capture the effect of queues that formed on the APIA and to ensure adequate storage for entering demands, long approach links upstream of the entrance ramp were coded on the freeway mainline. Likewise, to ensure that the freeway traffic had adequate time to recover after clearing the

weaving area, the link downstream of the access point opening area was also set sufficiently long. The configuration used in the simulation is shown in Figure 30.

One of the factors that varied significantly in the experimental design was the length of $L_{CW\text{-}Min}$ and $L_{CW\text{-}Max}$. Several combinations of the factors were identified from field data, and listed in Table 24. The design length for a BOA normally ranges between 1,300 ft and 2,000 ft. The simulation experiments used 1500 ft for the BOA for all cases and three different $L_{CW\text{-}Min}$ lengths (Case 1: 1,500 ft; Case 2: 2,000 ft; Case 3: 2,500 ft) to examine the impacts of $L_{CW\text{-}Min}$ on cross-weave behavior.

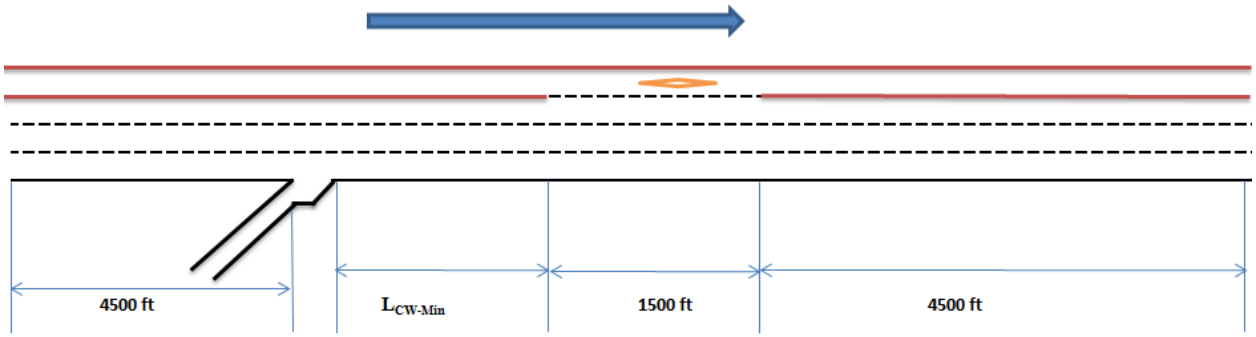

FIGURE 30 Configuration Used in VISSIM Simulation

TABLE 24 Field Data Reference for $L_{CW\text{-}Min}$ and $L_{CW\text{-}Max}$

Facility Name	$L_{CW\text{-}Min}$ (ft)	$L_{CW\text{-}Max}$ (ft)	Buffer Opening Area (ft)
I-394 EB, Minneapolis, Minnesota	2737	5082	2345
	2278	4623	2345
	1500	2984	1484
	2095	3577	1482
	2240	3722	1482
I-394 WB, Minneapolis, Minnesota	415	4044	3629
	2029	3226	1197
	1710	2907	1197
	3484	6462	2978
SR 167 NB, Seattle, Washington	2008	3460	1452
	2982	4434	1452
	2302	3798	1496
	2432	3928	1496
	2474	3951	1477
	4814	6191	1377
SR 167 SB, Seattle, Washington	3386	4842	1456
	4213	5669	1456
	3757	5304	1547
	2041	3588	1547
	2101	3593	1492
	2688	4180	1492

The cross-weave intensity is postulated to be a function of the number of necessary lane changes, the cross-weave demand, and the surrounding GP traffic. Therefore, when evaluating its operational impact on the GP lanes, various traffic demands on both the GP on-ramp and the approaching GP lanes need to be tested in the simulation experiment. GP lane demand varied from 1,600 pcphpl to 2,400 pcphpl in 100 pcphpl increments. Cross-weave demand from the GP on-ramp to the ML was tested for five different levels (100, 200, 300, 450 and 600 pcphpl). Three GP lane configurations (two-lane, three-lane and four-lane) were tested. The full sets of simulations were run without considering truck volume.

In the test scenario simulation model, virtual sensors were deployed in all GP lanes starting at the ramp gore point and continuing through the end of the BOA to collect average speed and volume across all GP lanes. A spacing of 200 ft was configured between each set of sensors. Different vehicle types were also configured in the simulation model with the cross-weave flows labeled as "ramp". Therefore, the sensors could capture the frequency of each vehicle type at the cross section every 200 ft apart on a lane-by-lane basis. Lane change intensity could then be calculated at various points in the segment. Also within the GP segment before the BOA, the capacity reduction of the GP segment due to the cross-weave volume needs to be estimated. To achieve this, link evaluation was performed for the GP segment at a spacing of 500 feet. In other words, speed-flow-density data for the GP segment are aggregated in 500-foot segments. By regressing from the speed-flow curves using the link evaluation output, the capacity for each scenario could be determined and the Capacity Reduction Factor (CRF)/Capacity Adjustment Factor (CAF) for various configurations can be estimated as well.

In VISSIM, traffic generation depends on the random seed number to use. By employing different random seeds, simulation results change due to the stochastic nature of the underlying algorithms. To capture this stochastic variability, multiple simulation runs for each scenario are necessary. Therefore, for each scenario, three different random seeds were selected, which sufficiently increased the sample of speed-flow data points. The integrated results from these simulation runs are considered reliable and unbiased, and are consistent with what an agency may obtain in the field from sensor data.

5.3.3 Simulation Result Analysis

From the simulation, traffic volumes and speeds were collected within the segment every 500 ft apart in 15-minute increment. The speed-flow diagram can be drawn correspondingly and Van Aerde's curve fitting can be performed to determine the capacity of the GP segment (Van Aerde and Rakha, 1995). Figure 31 shows the speed-flow diagram for the four-lane GP scenarios with $L_{CW\text{-}Min}$ =1,500 ft, and cross-weave volumes ranging from 100 pcph to 600 pcph. Within each cross-weave setting, the GP mainline demand changes from 1,600 pcphpl to 2,400 pcphpl, such that a set of complete data points could be collected from the simulation.

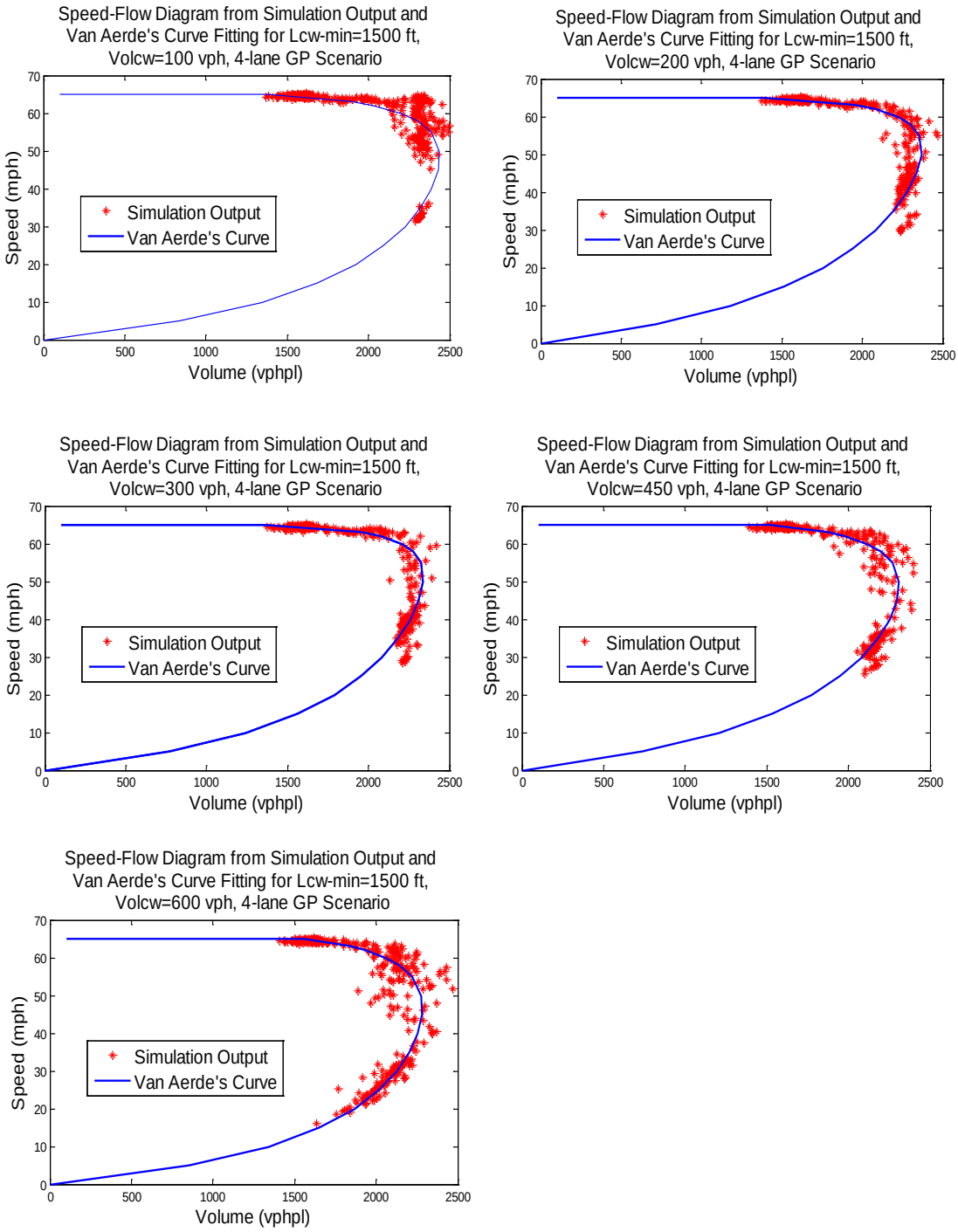

FIGURE 31 Speed-Flow Diagrams from Simulation Output and Van Aerde's Curve Fitting for 4-lane GP scenarios

A base scenario with no cross-weave flow was analyzed. The capacity from the Van Aerde's regression is calculated to be 2450 pcphpl, which is only slightly higher than the HCM 2010 freeway capacity for a 70 mph free-flow speed and is considered an acceptable match with the HCM. The remaining scenarios with varying cross-weave demands expectedly resulted in lower

capacities relative to the base. The CRF therefore can be expressed as a function of the base capacity C_{base} and the cross-weave capacity C_{cw} in Equation (5.1). Correspondingly, the CAF used in the HCM 2010 freeway facility chapter can be calculated as formulated in Equation (5.2).

$$CRF = \frac{C_{base} - C_{cw}}{C_{base}} \times 100\% \quad (5.1)$$

$$CAF = 1 - CRF \quad (5.2)$$

For each combination of cross-weave flow, number of lanes, and $L_{CW\text{-}Min}$, the capacity of the configuration is derived from the simulation model. The CRF for the combination is then consequently calculated. Figure 32 gives the graphical representation of the CRF for the 4-Lane GP scenarios. Note that as cross weave flow increases, the CRF increases as well. The general trend follows a logarithmic distribution. A longer $L_{CW\text{-}Min}$ would have less capacity reduction impact on the GP segment. Table 25 gives a complete result of the CRF for each configuration tested in the simulation model. Note that for the capacity calculated using the Van Aerde's model, all the calculated capacities were rounded to the nearest 5 or 0 in consideration of the underlying variability in the simulated speed-flow data. The results show reasonable trends since the CRF increases as the cross-weave flow increases, the $L_{CW\text{-}Min}$ decreases, and the number of GP lane increases. This result is as hypothesized, since as the cross-weave flow increases, more weaving would be generated within the GP segment, which brings more capacity disturbance to the area. With a longer weaving length ($L_{CW\text{-}Min}$), the cross-weave vehicles would have more time to position themselves onto the left-most lane to get into the ML. Therefore, the average LCI would be less intense and the CRF lower. Also, with fewer GP lanes, the number of lane changes required for the cross-weave flow would be correspondingly reduced, which also results in a lower disturbance frequency on the GP segment.

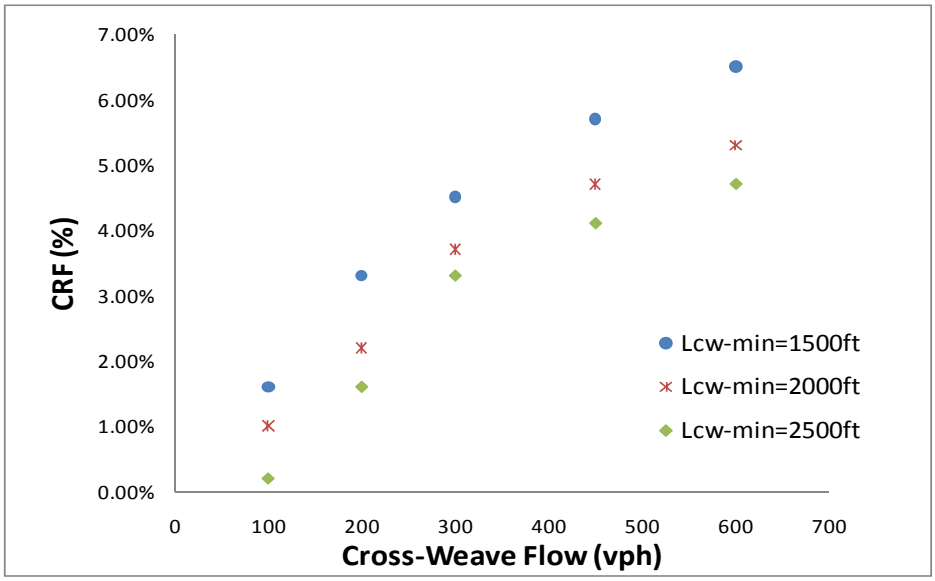

FIGURE 32 CRF as Response to Cross Weave Flow and Lcw-min under 4-Lane GP Scenarios

To further investigate the capacity reduction due to various configurations, lane change intensity analysis was performed for different scenarios. Figure 33 demonstrates the cumulative number of

lane changes profile for simulation scenarios with cross-weave flow of 300 pcph, and GP input demand of 2,400 pcphpl. The LCI is quite different for the three GP lane scenarios. With fewer lanes, the LCI is less due to the lower number of lane change maneuvers required for the cross-weave flow. Figure 34 gives the same configuration comparison, except that the changing variable is the length of $L_{CW\text{-}Min}$. Note that the shorter $L_{CW\text{-}Min}$ results in more intense lane changing, however, the significance is not that prominent. Also with a longer $L_{CW\text{-}Min}$, the total number of lane changes is increased due to the fact that more vehicles would position themselves on the left-most lane to be ready to get into the ML at the BOA. However, if analyzing the LCI on the entire length of $L_{CW\text{-}Min}$, the difference between the three scenarios would be quite pronounced. The LCI (total number of lane changes/$L_{CW\text{-}Min}$) are 0.48 LC/ft, 0.39 LC/ft and 0.32 LC/ft for $L_{CW\text{-}Min}$ =1500 ft, 2000 ft, and 2500 ft, respectively.

TABLE 25 CRF for Each Configuration Scenario

4 GP Lanes	$L_{CW\text{-}Min}$ (ft)	Cross-Weave Flow (pcph)				
		100	200	300	450	600
	1500	1.63%	3.27%	4.49%	5.71%	6.53%
	2000	1.02%	2.24%	3.67%	4.69%	5.31%
	2500	0.20%	1.63%	3.27%	4.08%	4.69%
3 GP Lanes	$L_{CW\text{-}Min}$ (ft)	Cross-Weave Flow (pcph)				
		100	200	300	450	600
	1500	1.22%	3.06%	3.88%	5.51%	6.12%
	2000	0.82%	2.04%	3.47%	4.29%	4.69%
	2500	0.20%	1.43%	2.65%	4.08%	4.29%
2 GP Lanes	$L_{CW\text{-}Min}$ (ft)	Cross-Weave Flow (pcph)				
		100	200	300	450	600
	1500	1.02%	2.65%	3.67%	5.10%	5.31%
	2000	0.61%	2.04%	3.06%	4.29%	4.90%
	2500	0.00%	1.22%	2.24%	3.27%	4.08%

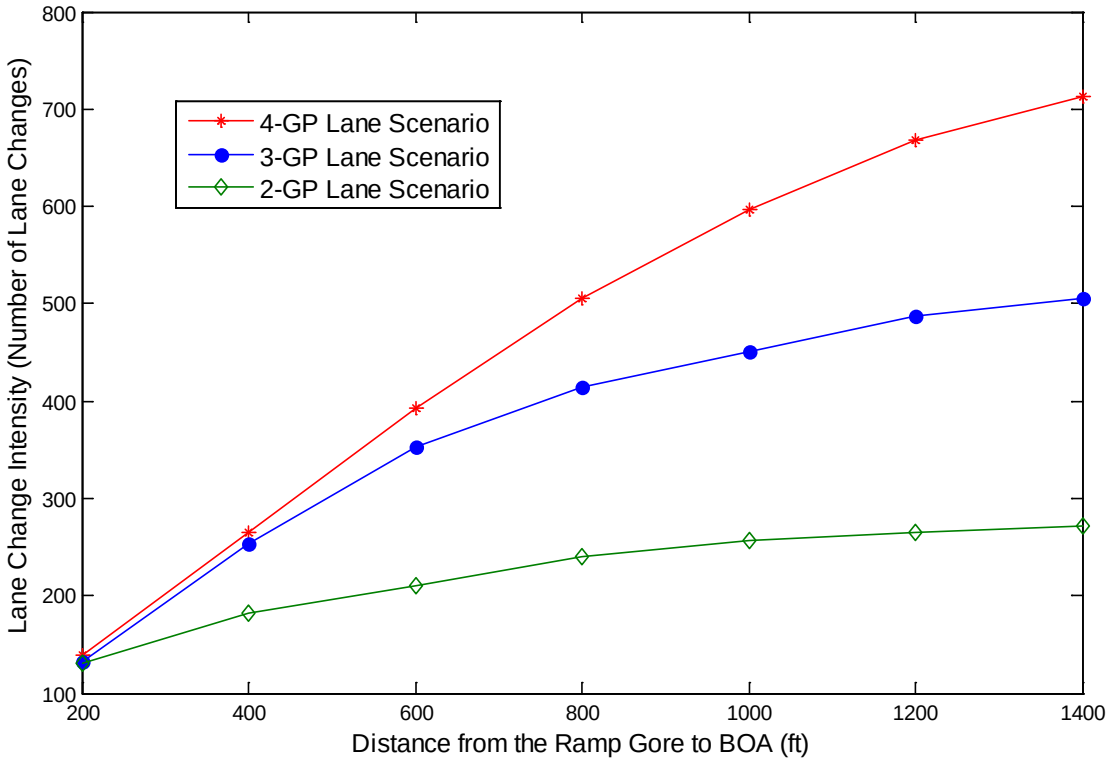

FIGURE 33 Cumulative Lane Change Intensity for Different GP Lanes Scenarios with Cross-Weave Flow 300 pcph, and GP Input Demand of 2400 pcphpl

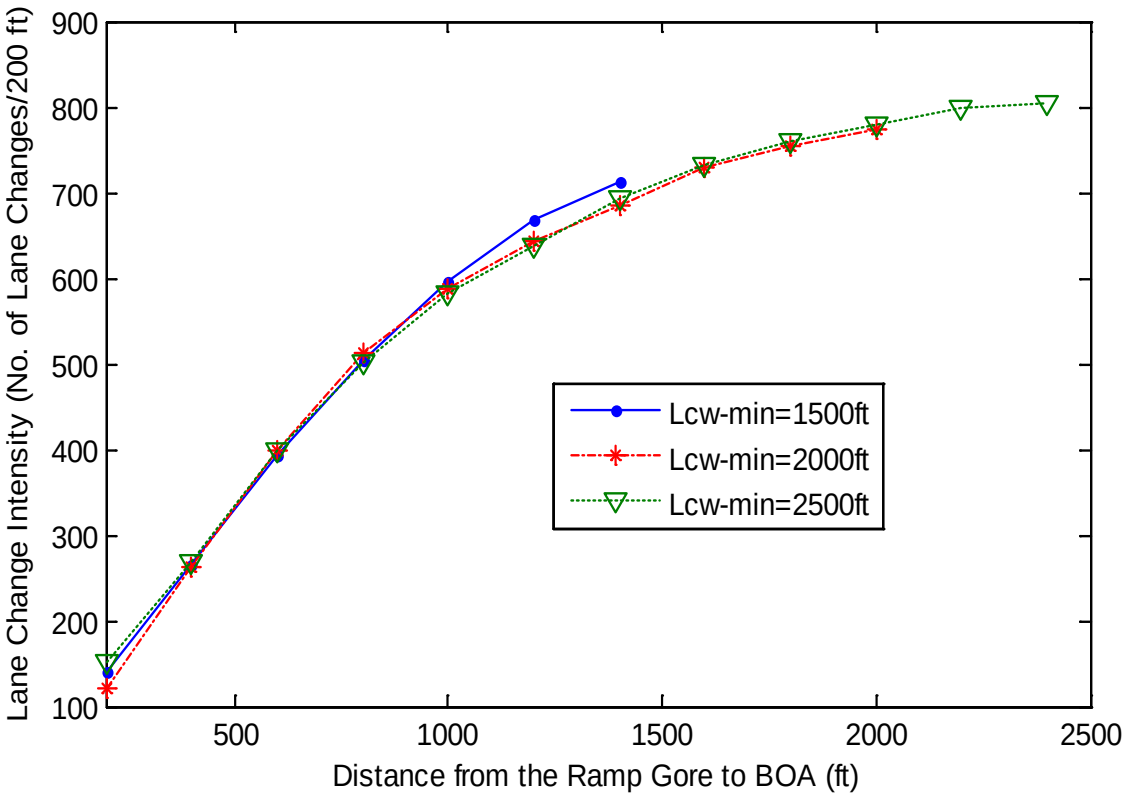

FIGURE 34 Cumulative Lane Change Intensity for Different $L_{CW\text{-}Min}$ Scenarios with Cross Weave Flow 300 pcph, and GP Input Demand of 2400 pcphpl

The calculated CRF was developed as a function of the number of GP lanes, cross-weave flows, and length of $L_{CW\text{-}Min}$. A regression model was performed to quantitatively establish the relation between the CRF and the other independent variables:

where CW is the cross-weave flow measured in pcph, $L_{CW\text{-}Min}$ is the length from the ramp gore to the beginning of BOA measured in ft, and number of GP lanes ranging from 2 to 4.

The regression result is shown in Table 26. All the independent variables yield a significant result at 95% confidence interval on the CRF, and the adjusted R-square value is 0.9837 which indicates an excellent fit.

TABLE 26 Linear Regression Output for CRI and the Corresponding Variables

Independent Variable	Estimated Parameter	T-statistic	P-Value
Constant (intercept)	-8.957	-24.063	0.000
ln(CW)	2.52	46.349	0.000
Lcw-min	-0.001453	-17.329	0.000
Number of GP Lanes	0.2967	7.075	0.001

Chapter 6 Sample Applications

6.1 Interface Description

The HCM 2010 Freeway Facilities method relies heavily on the use of the FREEVAL computational engine to apply and test the methodology, which is made available in HCM 2010 Volume 4. FREEVAL and the freeway facilities method have been in use for more than ten years. The method has been independently validated against empirical data for congested facility, and compared very favorably to simulation-based analyses. For consistency and compatibility, the NCHRP 03-96 research team developed an enhanced computational engine, FREEVAL-ML, for analyzing both GP and ML segments in parallel facilities. FREEVAL-ML was developed following the same *Excel/Visual Basic* structure as the HCM 2010 engine, which combines a user-friendly and intuitive spreadsheet interface with a flexible coding language to execute the computations. The updated FREEVAL-ML continues to be consistent with the HCM 2010 Freeway Facilities method for the GP-lane analysis, and reports outputs separately for GP lanes and MLs, as well as offering combined performance measures.

6.2 Example and Case study

To check the feasibility of the proposed framework, two existing ML facilities in Washington State are selected as the case study sites. The motivations for these case studies are (1) to demonstrate the applicability of the method to real-world facilities, (2) to test the sensitivity of input parameters, and (3) to identify limitations in the method. The purposes of the case studies are to demonstrate the capability of the methodology in replicating the geometry of actual facilities and do not attempt to perform a validation of actual performance. All volumes are therefore constructed to perform these tests, rather than using measured demands. Figures 35 and 38 show the proposed HCM segmentations for the two sites: “I-5 Reversible Northbound” and “SR 167 Northbound”, respectively.

Case 1: I5-Reversable Northbound

I-5 in Seattle, Washington has a set of reversible express lanes separated from the GP lanes by a concrete barrier. Therefore, no friction effect is present in this case study. Figure 35 shows the segmentation for this I-5 Reversible facility. There are three ramps (marked by red X in the figure) that should be ignored as the reversible lanes are operating in the northbound direction under the study period.

Based on the methodology presented in Chapter 3, 16 segments are identified, as shown in Figure 35. Since the freeway facilities methodology is directional, the opposite direction ramps on the reversible facility are ignored. Figure 35 also shows the resulting segment type for both GP and MLs. Note that the segment length of parallel lane groups is identical per the assumptions discussed above.

One important issue to consider in this facility is that Segments 11, 12 and 13 of the GP facility should be jointly coded as one weave segment per the HCM 2010 conventions, since the on- and off-ramps are connected by an auxiliary lane. However, on the parallel ML, the segment includes a ML off-ramp in Segment 11. To preserve the lane group concept, the analyst therefore needs to

decide whether to (A) code Segments 11 through 13 individually as is done here (thereby ignoring the weaving functionality) or to (B) code only one segment that captures the GP-Weave (but ignores the ML off-ramp). Considering the long length of GP weave segment (which is 3,700 ft), and the presumed focus of the analysis on the ML portion, option (A) is selected here. However, an analyst may decide to repeat the analysis with approach (B) to assure that the assumption to approximate the GP-weave by three separate segments is appropriate. If determined that the weave does have significant impacts on performance, the analyst may then decide to employ a capacity adjustment factor in Segments 11-13 in approach (A) to represent the weaving turbulence.

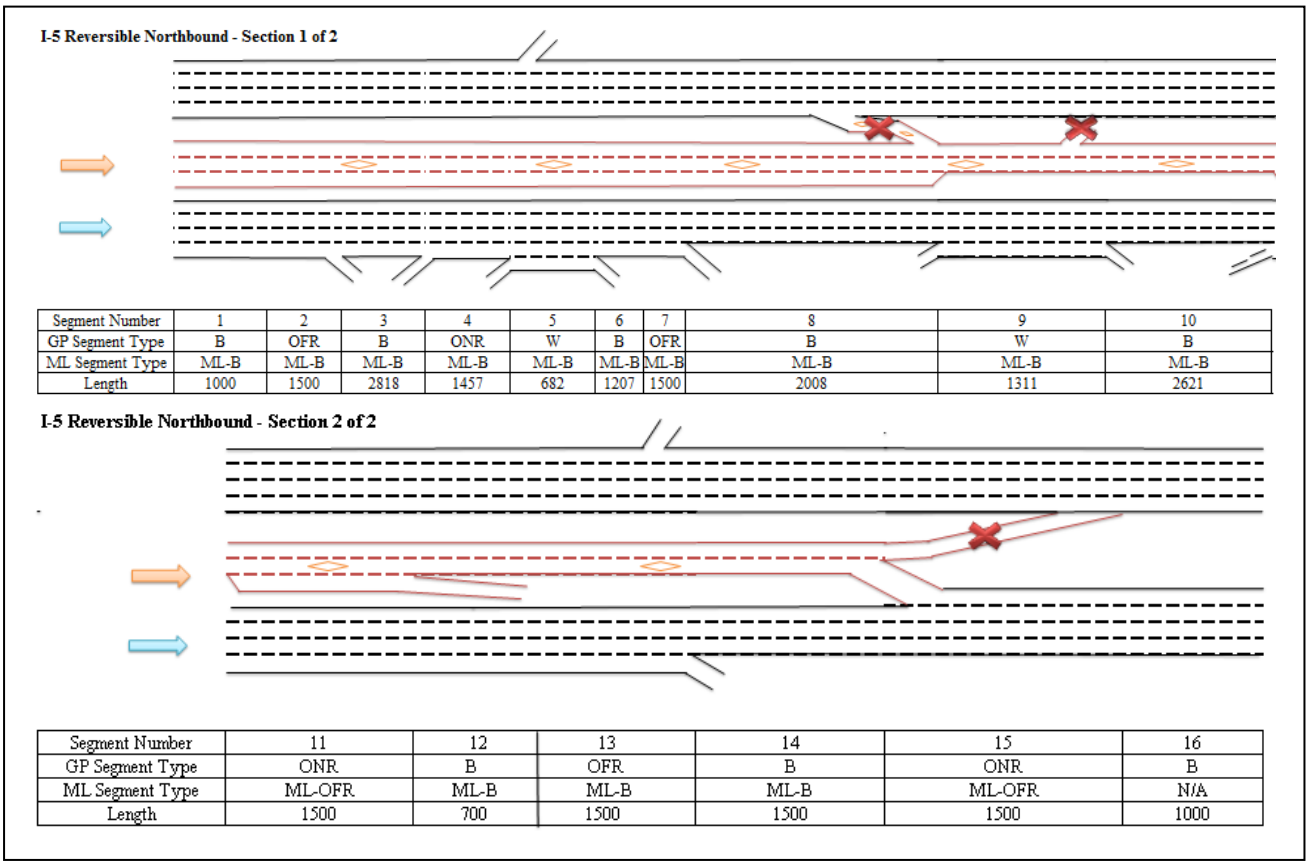

Segment Number	1	2	3	4	5	6	7	8	9	10
GP Segment Type	B	OFR	B	ONR	W	B	OFR	B	W	B
ML Segment Type	ML-B	ML-B	ML-B	ML-B	ML-B	ML-B	ML-B	ML-B	ML-B	ML-B
Length	1000	1500	2818	1457	682	1207	1500	2008	1311	2621

Segment Number	11	12	13	14	15	16
GP Segment Type	ONR	B	OFR	B	ONR	B
ML Segment Type	ML-OFR	ML-B	ML-B	ML-B	ML-OFR	N/A
Length	1500	700	1500	1500	1500	1000

FIGURE 35 Lane Group Segmentation for I-5 Reversible, Northbound

This facility was modeled in FREEVAL-ML for four consecutive 15-minute time periods (one hour total), although longer analysis periods would be feasible if desired. The facilities' performance is summarized in Figure 36 showing the distribution of LOS across all segments and time periods for both GP and MLs. This example was designed to result in GP lane congestion in time period 2, so the advantage of having MLs will be justified. Other performance measures for comparing the two facilities are available as well.

General Purpose (GP) Lanes DENSITY BASED Level Of Service

Time Period	Segment 1	2	3	4	5	6	7	8	9	10	11	12	13	14	15	16	FACILITY LOS
1	B	B	B	C	C	C	C	D	D	D	C	C	C	D	E	E	C
2	C	C	C	C	C	D	D	D	F	E	D	D	D	D	E	E	F
3	B	C	B	C	D	C	B	C	F	B	B	B	B	B	E	C	D
4	B	B	B	B	B	C	C	C	C	C	C	C	C	C	D	D	D

Managed Lanes (ML) DENSITY BASED Level Of Service

Time Period	Segment 1	2	3	4	5	6	7	8	9	10	11	12	13	14	15	16	FACILITY LOS
1	B	B	B	B	B	B	B	B	B	B	B	A	A	A	B	A	B
2	B	B	B	B	B	B	B	B	B	B	B	B	B	B	B	A	B
3	B	B	B	B	B	B	B	B	B	B	B	B	B	B	B	A	B
4	B	B	B	B	B	B	B	B	B	B	B	A	A	A	B	A	B

FIGURE 36 LOS Performance of I-5 Reversible (assumed traffic demands)

Figure 37 contrasts the average speed profiles (a) and the cumulative travel time difference (b) for the parallel facilities. Figure 37 (a) highlights the drop in speed due to congestion on the GP lanes, while the separated ML facility operates almost at FFS. Accordingly, the cumulative travel time in the GP lanes is affected by the drop in speed, showing the advantage of the MLs over the length of the facility. It is emphasized once again that the modeled demands are hypothetical, and developed only for demonstration purposes. The “combined” curve refers to the weighted average performance of ML and GP lanes.

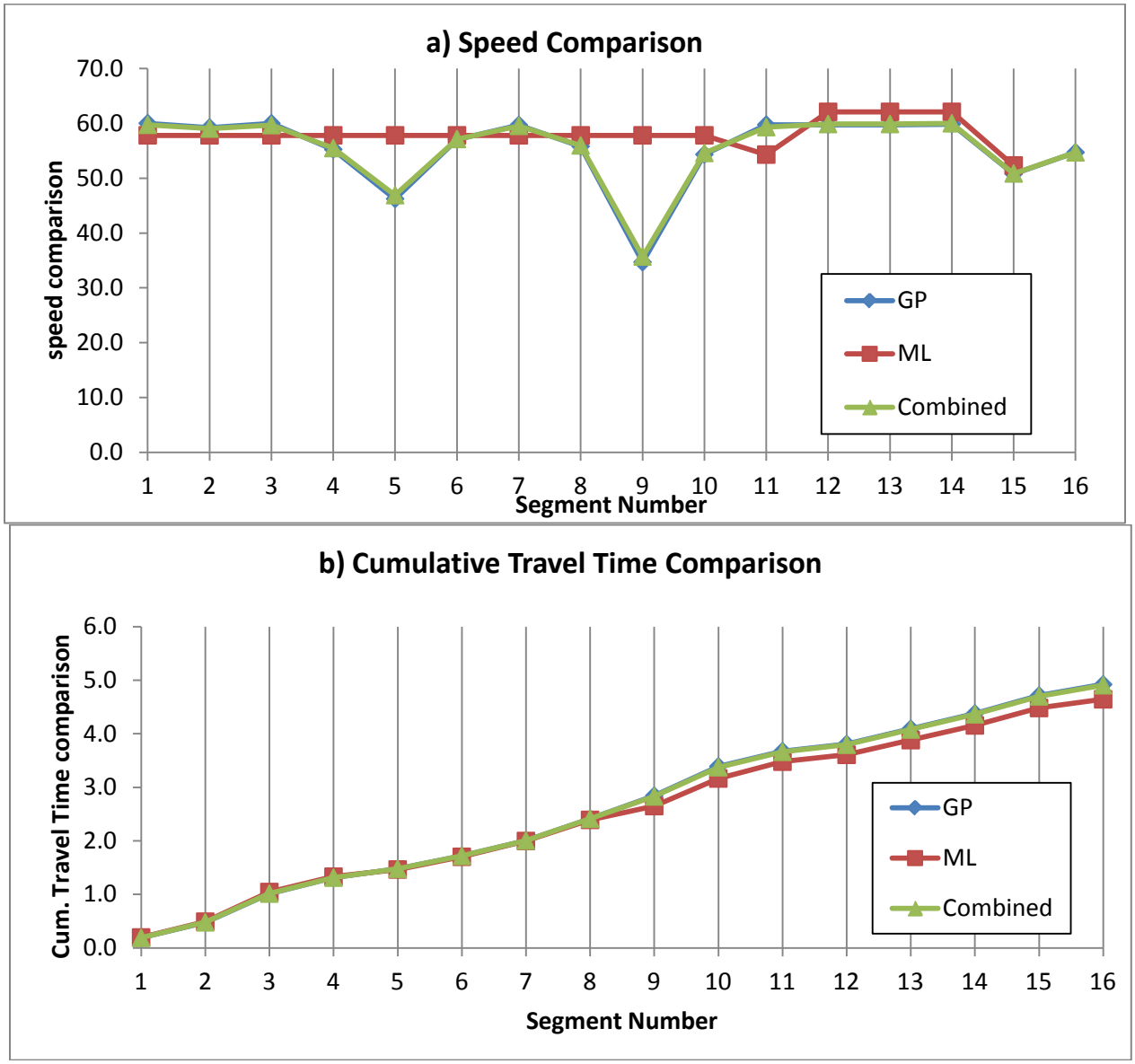

FIGURE 37 Cumulative Speed and Travel Time Comparison for ML and GP lanes

Case 2: SR-167 Northbound

The second sample facility SR 167 has northbound HOT lanes for 11.3 miles. In total, 38 segments are defined for this case study site. If ML were not presented, the GP facility would have only had 29 segments. However, 9 additional segments are added to satisfy the parallel lane group assumption. For example Segment 22, 23, and 24 would have been coded as one basic GP segment in the absence of ML, but are now modeled as Basic, GP-Access, and Basic. The GP-Access segment must be coded in parallel to a ML-Access segment. Figure 38 shows all lane groups for this facility based on the developed methodology. The separation type in this facility is buffer separation, where frictional effect will be modeled when the GP density exceeds 35 pcpmpl. There are a total of five access segments between ML and GP lanes.

SR-167 Northbound - Section 1 of 3

Segment Number	1	2	3	4	5	6	7	8	9	10	11	12
GP Segment Type	B	OFR	B	ONR	ONR	GP-ACS	OFR	B	ONR	B	GP-ACS	B
ML Segment Type	ML-B	ML-B	ML-B	ML-B	ML-B	ML-ACS	ML-B	ML-B	ML-B	ML-B	ML-ACS	ML-B
Length (feet)	10	740	3274	1450	1050	2300	720	2500	1500	700	1500	2900

SR-167 Northbound - Section 2 of 3

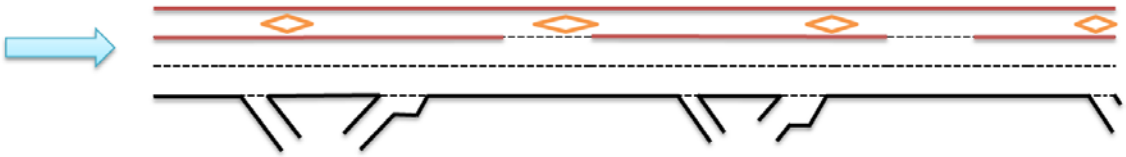

Segment Number	12	13	14	15	16	17	18	19	20	21	22	23	24	25
GP Segment Type	B	OFR	B	ONR	B	GP-ACS	B	OFR	B	ONR	B	GP-ACS	B	OFR
ML Segment Type	ML-B	ML-B	ML-B	ML-B	ML-B	ML-ACS	ML-B	ML-B	ML-B	ML-B	ML-B	ML-ACS	ML-B	ML-B
Length (feet)	2900	1500	2587	1500	802	1500	932'	1500	2800	1500	750	1500	1300	1500

SR-167 Northbound - Section 3 of 3

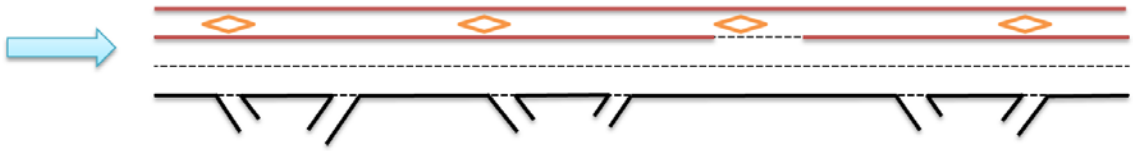

Segment Number	25	26	27	28	29	30	31	32	33	34	35	36	37	38
GP Segment Type	OFR	B	ONR	R	OFR	B	ONR	B	GP-ACS	B	OFR	B	ONR	B
ML Segment Type	ML-B	ML-B	ML-B	ML-B	ML-B	ML-B	ML-B	ML-B	ML-ACS	ML-B	ML-B	ML-B	ML-B	ML-B
Length (feet)	1500	2640	1200	82	1200	1848	1500	974	1500	3314	1500	3300	1500	200

FIGURE 38 Lane Group Segmentation for SR-167, Northbound

This facility does not have an active bottleneck, but still has several GP segments operating at a density above 35 pcpmpl. For these segments, the methodology invokes the friction effect module, resulting in a reduction in operating speed on the adjacent ML lane group. The corresponding ML speed drops by up to 8.5 mph in Segments 27 through 29 due to the frictional effect imposed onto ML. Note that if the facility had been designed with barrier separation, then no friction effect would have been modeled. The speed comparison is shown graphically in Figure 39 (a). The figure also clearly shows speed drops in both ML and GP lanes in the five ML/GP Access segments along the facility (Segments 6, 11, 17, 23, and 33). The speed-drops are likely the direct results of lane-change turbulences in those access segments. The cumulative travel time comparison is shown in Figure 39 (b), which again demonstrates the superior performance of the

ML, as opposed to the GP lanes with a bottleneck. Note that the travel time difference across this very long facility is smaller in magnitude than for the earlier case study.

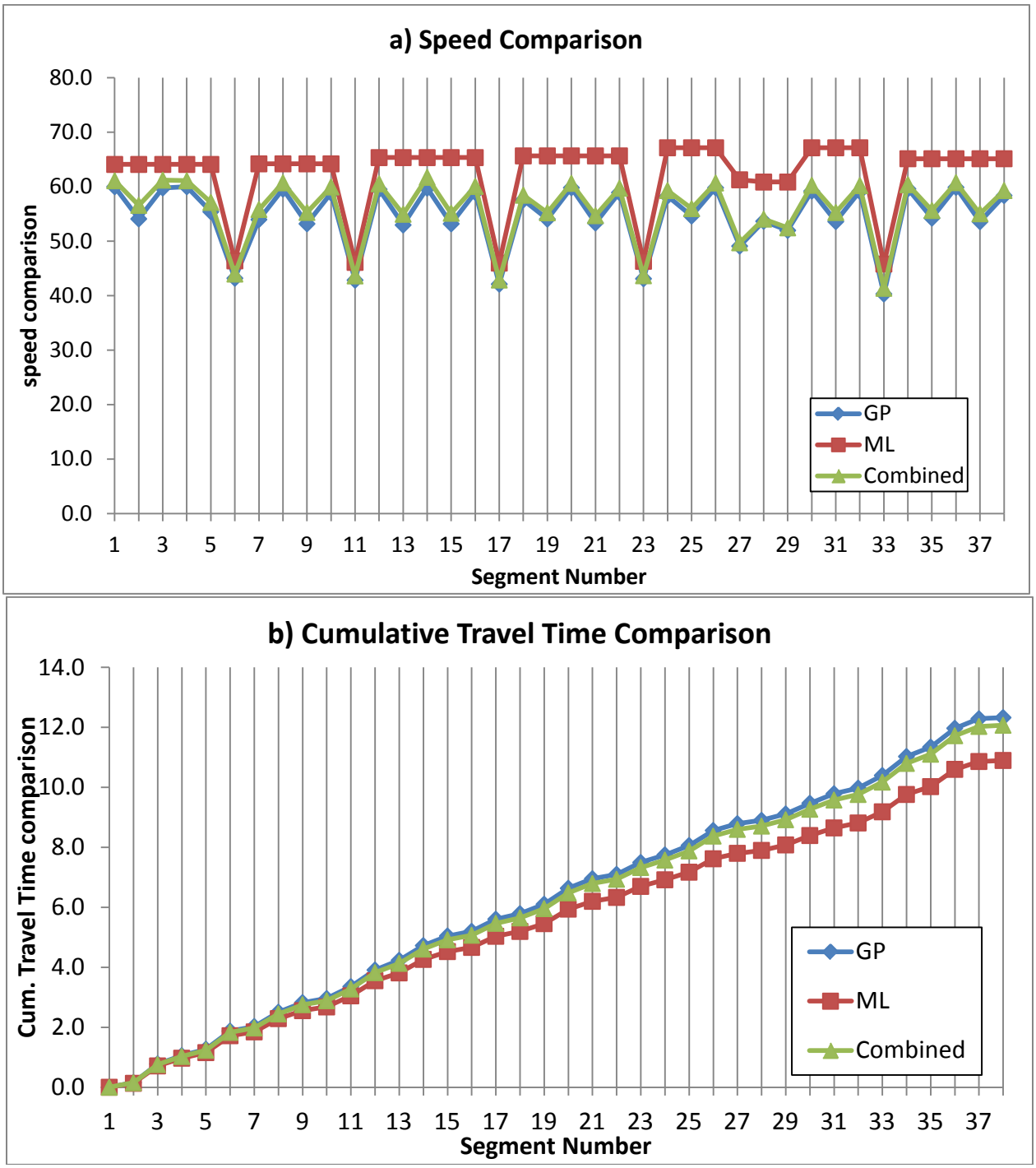

FIGURE 39 Speed and Travel Time Comparison for the ML and GP Lanes on NB SR-167

Chapter 7 Conclusions and Recommendations

Based on the findings of this study, MLs are considered an effective countermeasure against freeway congestion. A methodological framework along with a computational engine (available at http://sites.kittelson.com/hcqs-fwy) for the performance evaluation of freeway facilities with MLs is developed in this research. Major conclusions from the NCHRP 03-96 research team are summarized as follows.

Parallel Lane Groups of MLs and GP Lanes

This research adopts the lane group concept widely used in the signalized intersection analysis in HCM 2010 to ascribe separate attributes to parallel ML and GP facilities, while retaining the ability to model a certain degree of interaction between the two. As widely observed, the ML and GP lane groups may have different geometric characteristics, such as number of lanes, lane width, segment types. They may also have distinctive behavioral and traffic attributes, such as FFS, segment capacity, traffic demand, etc. Besides these dichotomies, the two lane groups would impose interaction onto each other under certain circumstances. For example, a congested GP lane may have an adverse frictional effect on the adjacent MLs. To accommodate all these features, the lane group concept is well-suited under the umbrella of a deterministic analytical framework for the two parallel facilities. The frictional effect was empirically derived from field collected data. It can be user-calibrated based on the types of physical separation, number of lanes, and FFS.

Unique Speed-Flow Features for Basic ML Segments

As a major component of the NCHRP 03-96 project, speed-flow models for the basic ML segments are developed following the HCM 2010 methodology. The models were developed based on an extensive amount of traffic sensor data collected nationwide. Fifteen-minute speed and volume data were used for consistency with HCM 2010. Traffic behavior characteristics of various ML design and strategies were carefully identified and studied, and a total of 63,656 fifteen-minute data points were extracted from 10 different freeway facilities with MLs. Five basic ML segment types are proposed based on field observation, including Continuous Access, Buffer 1, Buffer 2, Barrier 1, and Barrier 2. Operational performance and traffic flow characteristics were analyzed from intensive data sites for each segment type. To this end, the speed-flow models for the five segment types were developed. It was found that the separation type and number of lanes distinguish the traffic flow behavior of ML facilities. The developed models also incorporated and quantified the frictional effect imposed onto the ML facilities when the GP lanes are congested.

Cross-Weave Effect Imposed onto the Parallel GP Lanes

As the adjacent ML facilities would be readily impacted by traffic conditions on the GP lanes, there is an interdependent effect with the GP lanes. For example, when the GP on-ramp traffic tries to weave-across multiple GP lanes over a relatively short distance to get into MLs, there is a capacity-reducing effect on the GP segments called cross-weave effect. This cross-weave effect is quantified in this study through a multi-scenario simulation model that is carefully calibrated

using field collected video data. The simulation sensitivity is verified in that the capacity reduction in the simulation model is responsive to the cross-weave distance, cross-weave demand, and the number of GP lanes. As expected, the capacity reduction effect is more significant with shorter cross-weave distances, increased cross-weave demand, and the number of GP lanes. With these results, Capacity Reduction Factors (CRFs) that are compatible with the deterministic analysis approaches in the HCM is developed in the study. The CRF is the percentage of capacity reduction compared to the base scenario where no cross-weave flow is present. CRFs are analogous to the Capacity Adjustment Factor (CAF) used in the HCM freeway facilities method. This feature quantitatively describes the ML cross-weave impact on the GP segment. It also allows for an appropriate integration of this phenomenon into the ML methodology developed under research project NCHRP 03-96 for evaluating the performance of freeway facilities with MLs.

Future Research

For future research, this team identifies several areas that warrant further study and investigation:

- Future research should explore congested managed lane facilities, with a special emphasis on queuing patterns at intermittent access points, and queue spillback allocation between ML and GP lanes.
- Future research should investigate the beginning and end point designs of ML facilities. Variations in the design of these termini is expected to impact operations of the overall facility, and future research should explore what design aspects minimize the turbulence created at these locations.
- Future research should tie the operational HCM methodologies with demand-estimation procedures. Since many ML facilities in the US feature a congestion-pricing component, the distribution of corridor demands between ML and GP lanes has been shown sensitive to pricing. While the HCM is traditionally not focused on demand estimation (demand is generally treated as an input), a closer scrutiny on the supply and demand tradeoffs is needed for ML design and operations.
- Future research should take a more detailed look at special configurations of ML access points. In addition to the lane-change or weaving access mentioned above, grade-separated ramp access points also warrant further scrutiny, especially ramps to and from single-lane ML facilities. The methodology for merge and diverge sections in the HCM generally assumes a ramp-influence-area (RIA) of two lanes, and it is likely that ramps on single-lane facilities have different operational attributes.
- Future research should take a field data based approach to estimating capacity-reducing effects of ML cross-weave maneuvers on the GP lanes. The simulation-based approach taken in this research showed the hypothesized sensitivity, but this should be confirmed by field data.
- Finally, future research should focus on applying the methodology developed in this project to real-world case studies, and validating the predicted performance with field-measured performance data.

References

Bloomberg, L., and J. Dale. Comparison of VISSIM and CORSIM Traffic Simulation Models on a Congested Network. *Transportation Research Record: Journal of the Transportation Research Board*, Vol. 1727, 2000, pp. 52-60.

Brilon, W., and Ponzlet, M., Application of Traffic Flow Models. *Proceedings of the International Workshop on Traffic and Granular Flow*, Juelich, Germany, World Scientific Publishing, 1995.

Chang, J. Wiegmann, A. Smith, C. Bilotto. FHWA. A Compendium of Existing HOV Lane Facilities in the United States. Report No. FHWA-HOP-09-030. Dec. 2008.

Carson, J.L. *Monitoring and Evaluating Managed Lane Facility Performance*. Publication FHWA/TX-06/0-4160-23. Texas Transportation Institute, Texas Department of Transportation, Federal Highway Administration. 2005.

California Department of Transportation (Caltrans), Department of Transportation, Division of Traffic Operations *High Occupancy Vehicle (HOV) Guidelines for Planning, Design and Operations*, California Department of Transportation, 2003.

Eads, B., N. Rouphail, A. May, and F. Hall. Freeway Facility Methodology in Highway Capacity Manual 2000. *Transportation Research Record: Journal of the Transportation Research Board*, Vol. 1710, 2000, pp. 171-180.

Rodrigues, J., K. Kawamura, and A. Samimi. FREQ Simulation and Ramp Meter/HOV bypass Optimization for the Northwest Study Area. *Transport Chicago 2008*. Illinois Institute of Technology. June 2008.

Gomes, G., A. May, and R. Horowitz. Congested Freeway Microsimulation Model Using VISSIM. *Transportation Research Record: Journal of the Transportation Research Board*, Vol. 1876, 2004, pp. 71-81.

Guin, A., Hunter, M., and Guensler, R., Analysis of Reduction in Effective Capacities of High Occupancy Vehicle Lanes Related to Traffic Behavior, *Transportation Research Record 2065*, Transportation Research Board, Washington, D.C., 47-53, 2008.

Hall, F., L. Bloomberg, N. Rouphail, B. Eads, and A. May. Validation Results for Four Models of Oversaturated Freeway Facilities. *Transportation Research Record: Journal of the Transportation Research Board*, Vol. 1710, 2000, pp. 161-170.

Transportation Research Board (TRB). Highway Capacity Manual (HCM) 2010. Washington, D.C.

Wang, Y., X. Liu, N. Rouphail, B. Schroder, L. Bloomberg, Y. Yin. Interim Report of NCHRP 03-96: Analysis of Managed Lanes on Freeway Facilities. *Transportation Research Board*. August, 2009.

Kuhn, B., G. Goodin, A. Ballard, M. Brewer, R. Brydia, J. Carson, S. Chrysler, T. Collier, K. Fitzpatrick, D. Jasek, C. Toycen, and G. Ullman, *Managed Lanes Handbook*, Texas Transportation Institute, Texas Department of Transportation, Federal Highway Administration, 2005.

Kwon, J., and Varaiya, P., "Effectiveness of California's High Occupancy Vehicle System," *Transportation Research Part C 16*. 98-115, 2008.

Liu, X., G. Zhang, Y. Lao, and Y. Wang. Quantifying the Attractiveness of High Occupancy Toll (HOT) Lane under Various Traffic Conditions using Traffic Sensor Data. *Transportation Research Record: Journal of Transportation Research Board*, 2011. No. 2229, pp 102-109.

Liu, X., B. Schroeder, T. Thomson, Y. Wang, N. Rouphail, and Y. Yin. Analysis on Operational Interactions between Freeway Managed Lanes and Parallel General Purpose Lanes, *Transportation Research Record*: *Journal of Transportation Research Board*, In Print, 2011.

Liu, X., Y. Wang, B. Schroeder, and N. Rouphail. *Quantifying Cross-Weave Impact on Capacity Reduction for Freeway Facilities with Managed Lanes*. Transportation Research Board 91st Annual Meeting, 2012.

Loudon, W., Improving the Estimation of Potential Travel-Time Savings from HOV Lanes, Transportation Research Board 86th Annual Meeting, Washington D.C., 2007.

Martin, P., Perrin, J., Lambert, R., and Wu, P., *Evaluate Effectiveness of High Occupancy Vehicle* (HOV) Lanes. Utah Department of Transportation Research Division, 2002.

Nee, J., Ishimaru, J., and Hallenbeck, M., *Evaluation Tools for HOV Lane Performance Monitoring*, Washington State Transportation Center, Washington State Department of Transportation and FHWA Report, 1999.

Obenberger, J. Managed Lanes: Combining access control, vehicle eligibility, and pricing strategies can help mitigate congestion and improve mobility on the Nation's busiest roadways. *Public Roads*, Vol. 68, No. 3, 2004, pp. 48~55.

Orange County Transportation Authority (OCTA). *91 Express Lanes 2007 Annual Report*. http://www.octa.net/91annual07.aspx. Accessed 10/10/2008.

Park, B., and H. Qi. Development and Evaluation of a Procedure for the Calibration of Simulation Models. *Transportation Research Record: Journal of the Transportation Research Board*, Vol. 1934, 2005, pp. 208-217.

POET-ML Users Guide and Methodology Description, *POET-ML Purposes*, http://ops.fhwa.dot.gov/publications/fhwahop09031/purpose.htm Accesses July 26, 2011

Roess, R., Speed-Flow Curves for Freeways in the 2010 HCM, Transportation Research Board 90th Annual Meeting, Washington D.C., 2011.

Rakha, H. Traffic Stream Calibration Software.www.filebox.vt.edu/users/hrakha/Software.htm.

Schroeder B., S. Aghdashi, N. Rouphail, X. Liu and Y. Wang. Deterministic Approach to Modeling Managed Lanes on Extended HCM Freeway Facilities. Transportation Research Board 91st Annual Meeting, 2012.

Texas Transportation Institute (TTI). Current State-of-the-Practice for Managed Lanes. Texas Department of Transportation. 2001.

Tian, Z., T. Urbanik, R. Engelbrecht, and K. Balke. Variations in Capacity and Delay Estimates from Microscopic Traffic Simulation Models. *Transportation Research Record: Journal of the Transportation Research Board*, Vol. 1802, 2002, pp. 23-31.

Thomson, T., X. Liu, Y. Wang, B. Schroeder, and N. Rouphail. Operational Performance and Speed-Flow Relationships for Basic Managed Lane Segments. Transportation Research Board 91st Annual Meeting, 2012.

Varaiya, P., *What We've Learned About Highway Congestion*, University of California Transportation Center Report, University of California, Berkeley, 2005.

Van Aerde, M., Rakha, H. Multivariate Calibration of Single-Regime Speed-Flow-Density Relationships, *Vehicle Navigation and Information Conference (VNIS)*, IEEE, Piscataway, NJ, 334-341, 1995

Vo, P., *Capacity Estimation of Two-Sided Type C Weaves on Freeways*, Ph.D. dissertation, University of Texas at Arlington. 2008.

Venglar, S., D. Fenno, S. Goel, and P. Schrader, *Managed Lanes–Traffic Modeling*, TxDOT Research Report FHWA/TX-02/4160-4, Texas Transportation Institute, January 2002.

Williams, J., S. Mattingly, and C. Yang. *Assessment and Validation of Managed Lanes Weaving and Access Guidelines*. FHWA/TX-09/0-5578-1, 2010.

Zhang, G,, S. Yan, and Y. Wang. Simulation-based Investigation on High Occupancy Toll (HOT) Lane Operations for Washington State Route 167. ASCE *Journal of Transportation Engineering*. Vol. 35, No. 10, 677-686, 2009.

Appendix A

Simulation Model Calibration for Evaluation of the Cross-Weave Effect

A VISSIM simulation model has been developed to investigate how the cross-weave flow would impact the General Purpose (GP) lane operational performance. Cross-weave flow refers to those vehicles get on rightmost GP lane from an on-ramp and change multiple GP lanes to enter the ML. Cross-weave data extracted from the University of Texas at Arlington (UTA) video footage collected from IH 635 in Dallas, Texas were used for the calibration of the simulation model. The site with the extracted ground-truth data is on the WB IH 635 with four GP lanes and one buffer-separated HOV lane. An aerial photograph of this site from Google map and a schematic layout of site configuration are shown in Figure A-1.

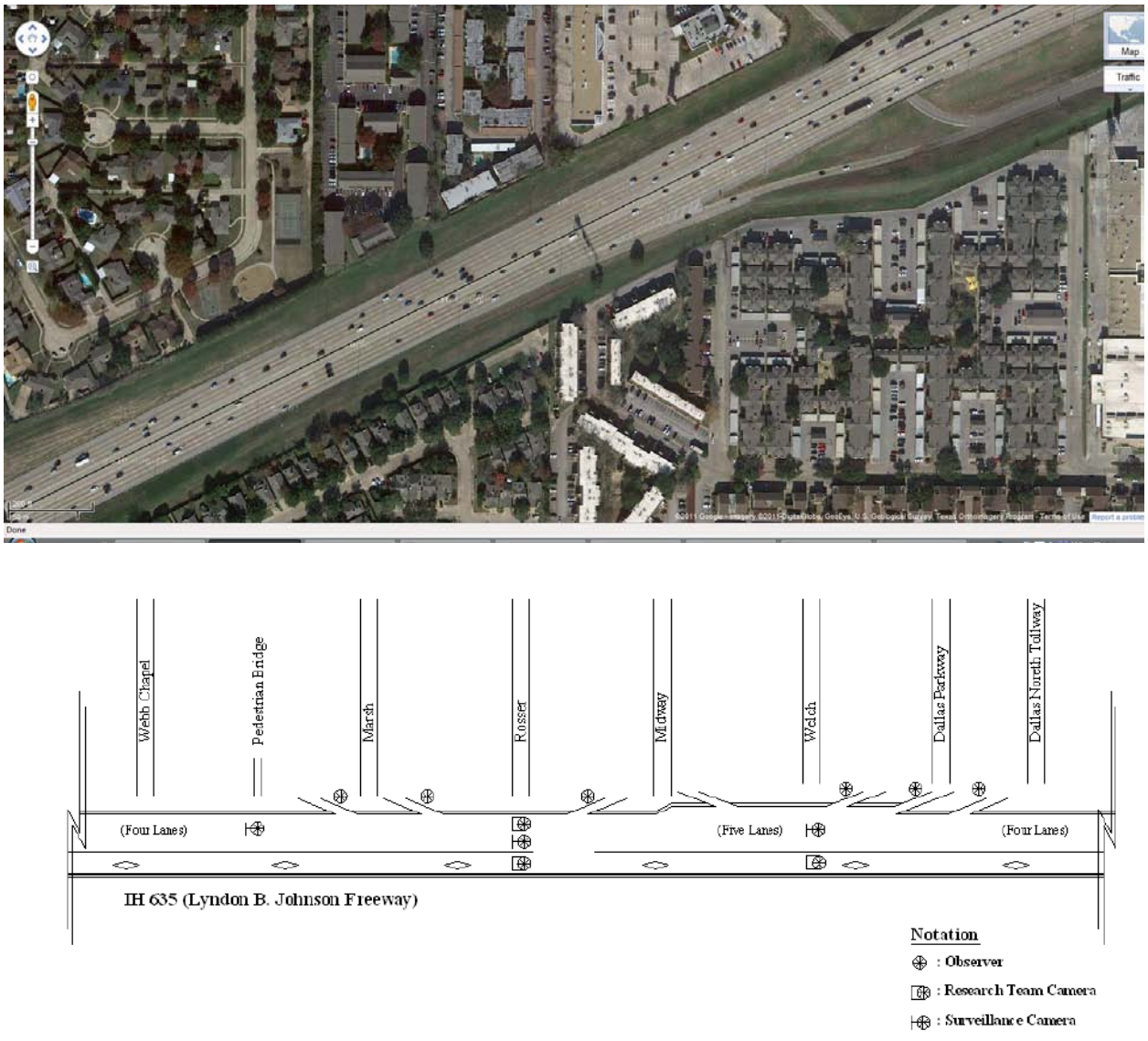

FIGURE A-1 Aerial Photograph and Schematics of Site Configuration

The access point of this data site is 1160 feet long. There is a pedestrian bridge at the downstream end of the access point, which allowed a camcorder to be set up to record traffic along the entire access point. A sample image of the video data is shown in Figure A-2.

FIGURE A-2 Sample Image from Video Data at IH 635 Access Point

Two one-hour video datasets were collected at this site:
− Friday, March 14, 2008, 10:20 a.m. to 11:20 a.m.
− Friday, March 14, 2008, 3:25 p.m. to 4:25 p.m.

The late morning dataset represents a moderate flow condition, while the late afternoon dataset shows an instance of heavy flow condition. The video datasets were processed to count the throughputs of GP and HOV lanes, respectively, and lane changes between the lane groups. Speed data were also collected from the same video by randomly selecting vehicles in each lane and recording their travel times as they travelled the entire length of the access point (1,160 ft).

Simulation Model Build-up

The research team relied on the UTA collected free-flow speed data to revise the distribution of desired speeds of cars and trucks in VISSIM. A RADAR gun was used to collect the speed information by randomly targeting vehicles that were not directly following other vehicles in the light traffic condition. The NCHRP 03-96 team used the UTA collected speed data to revise the desired speeds in the VISSIM configuration. The revised distributions of desired speeds for cars and trucks were coded in VISSIM as shown in Figure A-3.

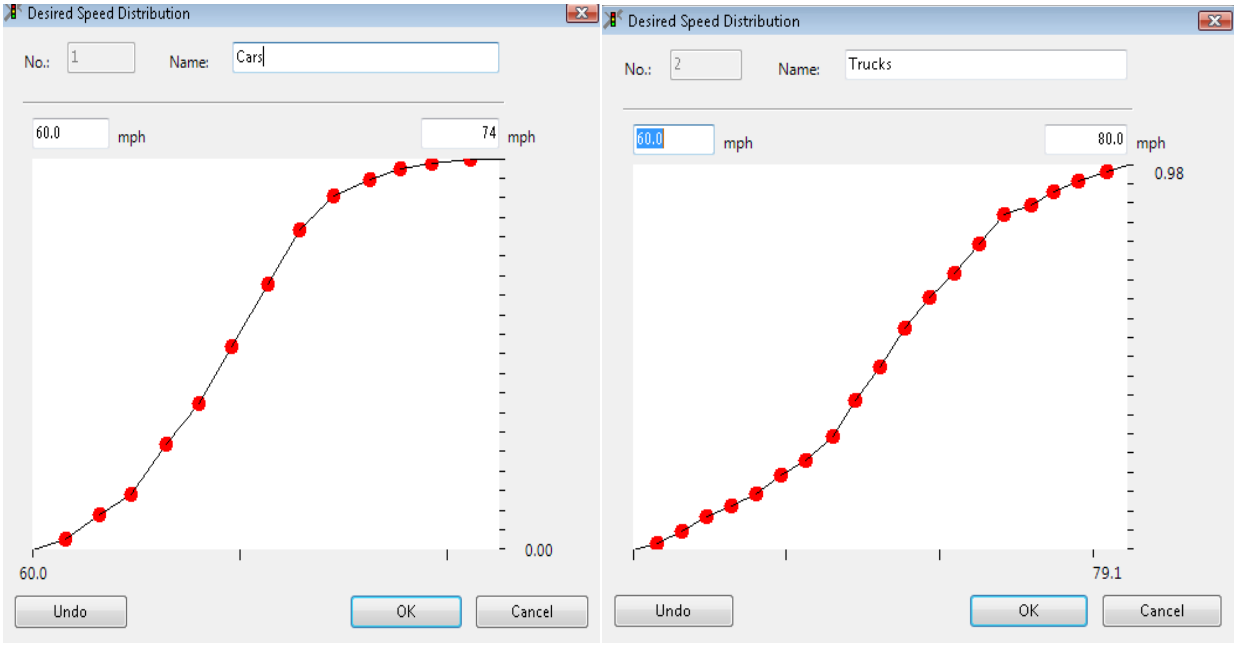

FIGURE A-3 Distributions of Desired Speeds for Cars and Trucks

For the convenience of calibration, three vehicle classes/types were defined including HOV, Car (SOV), and Truck as shown in Figure A-4. The vehicle composition includes GP traffic, Ramp Traffic, and HOV traffic.

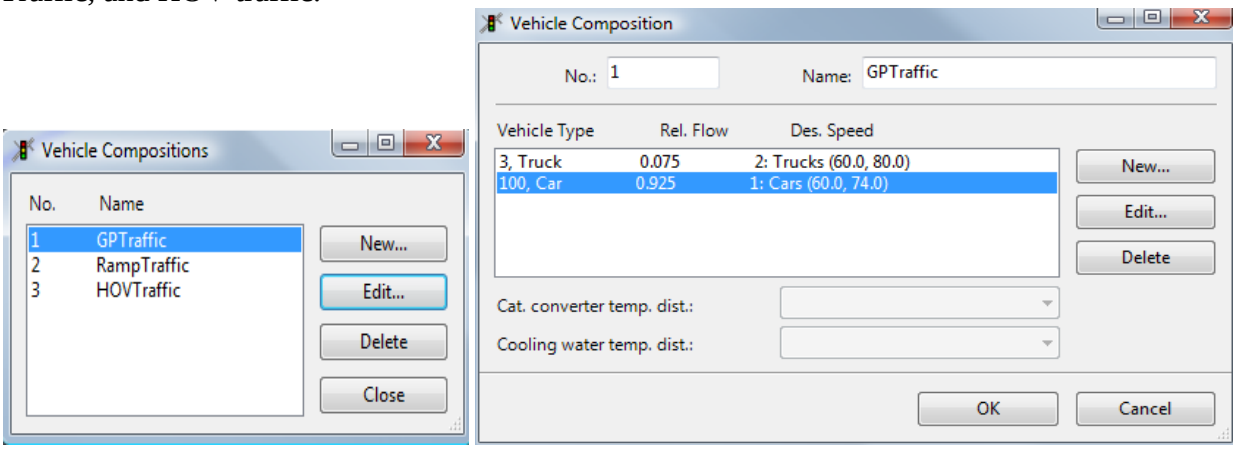

FIGURE A-4 Vehicle Composition

Using the processed video data, the Origin-Destination (OD) information was collected and aggregated at 10-min intervals to facilitate the routing input in VISSIM. The processed data are summarized in Figure A-5.

	Approaching Volume (vphpl)								Speed (mph)	
	GP	HOV	Ramp	Lane Change from GP Into HOV (veh/hr)	Lane Change from Ramp Into HOV (veh/hr)	Lane Change Out of HOV (veh/hr)	Lane Change Total (veh/hr)	Lane Change Intensity (veh/hr/100ft)	AVG GP	HOV
10:20 AM-10:30 AM	1650	300	894	132	18	60	210	18	61.4	68.9
10:30 AM-10:40 AM	1622	354	720	156	0	90	246	21	62.7	68.2
10:40 AM-10:50 AM	1650	378	822	156	0	84	240	21	62.6	66.8
10:50 AM-11:00 AM	1578	372	816	90	18	54	162	14	63.3	67
11:00 AM-11:10 AM	1589	420	870	108	0	66	174	15	63.1	65.9
11:10 AM-11:20 AM	1692	402	960	108	12	36	156	13	60.8	63.4
3:25 PM- 3:35 PM	1679	996	996	222	36	108	366	32	30.6	56.5
3:35 PM- 3:45 PM	1818	1212	996	300	60	132	492	42	33.7	56.5
3:45 PM- 3:55 PM	1725	1290	1002	246	72	210	528	46	27.8	49.4
3:55 PM- 4:05 PM	1598	1176	996	246	60	162	468	40	25.5	49.3
4:05 PM- 4:15 PM	1541	1518	996	222	60	312	594	51	23.2	45.2
4:15 PM- 4:25 PM	1625	1260	1002	144	24	204	372	32	25.6	45.9

FIGURE A-5 Processed Video Data from IH 635, Dallas, Texas

The simulation model was built following the network layout shown in Figure A-1 and configured using the data described above. The parameters considered in the calibration process are listed as follows:

Lane-changing Parameter

- Lane change
- Maximum deceleration for the current vehicle
- Maximum deceleration for trailing vehicles
- Waiting time before diffusion
- Safety distance reduction factor

Car-following parameters

- Standstill distance (CC0)
- Headway time (CC1)
- Following variation (CC2)
- Threshold for entering “following ” mode (CC3)
- “Following” thresholds (CC4 and CC5)

Figure A-6 shows the values used for the simulation models.

Parameter	Description	Default	Range	
			Minimum	Maximum
p_1	Lane Change	656 feet	1500	5000
p_2	Max. deceleration for own vehicle	-13.1 ft/sec^2	-20	-11
p_3	Max. deceleration for trailing vehicle	-9.8 ft/sec^2	-17	-8
p_4	Waiting time before diffusion	60 sec	2	30
p_5	Safety distance reduction factor	0.6	0.0	0.8
p_6	CC0 (Standstill distance)	4.9 feet	4	10
p_7	CC1 (Headway time)	0.90 sec	0.7	1.3
p_8	CC2 (Following variation)	13.1 feet	10	35
p_9	CC3 (Threshold for entering "following" mode)	-8.00	-15	-5
p_{10}	CC4 (Negative "following" threshold)	-0.35	-2.4	-0.2
p_{11}	CC5 (Positive "following" threshold)	0.35	0.2	2.4

FIGURE A-6 Parameters Description

Several indicators were selected for the calibration quality assessment, including:

- Cumulative number of vehicles entering the ML from the GP lanes and from the Midway ramp at Z4, Z7 and Z10 (the exact location of zones Z4, Z7, and Z10 can be found in Figure A-7);
- Number of vehicles entering the section from GP mainline to exit to the MLs;
- Number of vehicles entering the section from ML to exit to the GP lanes; and
- Speed in GP lanes

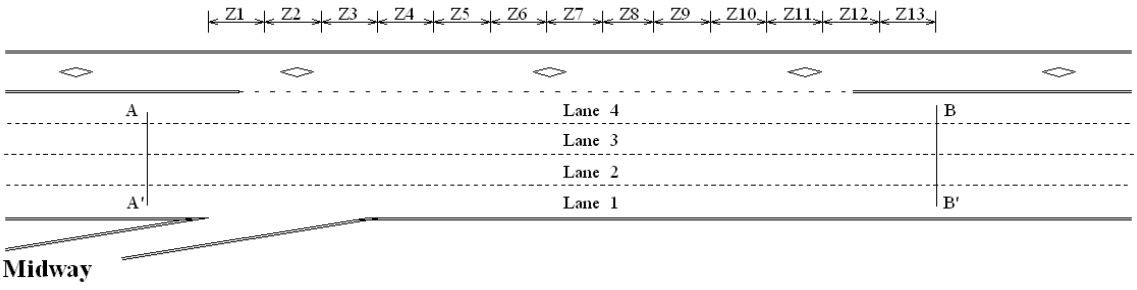

FIGURE A-7 Schematic of Configuration for the UTA Data Collection Site

A snapshot of the simulation model is in Figure A-8.

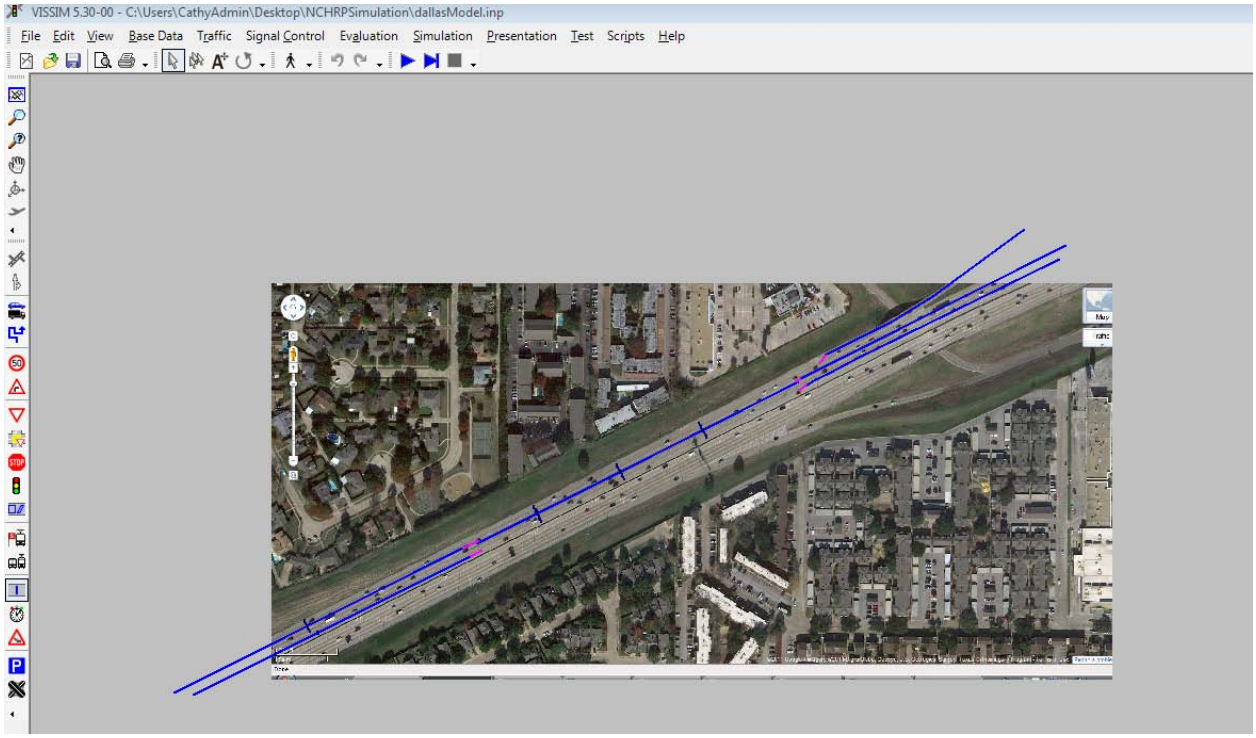

FIGURE A-8 VISSIM Simulation Model

Calibrated Model

The calibrated simulation model parameter values are shown in Table A-1 below:

TABLE A-1 Calibrated Parameters using the Dallas Dataset

Parameter	P1	P2	P3	P4	P5	P6	P7	P8	P9	P10	P11
Default	656	-13.1	-9.8	60	0.6	4.9	0.9	13.1	-8.0	-0.35	0.35
Calibrated	1750	-16	-13	12	0.4	6.0	1.3	16	-7	-1.5	1.5

Definitions of the parameters can be found in Figure A-6. Three simulation experiments were conducted with different randomly selected random seeds (42, 19, and 76) for each run. The calibration quality indicators were then averaged through the three simulation runs as show in Table A-2 and Table A-3 for moderate traffic flow and heavy traffic flow, separately.

TABLE A-2 Calibration Quality Indicators Comparison for Moderate Traffic Flow

Measurements	Entering ML from GP and Ramp			No. of HOV Leaving in GP					
	Z4	Z7	Z10	10-min	20-min	30-min	40-min	50-min	1 hour
Field Data	68	91	108	10	15	14	9	11	6
Simulated Data after Calibration	67	95	108	12	17	15	10	11	6

Measurements	No. of HOV Entering from GP leaving in HOV lanes					
	10-min	20-min	30-min	40-min	50-min	1 hour
Field Data	25	26	26	18	18	20
Simulated Data after Calibration	25	26	24	25	16	19

Measurements	Average Speed			
	L1	L2	L3	L4
Field Data	57.1	62.7	63.5	65.9
Simulated Data after Calibration	53.2	57.5	58.2	63.9

TABLE A-3 Calibration Quality Indicators Comparison for Heavy Traffic Flow

Measurements	Entering ML from GP and Ramp			No. of HOV Leaving in GP					
	Z4	Z7	Z10	10-min	20-min	30-min	40-min	50-min	1 hour
Field Data	146	198	235	18	22	35	27	52	34
Simulated Data after Calibration	152	203	234	19	23	32	26	54	41

Measurements	No. of HOV Entering from GP leaving in HOV lanes					
	10-min	20-min	30-min	40-min	50-min	1 hour
Field Data	43	60	53	51	47	28
Simulated Data after Calibration	39	52	49	53	47	27

Measurements	Average Speed			
	L1	L2	L3	L4
Field Data	22.6	27	29.3	32.3
Simulated Data after Calibration	25.3	32.7	35.2	28.7

Simulation Modeling and Calibration Summary

The UTA research team has used this Dallas dataset to build VISSIM simulation models to quantify the weaving effect at the buffer opening area of the HOV facility. They built two different simulation models, one for moderate traffic condition and the other for heavy traffic condition. However, the NCHRP 03-96 team reached a consensus that a properly calibrated model should be responsive to various traffic conditions. Therefore, in this study, one simulation model was developed and one set of parameter settings was used to account for all traffic conditions. The simulation results were validated using the ground-truth data manually extracted from the UTA video data. As shown in Tables A-2 and A-3, the simulated results match the observed data reasonably well, indicating that the calibration result is quite satisfactory. The calibrated simulation model was successfully used for the cross-weave analysis in this study.

Appendix B

Draft Text for
HCM Final Chapter: Managed Lane Facilities

CONTENTS

LIST OF EXHIBITS

1. INTRODUCTION

This chapter serves as an extension of Chapter 10 of the Highway Capacity Manual (HCM) 2010 and is designated for the analysis of freeway facilities with a Managed Lane (ML) component. The methodology described in this chapter is largely based on results of NCHRP 03-96 *(1)*. MLs (as defined in this chapter) may include High-Occupancy Vehicle (HOV) lanes, High-Occupancy/Toll (HOT) lanes, or express toll lanes. Freeways, as defined in the HCM, are classified into a variety of segment types that may be analyzed to determine the capacity and level of service at the segment or facility level. Three different freeway segments are defined in previous HCMs including *Freeway Merge and Diverge Segments*, *Freeway Weaving Segments*, and *Basic Freeway Segments*.

The procedures for General Purpose (GP) lanes that are adjacent to the MLs build upon this classification. In addition, a lane group concept is introduced to allow analysts to ascribe separate attributes to MLs and GP lanes, while still retaining a certain degree of interaction between the two facilities. The adjacent lane groups (one GP and one ML segment) are required to have the same segment length, but their segment types or separations do not have to be the same. For the ML lane group, five new ML segment types are defined in this chapter, including *ML Basic*, *ML On-Ramp*, *ML Off-Ramp*, *ML Weave*, and *ML Access Segment*.

The NCHRP 03-96 research leading to this chapter found that the composition, driver type, free-flow speed, capacity, and behavior characteristics of ML traffic streams are quite different from those of the GP lanes. In addition, there was evident interaction between the two facilities, especially for ML facilities without a physical barrier separation from the GP lanes either en route or at access points. Therefore, these newly-defined ML segment types have certain new features added.

SEGMENTS AND INFLUENCE AREAS

The five new ML segment types are presented in Exhibit 1 and discussed below:

- ML Basic: This is analogous to the basic freeway segment, but serves for ML traffic demands. Five different ML Basic segment types are identified based on the number of MLs and the type of separation between the two lane groups. New speed-flow models for these basic segments are developed through NCHRP 3-96 research and are presented in Section 2. Note that Continuous Access ML segment type, where access between the ML and GP lanes is allowed at any point, is classified as one of the five ML Basic types. It should be distinguished from the ML Access Segment (ML-AcS) which is introduced later in this section.
- ML On-Ramp and ML Off-Ramp: These are analogous to GP Lane On-Ramp and Off-Ramp segments, but with ML traffic demands. The ML On-Ramp and Off-Ramp segments are

suitable for using the existing GP lane procedures for ramps in the HCM 2010 with some necessary assumptions, as will be discussed later.

- ML Weave: This is analogous to the GP Weave segment, but with ML weaving traffic demands. The operational characteristics of an ML Weave segment are reasonably close to those of a GP Weave segment. Hence, the existing GP lane procedure for weaving segments can be applied.
- ML Access Segment (ML-AcS): This is a new segment type that is unique to ML facilities with intermittent access. Lane changing between GP and ML lanes can occur throughout the segment while prohibited in the segments just before and after it. It is treated as a weaving segment and the HCM 2010 weaving methodology is applied as an interim measure to compute its impact. By definition, an ML-AcS is always parallel to a GP Access Segment (GP-AcS) which is also shown in Exhibit 1. In the methodology, it is assumed that the operational performance of the concurrent ML and GP Access segments is estimated together for the entire cross section, and the results are applied to both ML and GP lane groups.

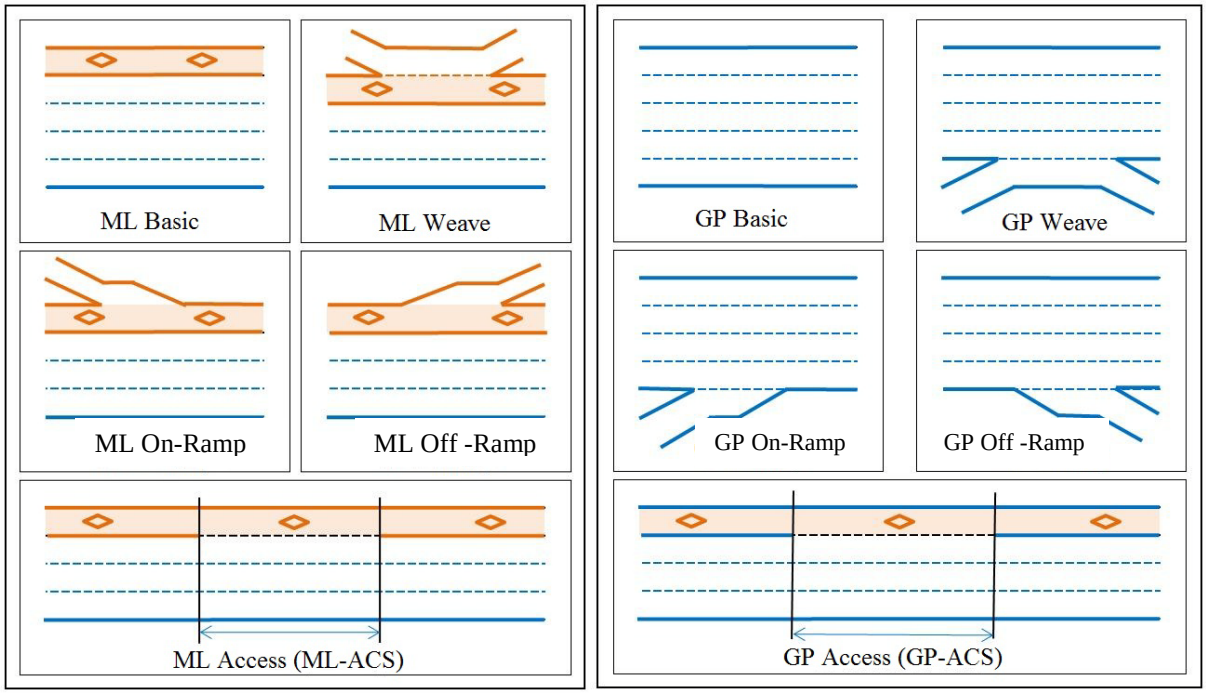

Exhibit 1 Different Segment Types for ML and GP Lanes

ML-AcS's are potential bottlenecks for an ML facility due to the interaction between ML-AcS and GP-AcS. ML access point design plays an important role in operational performance of ML facilities, in addition to the level of interactions between the ML and GP lanes. As illustrated in Exhibit 2, there are three principal types of ML access configurations in practice:

A. **At-Grade Lane-change Access (Type A)** occurs where ML traffic enters the GP lanes through a conventional on-ramp roadway (from the right), weaves across multiple GP lanes, and then enters the ML facility. ML traffic exits in the same segment, so this configuration is also a

form of a weaving movement. This access strategy is common for concurrent ML facilities. Access between ML and GP lanes is sometimes constrained to specific locations or openings, which affects the weaving intensity at these access points, as well as the intensity of the two-sided weaving maneuver across the GP lanes. The Type A access configuration requires a *cross-weaving* movement across GP lanes for drivers to position themselves prior to the access point, and a *lane-change movement* to get from the GP lane into the ML.

B. **At-Grade Ramp Access (Type B)** occurs where ML traffic enters the GP lanes through a conventional on-ramp roadway (from the right). Entering/exiting traffic may weave across multiple GP lanes (similar to Case A above), but the entrance to (or exit from) the ML facility is confined to an at-grade on-ramp or off-ramp. Operationally, the GP lanes may be affected by the cross-weaving flow, as well as by the friction caused by the on- and off-ramps. The ML lane operations are in turn affected by the cross-weaving maneuvers to and from the access points at the ramps. The Type B access configuration requires a *cross-weaving* movement across GP lanes for drivers to position themselves prior to the access point, and a *ramp movement* to get from GP into the ML.

C. **Grade-Separated Ramp access (Type C)** occurs where access to the MLs occurs on a grade-separated structure (i.e. flyover, bridge, or underpass). The operational impact to the GP lanes is minimal in this case, since the cross-weaving movement is eliminated entirely. The MLs are affected by friction from the entering or exiting ramp flows in the normal fashion as GP lanes. The Type C access configuration does not require any cross-weaving across GP lanes due to a grade separated ramp, and the ML access is handled by a *ramp movement*.

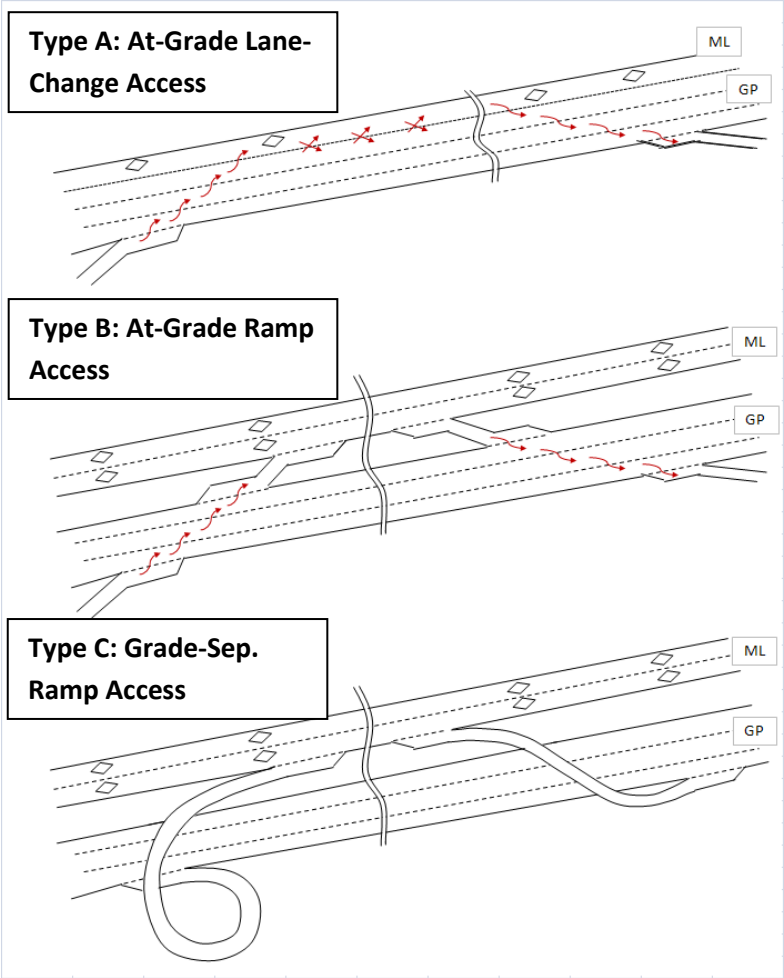

Exhibit 2 Typology of ML Access Point Designs

The spatial extent of the *Access-Point Influence Area* (APIA) for Type C is already defined in HCM ramp junction methodologies. The ramp influence area for GP facilities is defined as 1,500 feet from the ramp gore for both on-ramps (measured downstream) and off-ramps (measured upstream). The APIA for Type-C ML access points is assumed to follow the same convention.

For Types A and B access points, the intensity and impact of the *cross-weaving (CW) flows* between a GP ramp and the access region between the GP and MLs need to be analyzed. The minimum cross-weave length ($L_{CW\text{-}Min}$) is defined as the distance between the closest upstream GP on-ramp gore and the start of the ML access opening. The maximum cross-weave length ($L_{CW\text{-}Max}$) is defined as the distance from the ramp gore to the end of the access opening. Exhibit 3 illustrates this concept for a concurrent single ML next to three GP lanes with stripe-separation. In this case, on-ramp vehicles trying to enter the ML must complete all three lane-change maneuvers (not counting the merge from the acceleration lane), resulting in a cross-weave friction on the GP lane traffic. It is indicated in the report for NCHRP 03-96 *(1)* that most drivers attempt to complete the lane change maneuver as early as possible, resulting in lower operating

speed and capacity on the GP lanes prior to the ML access point. The overall cross-weave intensity can be estimated based on the number of lane change maneuvers, minimum and maximum available distances to complete all lane changes ($L_{CW\text{-}Min}$ and $L_{CW\text{-}Max}$), as well as the cross-weave demand. Beyond the effect of cross-weaves, intermittent-access MLs are analyzed as regular weaving segments using the HCM 2010 procedures.

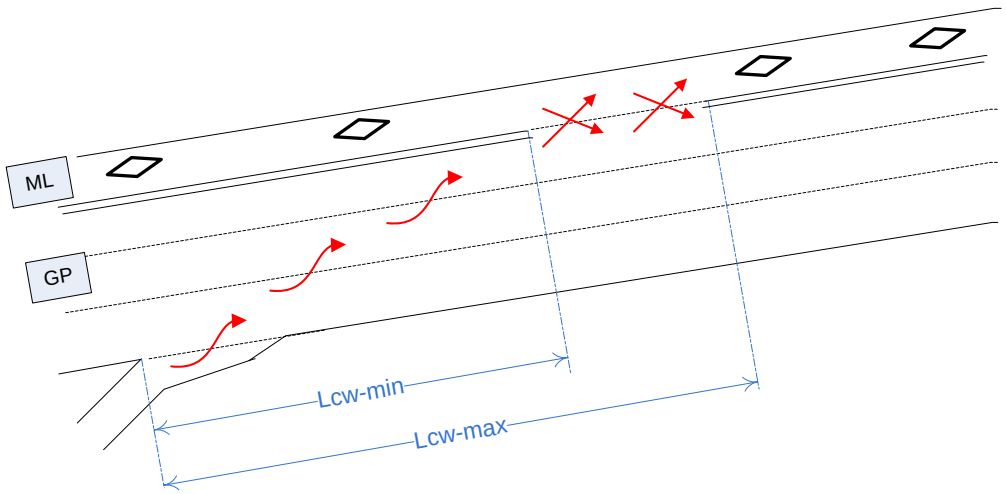

Exhibit 3 Defining Dimensions of APIA through Minimum and Maximum Cross-Weave Lengths

THE LANE GROUP CONCEPT

To capture the interaction effects between ML and GP lanes, while allowing for the varying demand, capacity, and speed inputs, the concept of *lane groups* is introduced for freeway MLs. The lane group concept is well-established in the signalized intersection methodology of the HCM 2010 *(2)*, where it is recognized that exclusive left turn lanes have different geometric and/or behavioral characteristics from the adjacent through lanes, or from shared lanes. By adopting the lane group concept in the ML context, the analyst will be able to ascribe separate attributes to parallel ML and GP facilities, while retaining the ability to model some degree of interaction between the two.

Each segment of a freeway facility is represented as having either one or two lane groups, depending on whether a concurrent ML segment is present. Input variables such as geometric characteristics (e.g., number of lanes), traffic performance attributes (e.g., free-flow speed, capacity), and traffic demands must be entered separately for each lane group. The methodology is then applied to assess the operational performance of each lane group, under consideration of empirically-derived interaction effects between the two lane groups. If a portion of the facility has no ML, then it is simply coded as a single GP lane group that serves all traffic demands.

The following principles apply to the proposed methodology:

- A freeway GP segment with a parallel ML segment is considered as two adjacent lane groups.
- Adjacent lane groups (one GP and one ML segment) must share the same segment lengths.
- Adjacent lane groups can be of different segment types. For example, a basic ML segment may be concurrent with an on-ramp GP segment.
- A lane group may have different geometric characteristics, including number of lanes, lane widths, shoulder clearance, etc.
- A lane group may have unique attributes, including free flow speed, segment capacity, or various capacity- or speed-reducing friction factors. The attributes representing the GP speed-flow relationships are those cited in the HCM 2010 (*2*) freeway facility methodology. Many ML-specific relationships have been derived empirically in NCHRP 3-96 (*1*).
- A lane group may have unique traffic demand parameters, which are entered by the user, and are obtained through an external process. As an operational methodology, the HCM does not make predictions on the split in demand between ML and GP lanes.
- The operational performance of adjacent ML and GP lane groups is interdependent in that congestion in one lane group may have a frictional effect on operations in the adjacent lane group. This friction effect was empirically-derived, can be user-calibrated, and is sensitive to the type of physical separation between lane groups (i.e., striping vs. buffer vs. barrier).

The method assumes that all ML segments operate at a demand-to-capacity ratio less than 1 (d/c<1), which means that no queuing or oversaturation would occur on ML segments. Oversaturated ML facilities are relatively rare in practice, as one of the underlying principles for ML operations (especially for the newly emerging HOT lanes) is to assure that ML traffic density is below the critical density even in peak periods, which in turn guarantees satisfactory service to ML customers. Congestion on GP lanes can and should be considered by the method, as many facilities operate in the peak periods with congested GP lanes and below-capacity ML volumes.

BASIC ML SEGMENTS SPEED-FLOW RELATIONSHIPS

Type of Segments

For this class of ML segments, the separation type and number of lanes are the key factors that affect traffic flow behavior. A basic ML segment can be categorized into one of the five segment types, including Continuous Access, Buffer 1, Buffer 2, Barrier 1, and Barrier 2. Each of the five segment types is described below:

1) **Continuous Access** – Skip-stripe or solid single line separated, single lane, continuous access

Continuous Access separation type refers to single lane, concurrent ML facilities in which access between the ML and GP lanes is allowed at any point. Entrances and exits to the MLs are

unrestricted. These facilities are typically located on the leftmost lane on freeways, parallel to the GP lanes. Exhibit 4 shows a schematic of this configuration. The solid single line separating the ML from the GP lanes can also be skip-striped. Either way, vehicles can cross between the ML and GP lanes at any time. I-5 in Seattle, Washington is the example of a Continuous Access facility shown in Exhibit 4. These types of facilities are very common and are more favorable to HOV than HOT lane operations though continuous access is more difficult to manage for most tolling schemes.

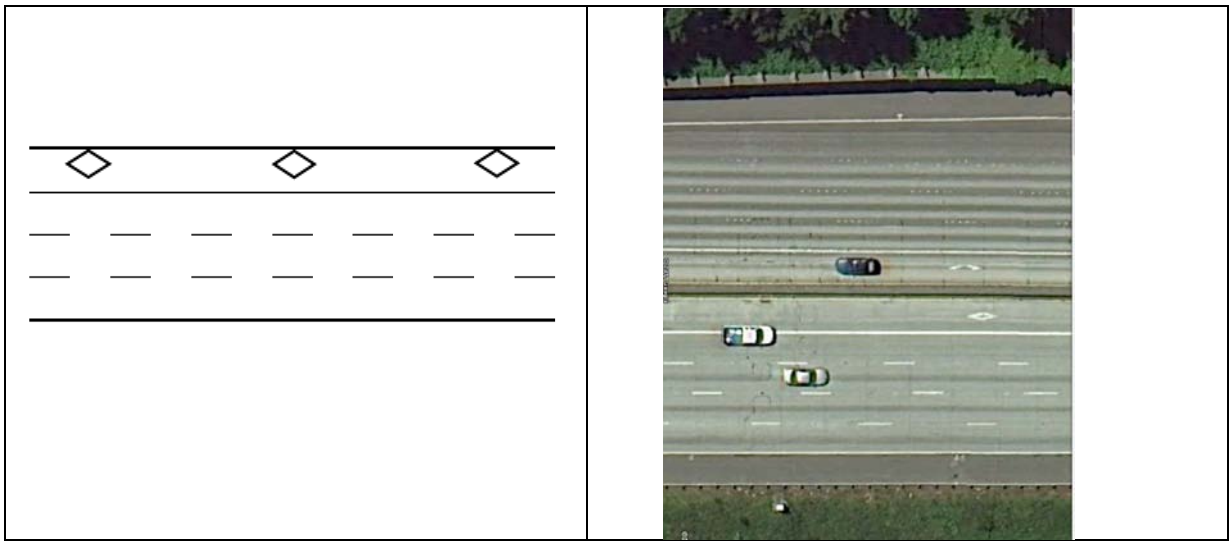

Exhibit 4 Schematic of Continuous Access and Example at I-5 Seattle, Washington (Source: Google Earth)

2) **Buffer 1** – Buffer-separated, single lane

Buffer 1 refers to a single, concurrent lane ML facility with intermittent access. Similar to Continuous Access, these facilities are located in the leftmost lane of the freeway cross section. They are separated from the GP lane with a striped buffer. The striping techniques for Buffer 1 vary by location, and can feature a double white line, a double yellow line, or two yellow stripes and one white stripe (as is typical in California). Access to and from the ML is limited to occasional buffer opening areas designated by dashed line separation. This geometry is commonly used for both HOV and HOT facilities. Exhibit 5 shows the basic schematic of a Buffer 1 facility along with an example at I-394 in Minneapolis, Minnesota. Note that the buffer opening itself is analyzed as a different ML segment type.

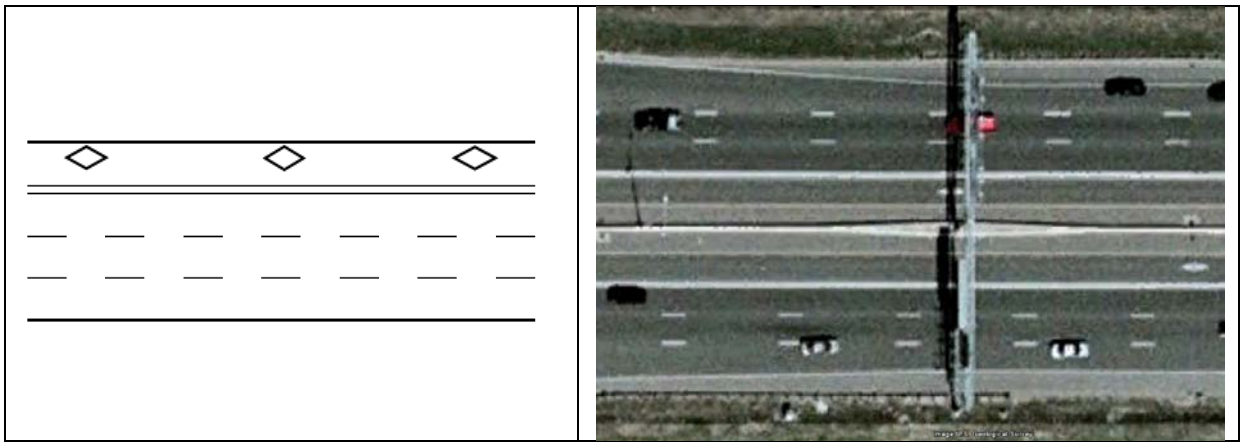

Exhibit 5 Schematic of Buffer 1 and Example at I-394 in Minneapolis, Minnesota (Source: Google Earth)

3) **Buffer 2** – Buffer-separated, multiple lanes

Buffer 2 is similar to type Buffer 1 but with multiple MLs. It is generally separated from the GP lanes with a buffer consisting of various painting schemes. This type of facility is the rarest of the five facility types studied, although it may become more common in future deployments. I-110 in Los Angeles, California is an example of a location with this type of configuration. Exhibit 6 displays a schematic of the facility type and an aerial view of I-110 in Los Angeles, California.

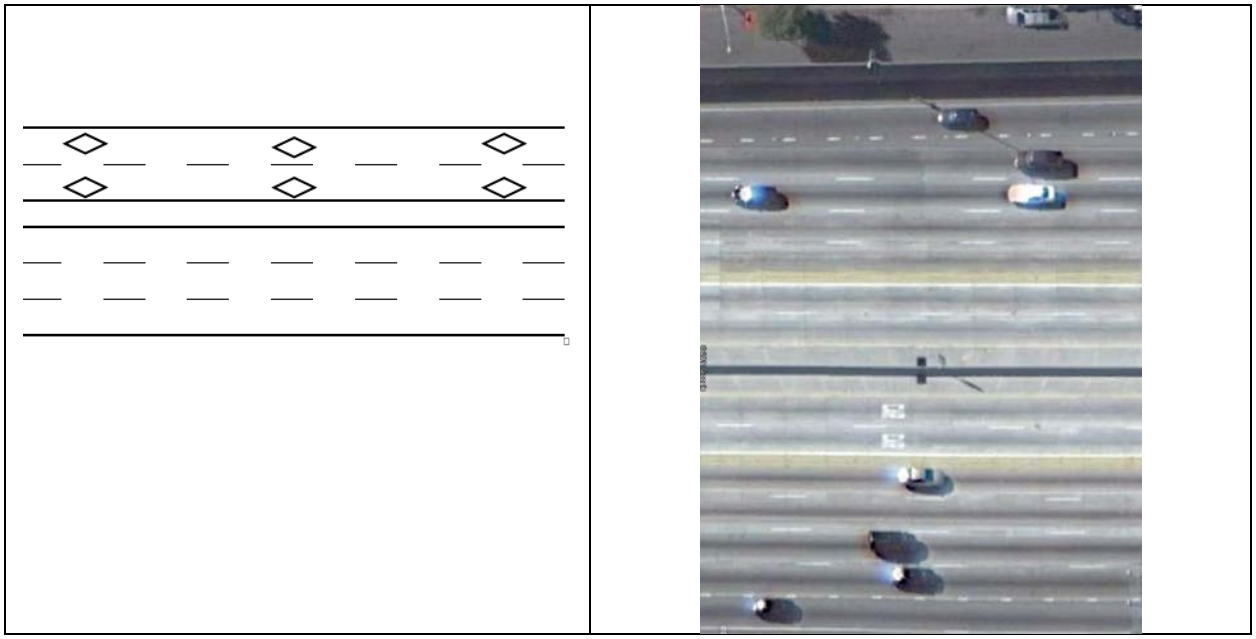

Exhibit 6 Schematic of Buffer 2 and Example at I-110 Los Angeles, California (Source: Google Earth)

4) **Barrier 1** – Barrier-separated, single lane

Barrier 1 refers to a barrier-separated ML facility with a single lane. The barrier in all facilities refers to a concrete barrier. Other physically separating schemes such as raised delineators or landscaping can also be considered as barrier-separated. This facility type is suitable for HOV, HOT, and express lanes. Exhibit 7 shows the schematic of Barrier 1 separation and an example of Barrier 1 with an aerial view of I-5 in Orange County, California.

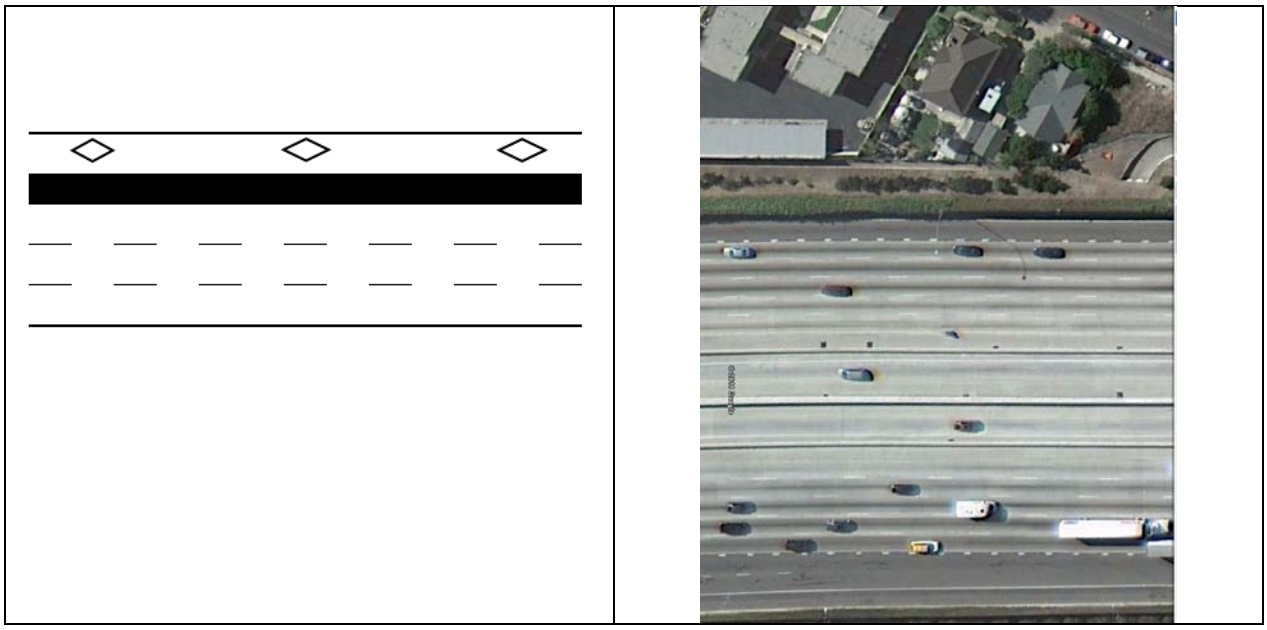

Exhibit 7 Schematic of Barrier 1 and Example at I-5 in Orange County, California (Source: Google Earth)

5) **Barrier 2** – Barrier-separated, multiple lane

Barrier 2 refers to a barrier-separated ML facility with multiple lanes. The barrier can consist of a concrete barrier, raised delineators or wide landscaped separation. Access between the MLs and GP lanes is limited and can be in the form of either a weave access, or direct ramp access. This type of facility is commonly used for HOV, HOT, and express lanes. Exhibit 8 shows a sample schematic of the Barrier 2 configuration and an image of I-5 in Seattle, Washington is shown as an example of a Barrier 2 facility.

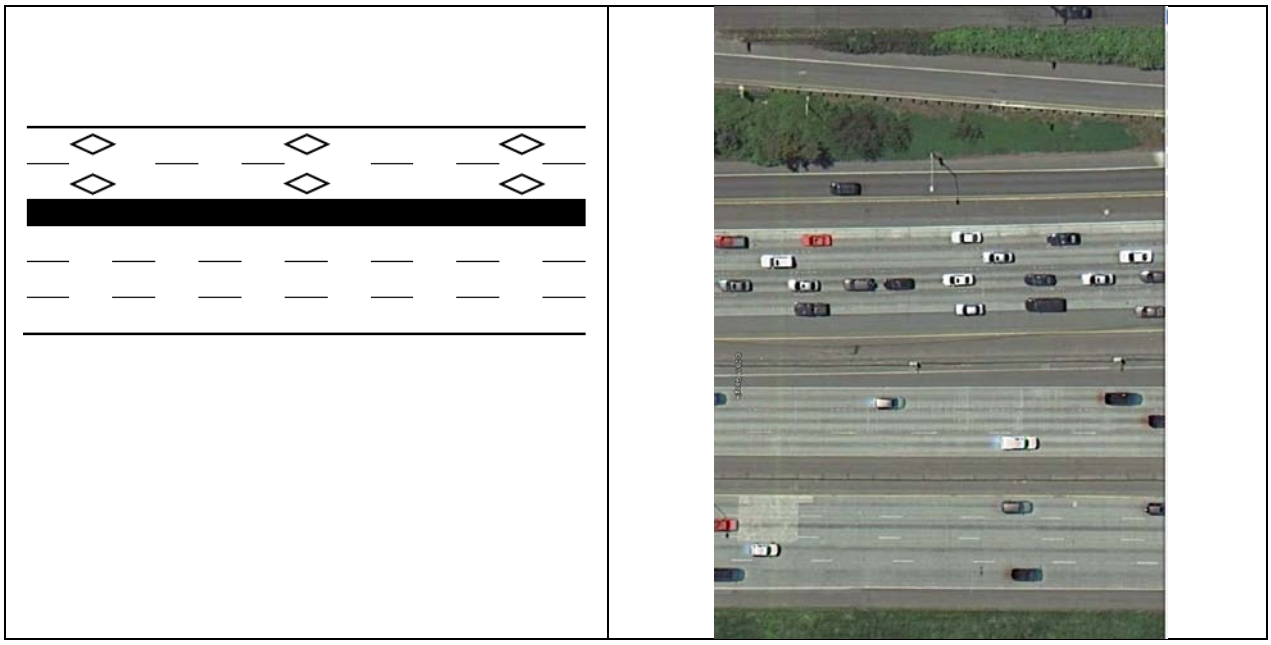

Exhibit 8 Schematic of Barrier 2 and Example at I-5 in Seattle, Washington (Source: Google Earth)

BASIC ML SEGMENT CHARACTERISTICS

Three traffic performance characteristics on ML facilities were found distinguishable from GP lanes. They can be categorized in the following three dimensions:

1) Single lane ML operations are affected by the inability to pass slow moving vehicles. This can result in slower facility speeds than those of GP lanes serving the same per-lane traffic demands.

The slow car following effect for ML facilities is defined as the degradation in speed in a single-lane ML facility, due to the inability for faster vehicles to pass slower vehicles. Exhibit 9a provides an example of the speed-flow plot for a Buffer 1 separated facility. Exhibit 9b provides an example of a speed flow plot for a Buffer 2 separated facility. The major difference between the two shapes of the curves can be seen on the left side of the data plot under low flow conditions. The Buffer 1 facility shows a negative slope in the low flow section of the curve while the Buffer 2 facility shows virtually a horizontal line in the same flow range. Under low flow demand, the Buffer 2 separation type maintains its relatively constant free flow speed while the Buffer 1 speed decreases with an increase in flow. Exhibit 9c shows an example plot of speed-flow data from a facility with Continuous Access. Although the Continuous Access facility consists of only one lane, passing can occur on the facility to and from the contiguous GP lane under low flow scenarios. Thus, as long as there is an acceptable gap in the adjacent GP lane and speeds in the GP lane are not below that of the vehicle in the ML, a passing maneuver

can be completed through the GP lane. Therefore, for the Continuous Access facilities, the speed is constant (equals FFS) and does not decline with increasing flow up until the break point.

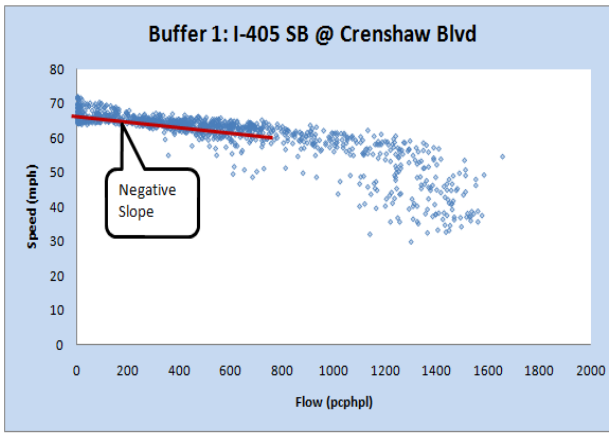

(a) Buffer 1 Facility

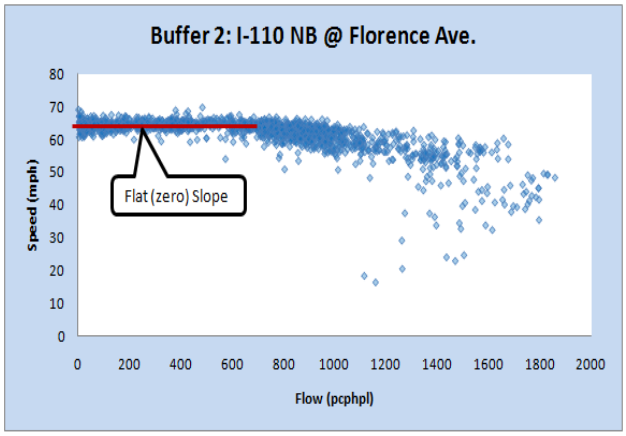

(b) Buffer 2 Facility

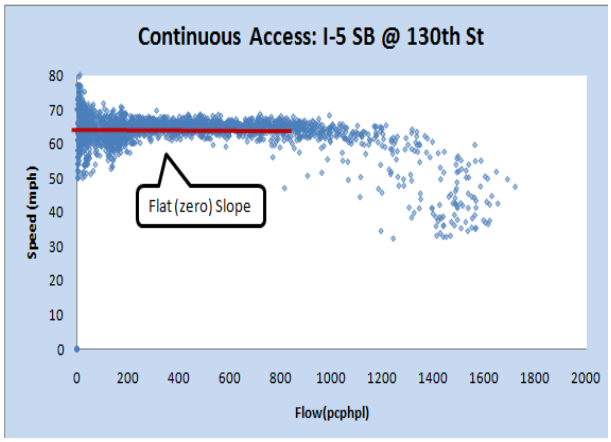

(c) Continuous Access Facility

Exhibit 9 Slow Vehicle Following Effect

2) ML operations are sensitive to congestion in GP lanes under certain separation conditions. Vehicles in the ML(s) will tend to slow down to reduce the discomfort associated with high speed differentials with adjacent traffic, possibly in anticipation of a sudden lane change from the slow GP to the faster ML. This phenomenon typically occurs when traffic density in the GP lanes is at or exceeds 35 pcpmpl.

Congested GP lanes have an adverse effect on the adjacent MLs. This frictional effect is stronger on facilities with minimal physical separation such as the Continuous Access and Buffer 1 cases *(3)*. Exhibit 10 visually illustrates this effect for a Continuous Access facility. In Exhibit 10a, all of the speed-flow data are shown. There is a wide spread in the data from a flow of 600 pcphpl to 1700 pcphpl. This trend is atypical for what is usually seen in GP lane speed flow curves, which normally show little variance in speed between conditions of equal flows.

When the data are segregated based on the quality of operations in the GP lanes as shown in Exhibit 10b, the reason for the dispersion of speed can be ascertained. A density of 35 pcpmpl is used as a threshold for the drop in performance of the GP facility. This particular threshold was selected as it serves as the transition point from LOS D to LOS E in the HCM 2010. During periods of time where the GP lane has a density greater than 35 pcpmpl, lower speeds can be observed on the ML. The lack of continuity of the curve can be seen as breakdown appears to occur at different levels of flow depending on the GP lane's performance.

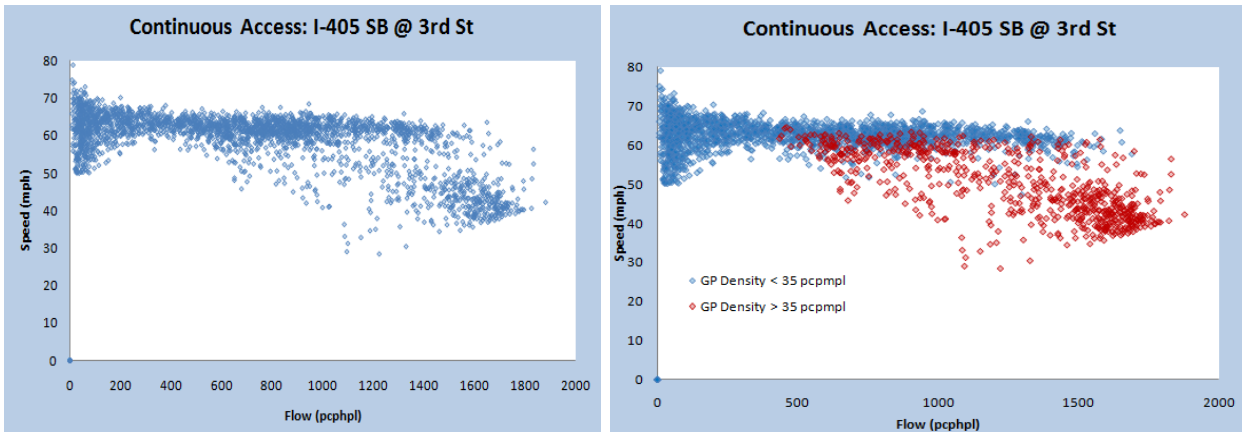

(a) All ML Data Points **(b) Paired ML Data Points by GP Density**

Exhibit 10 Continuous Access Facility at I-405 SB @ 3rd St, King County, Washington

3) Lower ML Capacity – Following the more restrictive speed-flow relationship of MLs as shown in Exhibit 10, ML capacity can be predicted lower than that of GP lanes under the same conditions. However, it should be mentioned that no recurrent breakdown conditions were observed in the MLs during the course of the field observations, so further studies are needed to quantify ML capacities under different traffic and geometric conditions.

2. BASIC ML SEGMENT SPEED-FLOW RELATIONSHIP

Speed-flow curves have been developed for the different basic ML segment types. For each segment type, there are five curves, one for each of the five free-flow speeds: 75 mi/h, 70 mi/h, 65 mi/h, 60 mi/h, and 55 mi/h. There are two clear ranges in the shape of the curves:

- At flow rates from 0 to the breakpoint, the segment is linear. For Buffer 1 and Barrier 1, the speed declines linearly with increasing flow due to the slow moving vehicle effect. For all other segment types, FFS prevails.
- At flow rates between the breakpoint and the maximum observed flows, speeds decline along a curvilinear trend.

For Continuous Access and Buffer 1 segment types, as the frictional effect takes hold, a second set of curves is adopted to show the speed-flow relationship under the frictional effect during GP lane congestion. When the adjacent GP lane is congested (GP density ≥ 35 pcpmpl), the frictional curve comes into play. It is a function of both the non-friction curve and the flow rate. FFS should be rounded to the nearest 5 mi/h as follows:

· ≥72.5 mi/h < 77.5 mi/h - use FFS = 75 mi/h.
· ≥67.5 mi/h < 72.5 mi/h - use FFS = 70 mi/h.
· ≥62.5 mi/h < 67.5 mi/h - use FFS = 65 mi/h.
· ≥57.5 mi/h < 62.5 mi/h - use FFS = 60 mi/h.
· ≥52.5 mi/h < 57.5 mi/h - use FFS = 55 mi/h.

No attempt should be made to interpolate between basic curves.

CONTINUOUS ACCESS SEGMENTS

Exhibit 11 shows the proposed speed-flow relationships for each FFS for the Continuous Access segment type. Non-friction curves are shown as solid lines, while the corresponding friction curves are shown as dashed lines. Exhibit 12 shows the models defining each of the curves in Exhibit 11.

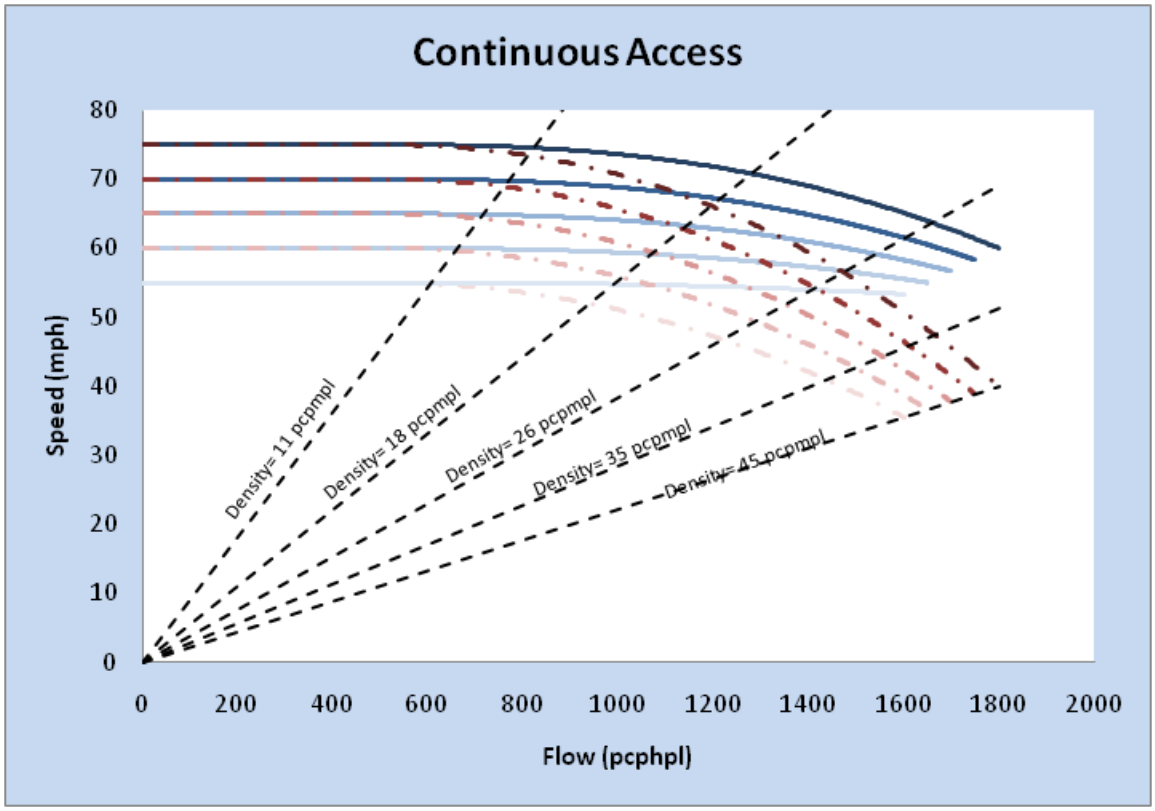

Exhibit 11 Continuous Access Speed-Flow Curves

Exhibit 12 Equations Describing Speed-Flow Curves for Continuous Access

FFS (mph)	Flow Rate Range	
	0 - 500 pc/hr/ln	500 pc/hr/ln - Max. Flow*
75	75	$75 - (2.46 \times 10^{-7}(v_p\text{-}500)^{2.5}) - (0/1)(1.18 \times 10^{-5}\ (v_p\text{-}500)^2)$
70	70	$70 - (2.12 \times 10^{-7}(v_p\text{-}500)^{2.5}) - (0/1))1.24 \times 10^{-5}\ (v_p\text{-}500)^2)$
65	65	$65 - (1.67\times 10^{-7}(v_p\text{-}500)^{2.5}) - (0/1)(1.31 \times 10^{-5}\ (v_p\text{-}500)^2)$
60	60	$60 - (1.12\times 10^{-7}(v_p\text{-}500)^{2.5}) - (0/1)(1.39 \times 10^{-5}\ (v_p\text{-}500)^2)$
55	55	$55 - (4.15\times 10^{-8}(v_p\text{-}500)^{2.5}) - (0/1)(1.47 \times 10^{-5}\ (v_p\text{-}500)^2)$

*(0/1) represents values for non-friction (0) and friction (1) curves, respectively

It should be noted here that the friction curves terminate at a density of 45 pcpmpl, which is consistent with the methodology used in HCM 2010 Chapter 11. The range of observed data for the non-friction curves never reached a density level this high. This is probably attributable to a low likelihood of observing non-friction cases in combination with high flow rates. As a result, the terminal density of the non-friction curves is 30 pcpmpl.

BUFFER 1 SEGMENTS

Exhibit 13 shows the speed-flow relationships for each FFS for the Buffer 1 segment type. Non-friction curves are shown as solid lines, while the corresponding friction curves are shown as dashed lines. The speed-flow equations are provided in Exhibit 14.

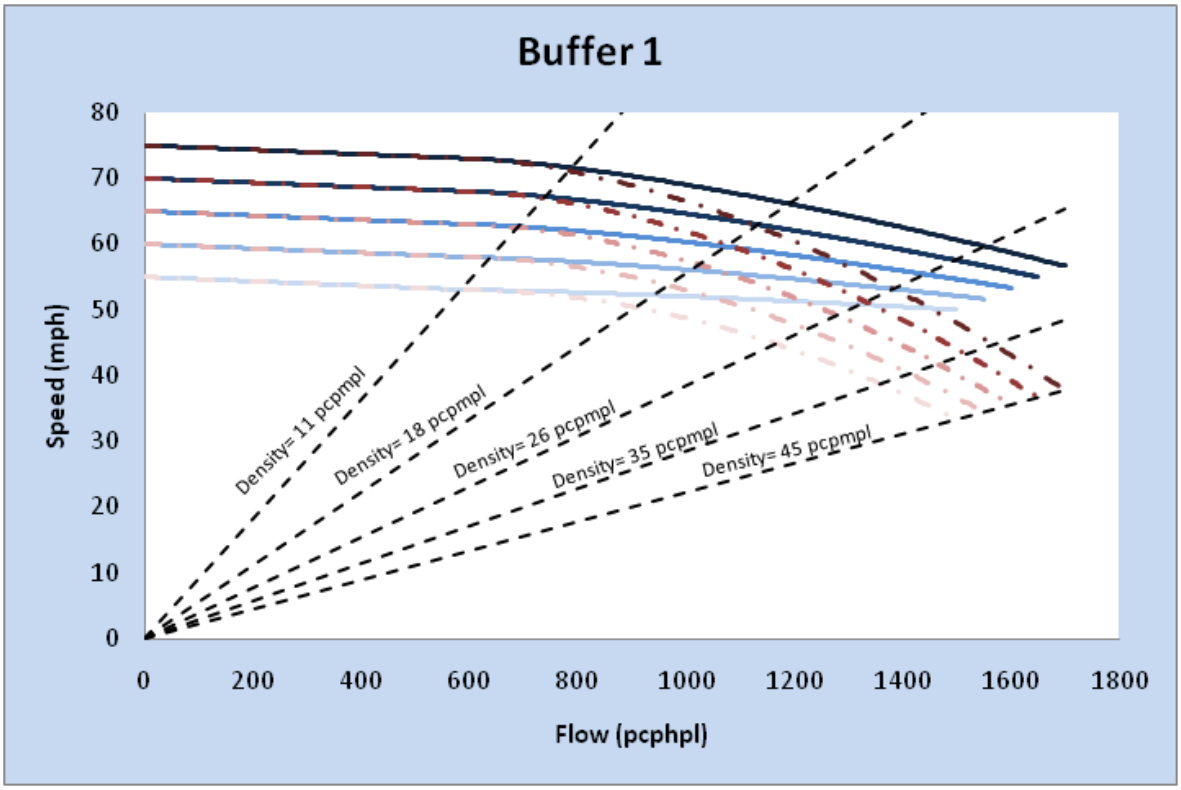

Exhibit 13 Buffer 1 Speed-Flow Curves

Exhibit 14 Equations Describing Speed-Flow Curves for Buffer 1

	Flow Rate Range	
FFS (mph)	**0 - 600 pc/hr/ln**	**600 pc/hr/ln – Max. Flow***
75	$75 - .00333(v_p)$	$73 - 0.00090(v_p\text{-}600)^{1.4} - (0/1)(1.38 \times 10^{-5} (v_p\text{-}600)^2)$
70	$70 - .00333(v_p)$	$68 - 0.00077(v_p\text{-}600)^{1.4} - (0/1)(1.46 \times 10^{-5} (v_p\text{-}600)^2)$
65	$65 - .00333(v_p)$	$63 - 0.00061(v_p\text{-}600)^{1.4} - (0/1)(1.56 \times 10^{-5} (v_p\text{-}600)^2)$
60	$60 - .00333(v_p)$	$58 - 0.00043(v_p\text{-}600)^{1.4} - (0/1)(1.66 \times 10^{-5} (v_p\text{-}600)^2)$
55	$55 - .00333(v_p)$	$53 - 0.00022(v_p\text{-}600)^{1.4} - (0/1)(1.65 \times 10^{-5} (v_p\text{-}600)^2)$

*(0/1) represents values for non-friction (0) and friction (1) curves, respectively

As with the Continuous Access curves, the non-friction curves terminate at a density of 30 pcpmpl as higher densities were not observed during periods of time where the GP lanes were not congested. The set of friction curves terminates at a density of 45 pcpmpl.

BUFFER 2 SEGMENTS

Exhibit 15 shows the speed-flow relationships for each FFS for the Buffer 2 segment type. There is only one set of curves, because there is no frictional effect observed for this type of segment. The formulae describing speed-flow relationships are provided in Exhibit 16.

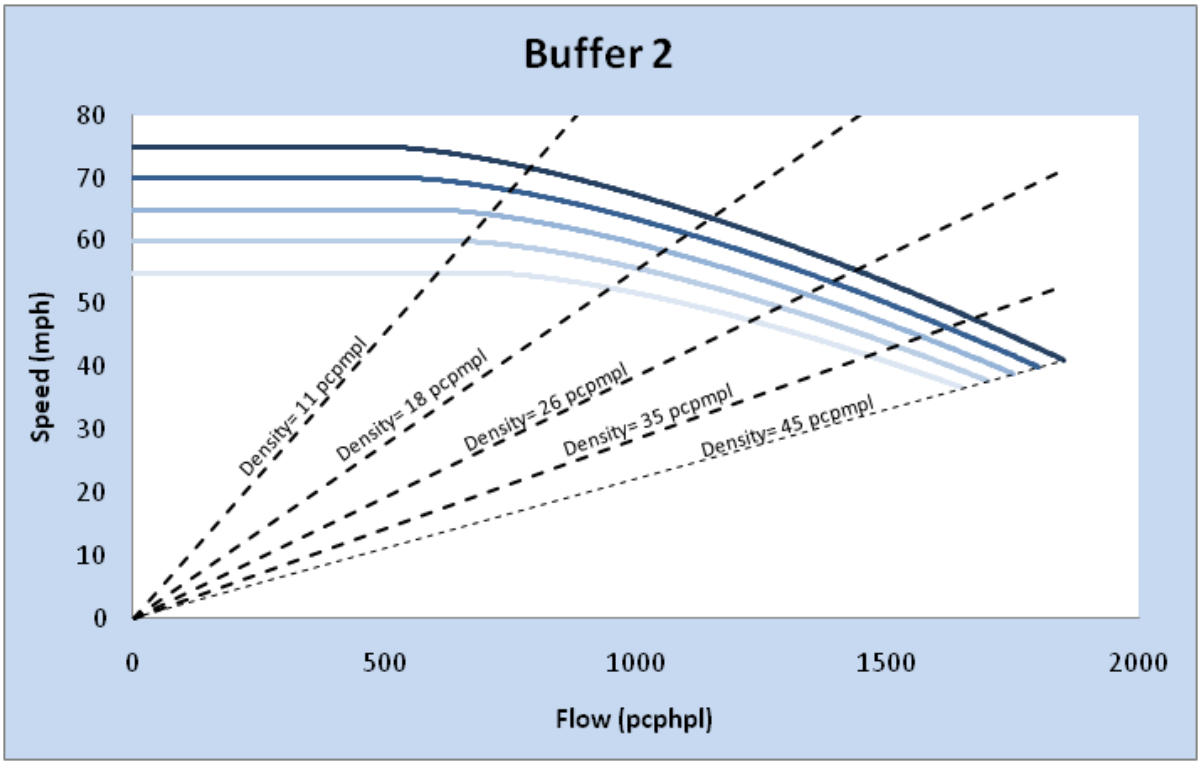

Exhibit 15 Buffer 2 Speed Flow Curves

Exhibit 16 Equations Describing Speed-Flow Curves for Buffer 2

FFS (mph)	Flow Rate Range	
	0 – Breakpoint pc/hr/ln	Breakpoint – Max Flow pc/hr/ln
75	75	$75 - 0.000683(v_p-500)^{1.5}$
70	70	$70 - 0.000679(v_p-550)^{1.5}$
65	65	$65 - 0.000670(v_p-600)^{1.5}$
60	60	$60 - 0.000653(v_p-650)^{1.5}$
55	55	$55 - 0.000626(v_p-700)^{1.5}$

BARRIER 1 SEGMENTS

Exhibit 17 shows the speed-flow relationships at each FFS level for the Barrier 1 segment type. The linear portion of the curve is sloped from the flow range of 0 to the breakpoint due to the slow-car following effect. The formulae showing speed flow relationships are provided in Exhibit 18.

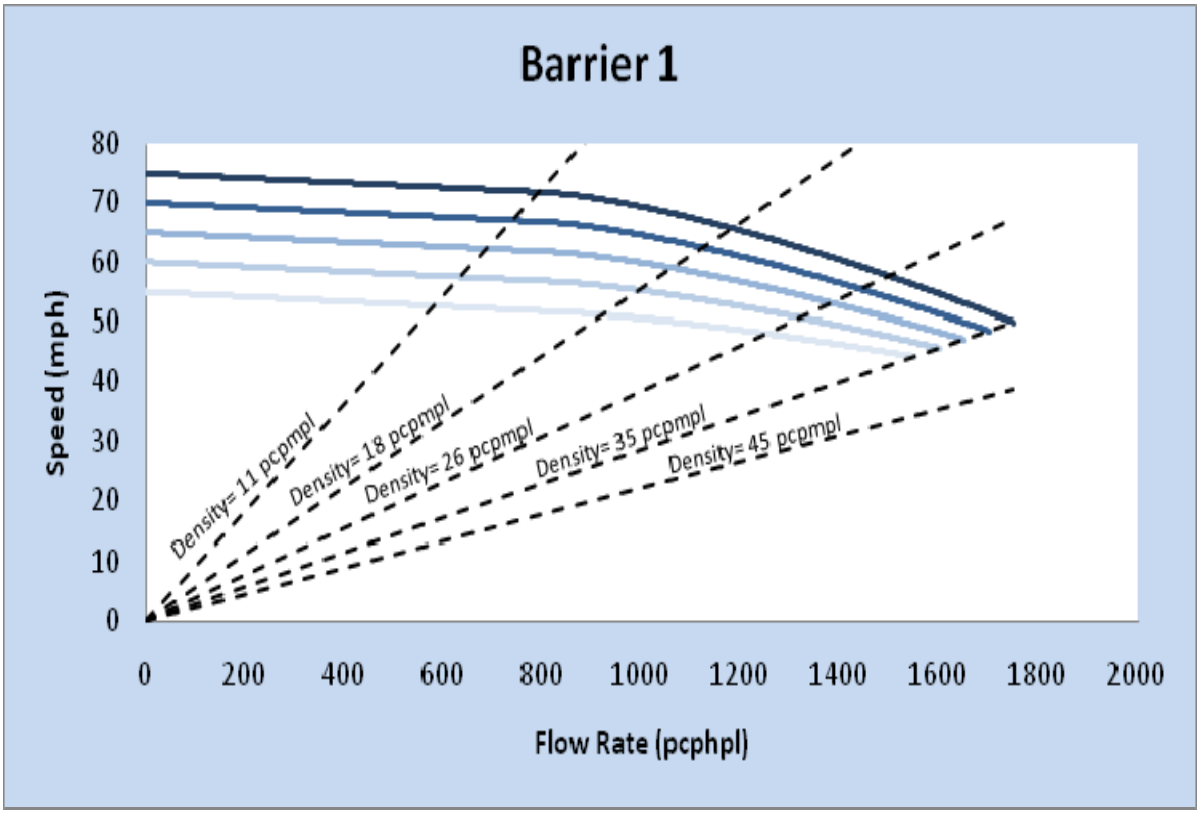

Exhibit 17 Barrier 1 Speed-Flow Curves

Exhibit 18 Equations Describing Speed-Flow Curves for Barrier 1

	Flow Rate Range	
FFS (mph)	**0 - Breakpoint pc/hr/ln**	**Breakpoint – Max. Flow (pc/hr/ln)**
75	$75-(0.004v_p)$	$71.8 - 00148(v_p-800)^{1.4}$
70	$70-(0.004v_p)$	$66.8 - 0.00133(v_p-800)^{1.4}$
65	$65-(0.004v_p)$	$61.8 - 0.00116(v_p-800)^{1.4}$
60	$60-(0.004v_p)$	$56.8 - 0.00096(v_p-800)^{1.4}$
55	$55-(0.004v_p)$	$51.8 - 0.00071(v_p-800)^{1.4}$

While the curves for many of the other facility types terminate at a density of 45 pcpmpl, the breakdown for Barrier 1 facilities was observed to occur at a lower density. The termination point for the Barrier 1 speed-flow curves was determined to be 35 pcpmpl. This lower density of

breakpoint could be attributable to driver behavior in this type of facility. Drivers may not feel as comfortable traveling at shorter headways. As barriers are present on both sides of the facility, there is little room to maneuver. Should a vehicle stop short, the trailing vehicle does not have the option of swerving to the right or left if the driver cannot brake in time due to the presence of the barriers. The reduction in acceptable car following headway would cause breakdown at a lower density.

BARRIER 2 SEGMENTS

The Barrier 2 speed-flow curve is similar to a basic freeway segment. It can essentially be thought of as its own independent facility as there is no slow car following or frictional effect. Exhibit 19 shows the speed-flow relationships for each FFS for the Barrier 2 type. The corresponding equations defining the curves are provided in Exhibit 20.

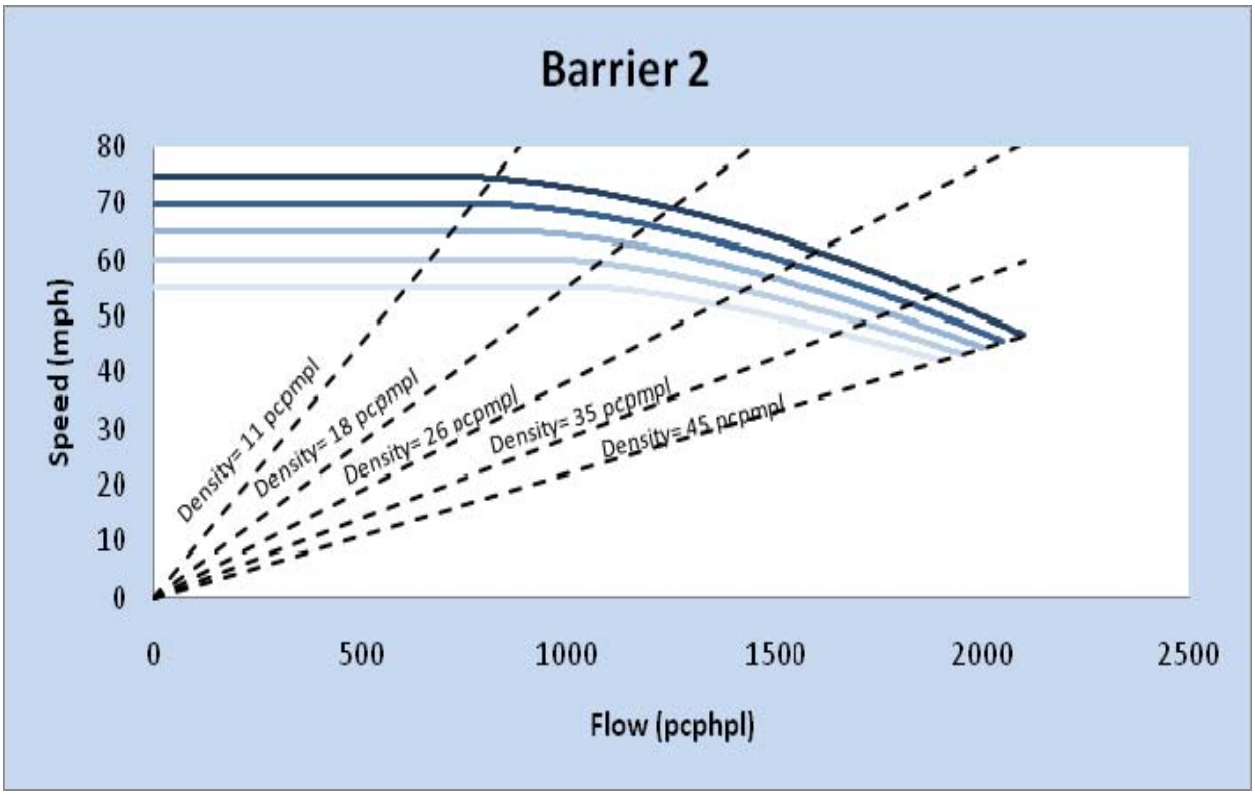

Exhibit 19 Barrier 2 Speed-Flow Curves

Exhibit 20 Equations Describing Speed-Flow Curves for Barrier 2

	Flow Rate Range	
FFS (mph)	**0 - BP pc/hr/ln**	**BP pc/hr/ln - Max. Flow**
75	75	$75 - (0.000127(v_p-700)^{1.7})$
70	70	$70 - (0.000271(v_p-800)^{1.6})$
65	65	$65 - (0.000563(v_p-900)^{1.5})$
60	60	$60 - (0.00113(v_p-1000)^{1.4})$
55	55	$55- (0.00215(v_p-1100)^{1.3})$

3. ADJUSTMENTS FOR CROSS-WEAVE EFFECTS

When estimating the GP segment capacity, the cross-weave adjustment should be taken into account to quantify the reduction in GP segment capacity from ML cross-weave flows. This adjustment should be applied where there is intermittent access to the ML over an access segment. If the upstream end of the access segment is relatively close to a GP entrance ramp, the resulting weaving maneuvers by vehicles attempting to access the ML will have a capacity-reducing impact on GP traffic operations. Research indicated that the impact of cross weave on *GP capacity reduction* is positively correlated with the level of cross-weave demand entering at the on-ramp and the number of lanes to be crossed. The impact of the cross-weave is negatively correlated with the distance between the on-ramp gore and the access point. One can think of that effect as akin to a 2-sided weaving segment in the HCM 2010. Due to the difficulties in observing these relationships on field, microscopic simulation models were developed and calibrated to quantify the cross-weave effects.

This *capacity reducing effect* is reflected through a set of Capacity Reduction Factors (CRF) or conversely the HCM Capacity Adjustment Factors (CAF). A CRF is expressed as a function of the base capacity C_{base} and the cross-weave capacity C_{cw}. The CRF and CAF can be estimated as follows:

$$CRF = \frac{C_{base} - C_{cw}}{C_{base}}, \quad CAF = 1 - CRF$$

The CRF is estimated as a function of the number of GP lanes, cross-weave flows, and length of $L_{CW\text{-}Min}$ (see Exhibit 3).

$$CRF(\%) = -8.957 + 2.52 \times \ln(CW) - 0.001453 \times L_{cw-min} + 0.2967 \times (No.\,of\ GP\ Lanes)$$

where CW is the cross-weave flow measured in pcph, $L_{CW\text{-}Min}$ is the length from the ramp gore to the beginning of BOA measured in ft, and number of GP lanes ranging from 2 to 4.

Exhibit 21 shows some sample results of CRF estimates for several common combinations of roadway geometries and cross-weave flow conditions.

Exhibit 21 CRF Estimates by Configuration Scenario

	$L_{CW\text{-}Min}$ (ft)	Cross-Weave Flow (vph)				
4 GP Lanes		100	200	300	450	600
	1500	1.6%	3.3%	4.5%	5.7%	6.5%
	2000	1.0%	2.2%	3.7%	4.7%	5.3%
	2500	0.2%	1.6%	3.3%	4.1%	4.7%
	$L_{CW\text{-}Min}$ (ft)	Cross-Weave Flow (vph)				
3 GP Lanes		100	200	300	450	600
	1500	1.2%	3.1%	3.9%	5.5%	6.1%
	2000	0.8%	2.0%	3.5%	4.3%	4.7%
	2500	0.2%	1.4%	2.6%	4.1%	4.3%
	$L_{CW\text{-}Min}$ (ft)	Cross-Weave Flow (vph)				
2 GP Lanes		100	200	300	450	600
	1500	1.0%	2.7%	3.7%	5.1%	5.3%
	2000	0.6%	2.0%	3.1%	4.3%	4.9%
	2500	0.0%	1.2%	2.2%	3.3%	4.1%

4. METHODOLOGY

This chapter's methodology can be used to analyze the capacity, level of service, and the effects of design features on the performance of ML freeway segments. The methodology is based upon the results of NCHRP 03-96 (*1*), which also referred to guidance provided by HCM 2010 (*2*). The methodology is implemented in the FREEVAL-ML 2011 computational engine. This chapter discusses the basic principles of the methodology.

LIMITATIONS

The methodology of this chapter does not apply to nor take into account (without modification by the analyst) the following impacts:

- Operational effects of oversaturated conditions in the MLs.
- Variations in the design of the start and end access points of ML facilities as well as the operational impact due to variations in the design of the termini.
- Demand-estimation for both ML and GP facilities, especially demand dynamics due to a pricing component that may be in effect on the ML.
- Facilities with free-flow speeds below 55 mi/h or above 75 mi/h.
- The spillback effect in the ML due to a downstream queue in the GP lanes.

In most of the cases cited above, an analyst would have to apply alternative tools or draw on other research information and/or apply customized modifications of this methodology to incorporate the effects of any of the above conditions.

OVERVIEW OF THE METHODOLOGY

The methodological flowchart that incorporates ML facilities is depicted in Exhibit 22. While both under-saturated and oversaturated scenarios are shown, the proposed enhancements to the method are limited to under-saturated conditions in the MLs. By design, the majority of ML facilities operate below capacity, especially when they include a pricing component (HOT lanes). It is therefore difficult to obtain ML performance data at breakdown, making the development of an empirical relationship impractical. It is therefore taken for granted that the operations of congested ML facilities are beyond the scope of the HCM method, and may be appropriate to analyze using simulation-based approach if necessary. This approach is consistent with the reference to alternative tools, a theme throughout the HCM 2010.

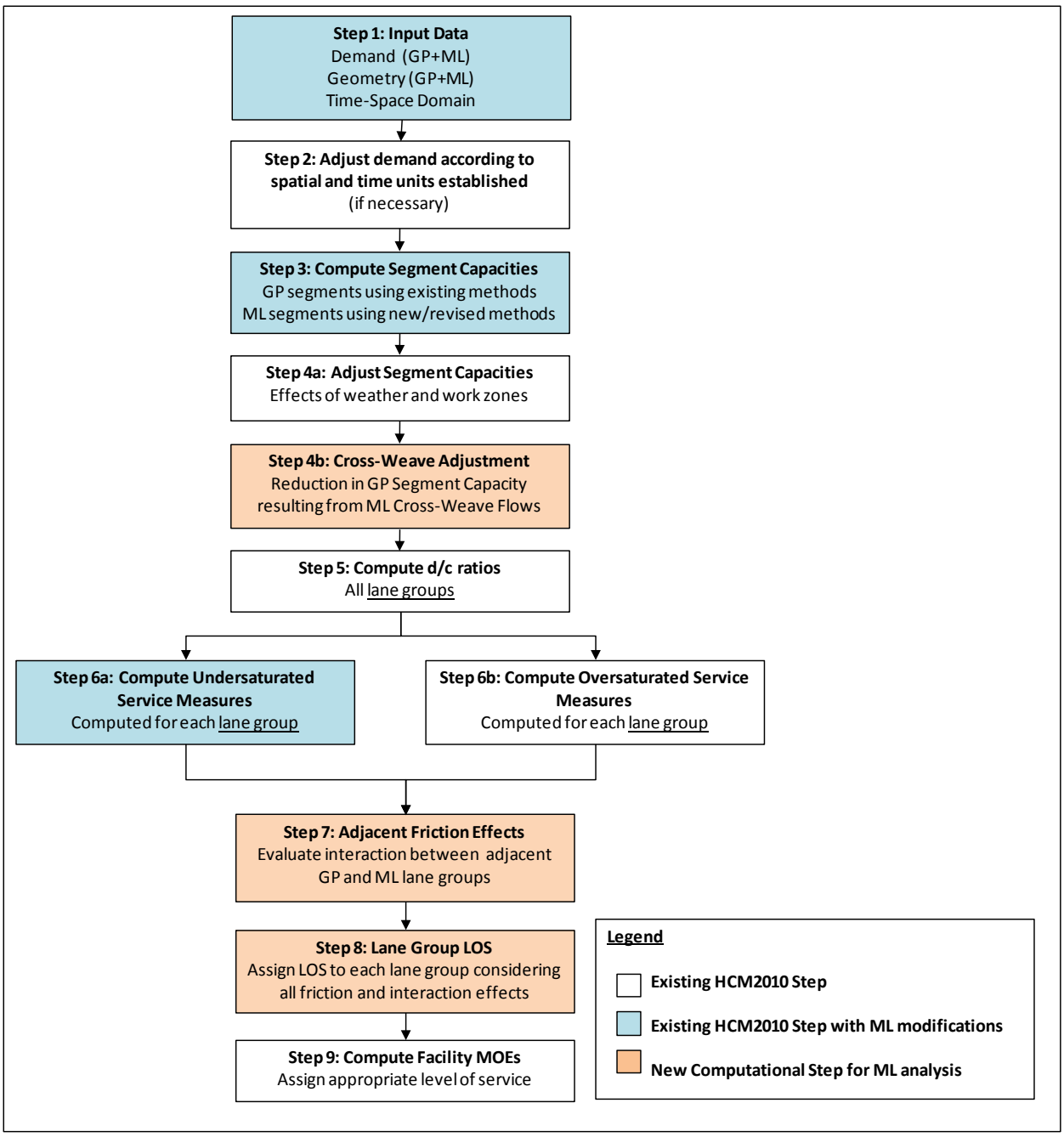

Exhibit 22 Methodological Flow Chart Incorporating MLs

COMPUTATIONAL STEPS

Step 1: Input Data

For a typical operational analysis, the analyst would need to specify demand volume, roadway geometric information, including number of lanes, lane width, right-side lateral clearance, total ramp density, percentage of heavy vehicles, peak hour factors, terrain, and driver population, just

as one would do for the freeway segment analysis following HCM 2010 Chapter 10. The only difference would be that with the introduction of lane group concept, the analyst would need to input the above information for ML and GP lane groups separately.

Also the time-space domain for the analysis needs to be established. When specifying the freeway sections included in the defined facilities, the segmentation would be slightly different from that for the GP-only freeway segment to preserve the lane group concept. Using Exhibit 23 as an example, with the absence of the parallel ML facility, the GP section would be treated as one weaving segment according to the HCM 2010 convention. However, since the ML lane group is presented, the segmentation needs to take into consideration of the ML segment types. Therefore, the GP lane group is divided into three segments: On-Ramp, Basic, and Off-Ramp.

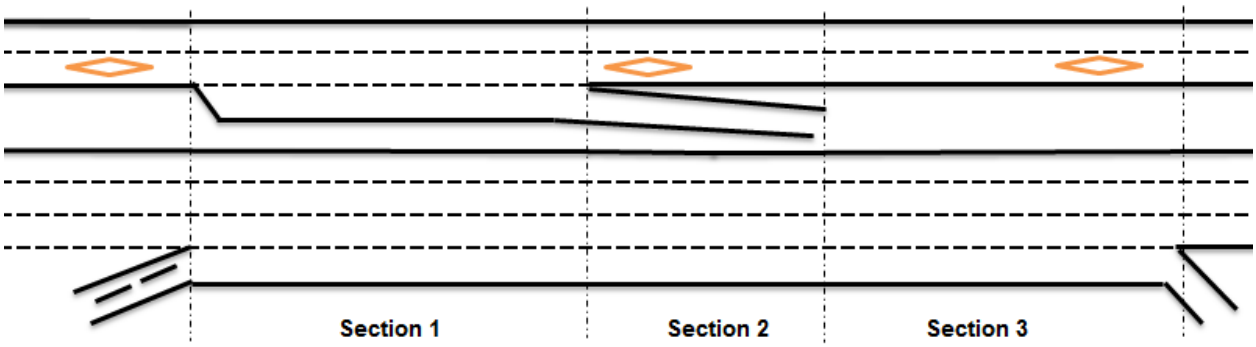

Exhibit 23 Graphical Representation of New Segmentation Method

Step 2: Adjust Demand According to Spatial and Time Units Established

This step is identical to the current HCM 2010 method. The sum of the input demands must equal to the sum of the output demands in every time interval. The demand estimation model proposed in HCM Chapter 10 is still valid for the freeway segments with ML component.

Step 3: Compute Segment Capacities

The capacity estimation for GP segments is not initially affected by the introduction of MLs. The GP segment capacity estimates are determined using the methodologies of Chapter 11 for basic freeway segments, Chapter 12 for weaving segments, and Chapter 13 for merge and diverge segments. For the ML segments, capacity estimates can be conducted using the speed-flow models developed for the ML basic segment, Chapter 13 for merge and diverge segments, and Chapter 12 for weaving segments.

Step 4a and Step 4b: Adjust Segment Capacities and Incorporate Cross-Weave Adjustments

Segment capacities would be adjusted in Step 4a for the presence of work zones, and/or due to adverse weather effects. The existing methods for estimating the capacity reduction in the HCM 2010 are adopted.

When adjusting the segment capacity, one unique segment, ML Access Segment, needs to be treated with care. This segment often exists in ML facilities with intermittent access. The segment itself is treated as weaving segment using HCM Chapter 12 to compute its impact. However, for the segments between an GP on-ramp and the ML Access Segment, or between the ML Access Segment and an GP off-ramp, the cross-weave module needs to be invoked to estimate the capacity reduction effects (if any) on the GP lanes due to the cross-weaving flows.

Step 5: Compute Demand-to-Capacity Ratios

Within each cell of the time-space unit, a demand-to-capacity ratio needs to be calculated for both lane groups. As explained in HCM 2010 Chapter 10, there are two possible outcomes:

1. If all cells have d/c ratios of 1.00 or less, then the entire time-space unit contains under-saturated flow.

2. If any cell has a d/c ratio greater than 1.00, then the time-space unit will contain both under-saturated and oversaturated cells. Analysis of oversaturated conditions is much more complex because of the interactions between freeway segments and the shifting of demand in both time and space. This condition may occur only for GP segments.

If Case 1 exists, the analysis moves to Step 6a. If Case 2 exists, the analysis moves to Step 6b. Note that for the ML group, the methodology is limited to the under-saturated conditions. It is assumed in this method that the operations of congested ML facilities are beyond the scope of the current HCM method, and will be reserved for a simulation-based analysis if necessary *(4)*.

Step 6a and 6b – Compute Undersaturated (6A) / Oversaturated (6B) Service Measures

Depending on the prevailing congestion levels in the GP lanes, either the under-saturated or oversaturated performance modules are invoked. It is assumed that the oversaturated methodology for GP lanes (Step 6b) will remain unchanged. For under-saturated operations (Step 6a), performance measures are estimated for each segment, under consideration of traffic demands and appropriate adjustments to segment capacity.

Step 7: Adjacent Friction Effects

The fact that ML performance is affected by GP lane traffic requires that the GP lane analysis be done prior to the ML analysis. When the GP lanes operate at densities above the specified

threshold, the friction-based speed prediction model should be invoked. When the GP lanes operate below the specified threshold, the non-friction-based speed prediction model needs to be invoked. This concept is applied to both Continuous Access and Buffer 1 Basic ML segments.

Step 8: Lane Group LOS

Upon the completion of the frictional effect adjustments, the LOS assignment for each segment within each 15-min time interval is performed.

Step 9: Compute Facility MOEs

Finally, facility Measures of Effectiveness (MOEs) are estimated as before, with the caveat that additional MOEs specific to MLs or the relative comparison of the two is needed. Aggregations of MOEs over the entire time-space domain of the analysis would be performed for each separate lane group. Cumulative travel time and average speed, weighted by both length of segments and number of lanes in segments, would be calculated and compared between the two lane groups.

5. EXAMPLE PROBLEMS

EXAMPLE PROBLEM 1

The Facility

The subject of this operational analysis is an urban freeway facility with a 4-mi long reversible ML separated from the GP lanes by a concrete barrier. Therefore, no friction effect is present in this study. The example is based upon an actual ML facility in the U.S. to demonstrate the capability of the methodology in replicating the geometry of actual facilities. It is assumed that the reversible MLs are operating in the northbound direction during the study period. Sixteen individual analysis segments are identified based on the methodology, as shown in Exhibit 24. Note that the segment length of parallel lane groups is identical per the assumptions discussed. Exhibit 24 also shows the geometric details of the facility.

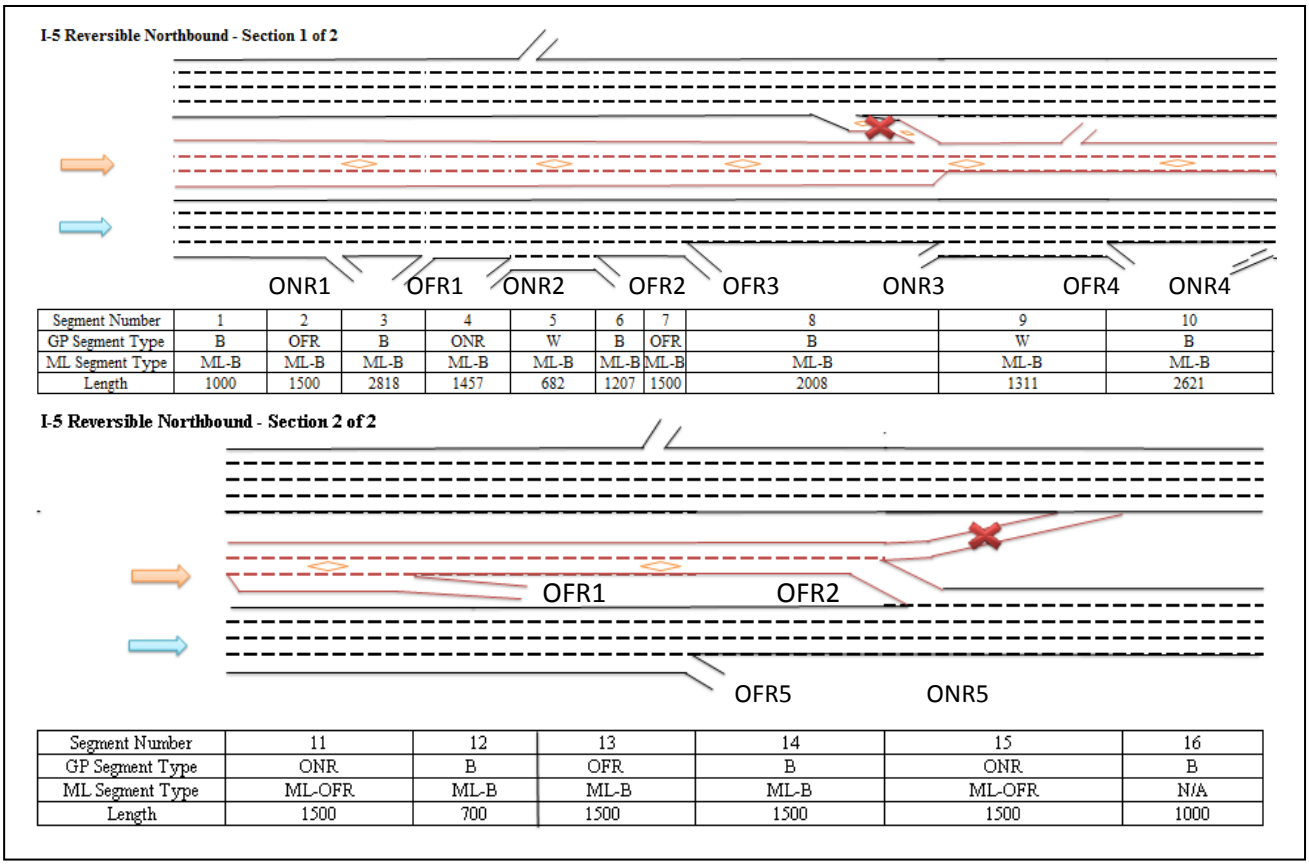

Segment Number	1	2	3	4	5	6	7	8	9	10
GP Segment Type	B	OFR	B	ONR	W	B	OFR	B	W	B
ML Segment Type	ML-B	ML-B	ML-B	ML-B	ML-B	ML-B	ML-B	ML-B	ML-B	ML-B
Length	1000	1500	2818	1457	682	1207	1500	2008	1311	2621

Segment Number	11	12	13	14	15	16
GP Segment Type	ONR	B	OFR	B	ONR	B
ML Segment Type	ML-OFR	ML-B	ML-B	ML-B	ML-OFR	N/A
Length	1500	700	1500	1500	1500	1000

Exhibit 24 Lane Group Segmentation for Example Problem 1

One important issue to consider in this facility is that for the GP lane group, Segments 11, 12, and 13 should be considered as one weave segment per HCM2010 conventions, since the on- and off-ramps are connected by an auxiliary lane. However, on the parallel ML, the segment includes an ML off-ramp in Segment 11. To preserve the lane group concept, the analyst

therefore needs to decide whether to (a) code Segments 11 to 13 individually as is done here (thereby ignoring the weaving functionality) or (b) code only one segment that captures the GP-Weave (but ignores the ML off-ramp). Considering the long length of GP weave segment (3700 feet), and the presumed focus of the analysis on the ML portion, option (a) is selected here.

Further, it should be emphasized that the MLs merge with the GP lanes in Segment 15. It is assumed in this analysis that this merge operates like an off-ramp segment on the MLs, and as an on-ramp on the GP lanes. For facilities, where this assumption is not valid, or where significant turbulence or congestion is expected at the ML terminus, the present methodology is no longer appropriate. In particular, the methodology in this chapter currently does not capture off-ramp congestion and queuing, and further does not model spillback from the GP lanes onto the ML portion of the facility. In these cases, the analyst is referred to the use of alternative analysis tools, like micro-simulation.

The analysis question is: What is the operational performance and level of service of the ML-freeway facility shown in Exhibit 24?

The Facts

In addition to the information contained in Exhibit 24, the following characteristics of the facility are known:

GP Lane Group:

FFS= 60 mi/h (all mainline segments)

Heavy vehicles= 0%

ML Lane Group:

FFS= 70 mi/h

Heavy vehicles= 0%

Analysis duration= 60 min (divided into four 15-min intervals)

Fifteen-minute demand flow rates are given in vehicles per hour under prevailing conditions. These demands must be converted to passenger cars per hour under equivalent ideal conditions for use in the parts of the methodology rated to segment LOS estimation.

Step 1: Input Data

Traffic demand inputs for all 16 segments and four analysis intervals are given in Exhibit 25 and Exhibit 26.

Exhibit 25 GP Lane Group Demand Inputs for Example Problem 1

Time Interval (15 min)	Entering Flow Rate (veh/h)	Ramp Flow Rate by Time Period (veh/h)										Exiting Flow Rate (veh/h)
		ONR1	ONR2	ONR3	ONR4	ONR5	OFR1	OFR2	OFR3	OFR4	OFR5	
1	4000	1000	1000	250	250	1299	250	250	250	250	350	6449
2	5500	500	500	2000	50	1549	350	50	500	500	2100	6645
3	5000	1300	1300	1200	200	1499	450	450	450	500	2100	6549
4	4000	500	500	400	258	1199	250	400	350	358	264	5235

Exhibit 26 ML Lane Group Demand Inputs for Example Problem 1

Time Interval (15 min)	Entering Flow Rate (veh/h)	Ramp Flow Rate by Time Period (veh/h)		Exiting Flow Rate (veh/h)*
		OFR1	OFR2	
1	1650	350	1299	1
2	1650	100	1549	1
3	1650	150	1499	1
4	1450	250	1199	1

*Due to the nature of the computational engine, a minimum flow of 1 veh/h is needed, to avoid a software crash

The volumes in Exhibit 25 and Exhibit 26 represent the 15-min demand flow rates on the facility. The actual volume served in each segment will be determined by the methodology. The demand flows are given for the extended time-space domain consistent with the HCM 2010 recommendations. Peaking occurs in the second 15-min period. Since inputs are in the form of 15-min flow rates, no peak hour factor adjustment is necessary. Since the ML portion of the facility ends in Segment 15, the ML-OFR (and corresponding GP ONR) demands are designed to empty out the ML facility. A flow rate of 1 veh/h is retained in the MLs related to the software implementation in FREEVAL-ML.

Step 2: Demand Adjustments

The traffic flows in Exhibit 25 and Exhibit 26 are already given in the form of actual 15-min demand flow rates. Therefore, no additional demand adjustment is necessary, since the flows represent true demand. Note that the FREEVAL-ML 2010 computational engine assumes that the user inputs true demand flows.

Step 3: Compute Segment Capacities

Segment capacities are determined using the methodologies of HCM Chapter 11 for basic GP segments, Chapter 12 for weaving segments, and Chapter 13 for merge and diverge segments and Section 2 of this chapter for Basic ML segments. The resulting capacities are shown in Exhibit 27 and Exhibit 28.

For the GP segment capacities shown in Exhibit 27, since the capacity of a weaving segment (Segments 5 and 9) is dependent on traffic patterns including the weaving ratio, it varies by time period. The remaining segment capacities are constant in all four time intervals. For the ML segment, the capacities for Segments 1 through 16 are the same, since the segments have the same cross-section. Note that Segment 16 is a "virtual" segment, which is designed to not carry any traffic.

Exhibit 27 GP Segment Capacities for Example Problem 1

Time Interval (15 min)	Capacities (veh/h) by Segment											
	1	**2**	**3**	**4**	**5**	**6**	**7**	**8**	**9**	**10**	**11**	**12**
1					9,772				8,348			
2	8,976	8,976	8,976	8,976	10,435	8,976	8,976	6,732	7,704	6,732	8,976	8,976
3					9,892				7,983			
4					10,123				8,142			

Time Interval (15 min)	**13**	**14**	**15**	**16**
1				
2	8,976	6,732	6,732	6,732
3				
4				

Exhibit 28 ML Segment Capacities for Example Problem 1

Time Interval (15 min)	Capacities (veh/h) by Segment											
	1	**2**	**3**	**4**	**5**	**6**	**7**	**8**	**9**	**10**	**11**	**12**
1												
2	4,683	4,683	4,683	4,683	4,683	4,683	4,683	4,683	4,683	4,683	4,683	4,683
3												
4												

Time Interval (15 min)	**13**	**14**	**15**	**16**
1				
2	4,683	4,683	4,683	n/a
3				
4				

Step 4: Adjust Segment Capacities

This step typically allows the user to adjust capacities of specific segments or time periods to model the effects of work zones and inclement weather, or incidents and such. It also allows for the capacity adjustment due to the cross-weave effect between a GP on-ramp and ML access point or the ML access point and a GP off-ramp. No additional capacity adjustment is performed for this example problem, since the MLs are separated from the GP lanes by barrier without intermediate access points, and since no work zone or weather effects are considered.

Step 5: Compute Demand-to-Capacity Ratios

The demand-to-capacity ratios are calculated based on the demand flows and segment capacities in Exhibit 25 through Exhibit 28 for GP and ML lane groups, separately, as shown in Exhibit 29 and Exhibit 30, respectively.

Exhibit 29 GP Segment Demand-to-Capacity Ratios for Example Problem 1

Time Interval (15 min)	Demand-to-Capacity Ratios by Segment											
	1	**2**	**3**	**4**	**5**	**6**	**7**	**8**	**9**	**10**	**11**	**12**
1	0.45	0.45	0.42	0.53	0.59	0.61	0.61	0.78	0.66	0.78	0.61	0.61
2	0.61	0.61	0.57	0.63	0.59	0.68	0.68	0.83	0.99	1.05	0.80	0.80
3	0.56	0.56	0.51	0.65	0.72	0.75	0.75	0.93	0.93	1.03	0.80	0.80
4	0.45	0.45	0.42	0.47	0.47	0.48	0.48	0.59	0.54	0.60	0.48	0.48

Time Interval (15 min)	**13**	**14**	**15**	**16**
1	0.61	0.77	0.96	0.96
2	0.80	0.75	0.98	0.98
3	0.80	0.75	0.97	0.97
4	0.48	0.60	0.78	0.78

Exhibit 30 ML Segment Demand-to-Capacity Ratios for Example Problem 1

Time Interval (15 min)	Demand-to-Capacity Ratios by Segment											
	1	**2**	**3**	**4**	**5**	**6**	**7**	**8**	**9**	**10**	**11**	**12**
1	0.35	0.35	0.35	0.35	0.35	0.35	0.35	0.35	0.35	0.35	0.35	0.28
2	0.35	0.35	0.35	0.35	0.35	0.35	0.35	0.35	0.35	0.35	0.35	0.33
3	0.35	0.35	0.35	0.35	0.35	0.35	0.35	0.35	0.35	0.35	0.35	0.32
4	0.31	0.31	0.31	0.31	0.31	0.31	0.31	0.31	0.31	0.31	0.31	0.26

Time Interval (15 min)	**13**	**14**	**15**	**16**
1	0.28	0.28	0.28	0.00
2	0.33	0.33	0.33	0.00
3	0.32	0.32	0.32	0.00
4	0.26	0.26	0.26	0.00

The computed demand-to-capacity ratio matrixes for GP and ML segments show that the GP lane group has an active bottleneck in Segment 10 in time intervals 2 and 3 with a d/c ratio of 1.05 and 1.03, respectively. For the ML lane group, no segment has a d/c ratio greater than 1.0 in any time interval. Therefore, for the GP segments, the oversaturation module is invoked, while

for ML segments, the facility is categorized as globally under-saturated, and the analysis proceeds with computing the under-saturated service measures. Exhibit 31 shows the volume-to-capacity ratios by segment and time interval for the two lane groups, separately. Notice that the volume served at the active bottleneck in Segment 10 is limited to the segment capacity, resulting in a v/c ratio of 1.0.

Exhibit 31 Volume-to-Capacity Ratio for the GP and ML Lane Group by Segment and Time Interval

GP Volume/Capacity Ratio

	Segment											
Time (15 min)	**1**	**2**	**3**	**4**	**5**	**6**	**7**	**8**	**9**	**10**	**11**	**12**
1	0.45	0.45	0.42	0.53	0.59	0.61	0.61	0.78	0.66	0.78	0.61	0.61
2	0.61	0.61	0.57	0.63	0.59	0.68	0.68	0.83	0.94	1.00	0.76	0.76
3	0.56	0.56	0.51	0.65	0.72	0.75	0.75	0.93	0.90	1.00	0.77	0.77
4	0.45	0.45	0.42	0.47	0.47	0.48	0.48	0.60	0.62	0.69	0.54	0.54

	Segment			
Time (15 min)	**13**	**14**	**15**	**16**
1	0.61	0.77	0.96	0.96
2	0.76	0.71	0.94	0.94
3	0.77	0.73	0.95	0.95
4	0.54	0.66	0.84	0.84

ML Volume/Capacity Ratio

	Segment											
Time (15 min)	**1**	**2**	**3**	**4**	**5**	**6**	**7**	**8**	**9**	**10**	**11**	**12**
1	0.35	0.35	0.35	0.35	0.35	0.35	0.35	0.35	0.35	0.35	0.35	0.28
2	0.35	0.35	0.35	0.35	0.35	0.35	0.35	0.35	0.35	0.35	0.35	0.33
3	0.35	0.35	0.35	0.35	0.35	0.35	0.35	0.35	0.35	0.35	0.35	0.32
4	0.31	0.31	0.31	0.31	0.31	0.31	0.31	0.31	0.31	0.31	0.31	0.26

	Segment			
Time (15 min)	**13**	**14**	**15**	**16**
1	0.28	0.28	0.28	0.00
2	0.33	0.33	0.33	0.00
3	0.32	0.32	0.32	0.00
4	0.26	0.26	0.26	0.00

Step 6: Compute Segment Service Measures

The methodology proceeds to calculate service measures for each segment and each time period starting with the first segment in time step 1. The computational details for each segment type

are exactly as described in HCM Chapters 11–13 for GP segments and this chapter for ML segments.

The basic performance measures computed for each segment and each time step are the segment speed (Exhibit 32) and density (Exhibit 33). Other performance measures for comparing the two facilities are available as well.

Exhibit 32 Speed Matrixes for Example Problem 1

GP Space Mean Speed

Time (15 min)	Segment 1	2	3	4	5	6	7	8	9	10	11	12
1	60.00	59.65	59.99	55.56	46.16	57.00	59.67	59.32	49.71	59.32	59.98	60.00
2	60.00	58.85	59.97	55.00	49.93	57.82	59.76	55.26	30.34	51.10	59.66	59.66
3	60.00	58.90	59.97	54.69	41.83	56.07	59.56	51.36	26.87	51.10	59.44	59.44
4	60.00	59.65	59.99	55.95	49.31	57.69	59.74	59.98	49.00	59.54	59.98	60.00

Time (15 min)	Segment 13	14	15	16
1	60.00	59.54	50.42	53.39
2	59.66	59.97	50.31	54.19
3	59.44	59.90	50.23	53.79
4	60.00	60.00	52.40	58.02

ML Space Mean Speed

Time (15 min)	Segment 1	2	3	4	5	6	7	8	9	10	11	12
1	56.81	56.81	56.81	56.81	56.81	56.81	56.81	56.81	56.81	56.81	54.05	64.36
2	56.81	56.81	56.81	56.81	56.81	56.81	56.81	56.81	56.81	56.81	54.47	59.21
3	56.81	56.81	56.81	56.81	56.81	56.81	56.81	56.81	56.81	56.81	54.39	60.33
4	61.42	61.42	61.42	61.42	61.42	61.42	61.42	61.42	61.42	61.42	54.22	66.05

Time (15 min)	Segment 13	14	15	16
1	64.36	64.36	52.48	70.00
2	59.21	59.21	52.06	70.00
3	60.33	60.33	52.15	70.00
4	66.05	66.05	52.65	70.00

Exhibit 33 Density Matrixes for Example Problem 1

GP Average Density

Time (15 min)	Segment 1	2	3	4	5	6	7	8	9	10	11	12
1	16.67	16.76	15.63	21.37	24.91	24.12	23.05	29.50	27.66	29.50	22.93	22.92
2	22.92	23.36	21.47	25.68	24.63	26.37	25.52	33.78	59.40	43.91	28.42	28.42
3	20.83	21.22	18.97	26.74	34.18	29.88	28.12	40.50	67.16	43.91	29.16	29.16
4	16.67	16.76	15.63	18.99	19.26	18.85	18.20	22.27	25.63	25.91	20.37	20.36

Time (15 min)	Segment 13	14	15	16
1	22.92	28.83	42.63	40.27
2	28.42	26.62	42.00	38.99
3	29.16	27.24	42.44	39.63
4	20.36	24.72	35.93	32.46

ML Average Density

Time (15 min)	Segment 1	2	3	4	5	6	7	8	9	10	11	12
1	14.52	14.52	14.52	14.52	14.52	14.52	14.52	14.52	14.52	14.52	15.70	10.10
2	14.52	14.52	14.52	14.52	14.52	14.52	14.52	14.52	14.52	14.52	15.70	13.09
3	14.52	14.52	14.52	14.52	14.52	14.52	14.52	14.52	14.52	14.52	15.70	12.43
4	11.80	11.80	11.80	11.80	11.80	11.80	11.80	11.80	11.80	11.80	13.98	9.08

Time (15 min)	Segment 13	14	15	16
1	10.10	10.10	12.69	0.01
2	13.09	13.09	14.84	0.01
3	12.43	12.43	14.41	0.01
4	9.08	9.08	11.83	0.01

Step 7: Adjacent Friction Effects

Since the two lane groups are separated by a concrete barrier in this sample problem, it is assumed that no friction effects exist based on this chapter. Therefore, no adjustment for the friction effect is performed.

Step 8: Lane Group LOS

Upon the completion of the frictional effect adjustments, the LOS assignment for each segment within each 15-min time interval is performed. Exhibit 34 shows the distribution of LOS across all segments and time periods for both GP lanes and MLs. The GP lane group experienced

congestion in time period 2, while the ML group maintained free flow travel at the same period. This demonstrates the operational advantage with the MLs.

Exhibit 34 LOS Matrixes for Example Problem 1

General Purpose (GP) Lanes DENSITY BASED Level Of Service

Time (15 min)	Segment 1	2	3	4	5	6	7	8	9	10	11	12	13	14	15	16	FACILITY LOS
1	B	B	B	C	C	C	C	D	D	D	C	C	C	D	E	E	C
2	C	C	C	C	C	D	D	D	F	E	D	D	D	D	E	E	F
3	B	C	B	C	D	C	B	C	F	B	B	B	B	B	E	C	D
4	B	B	B	B	B	C	C	C	C	C	C	C	C	C	D	D	D

Managed Lanes (ML) DENSITY BASED Level Of Service

Time (15 min)	Segment 1	2	3	4	5	6	7	8	9	10	11	12	13	14	15	16	FACILITY LOS
1	B	B	B	B	B	B	B	B	B	B	B	A	A	A	B	A	B
2	B	B	B	B	B	B	B	B	B	B	B	B	B	B	B	A	B
3	B	B	B	B	B	B	B	B	B	B	B	B	B	B	B	A	B
4	B	B	B	B	B	B	B	B	B	B	B	A	A	A	B	A	B

Step 9: Compute Facility MOEs

Exhibit 35 contrasts the average speed profiles (a) and the cumulative travel time difference (b) for the parallel facilities. Exhibit 35a highlights the drop in speed due to congestion on the GP lanes, while the separated ML facility operates almost at FFS at the same time. Accordingly, the cumulative travel time in the GP lanes is affected by the drop in speed, showing the advantage of the MLs over the length of the facility. The "combined" curve refers to the weighted average performance of ML and GP lanes.

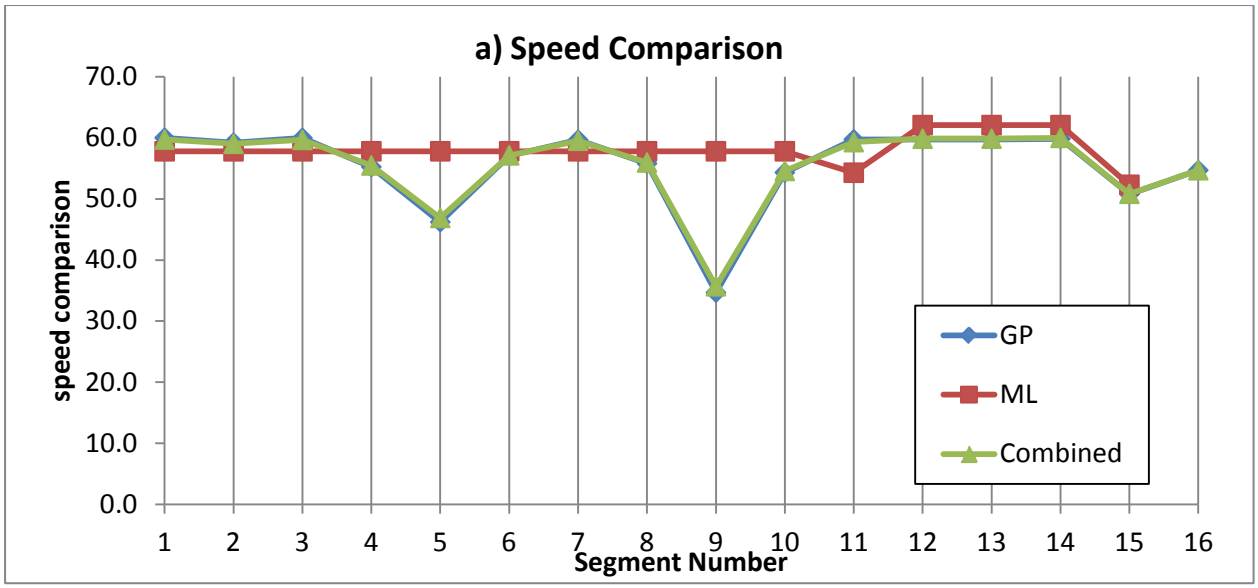

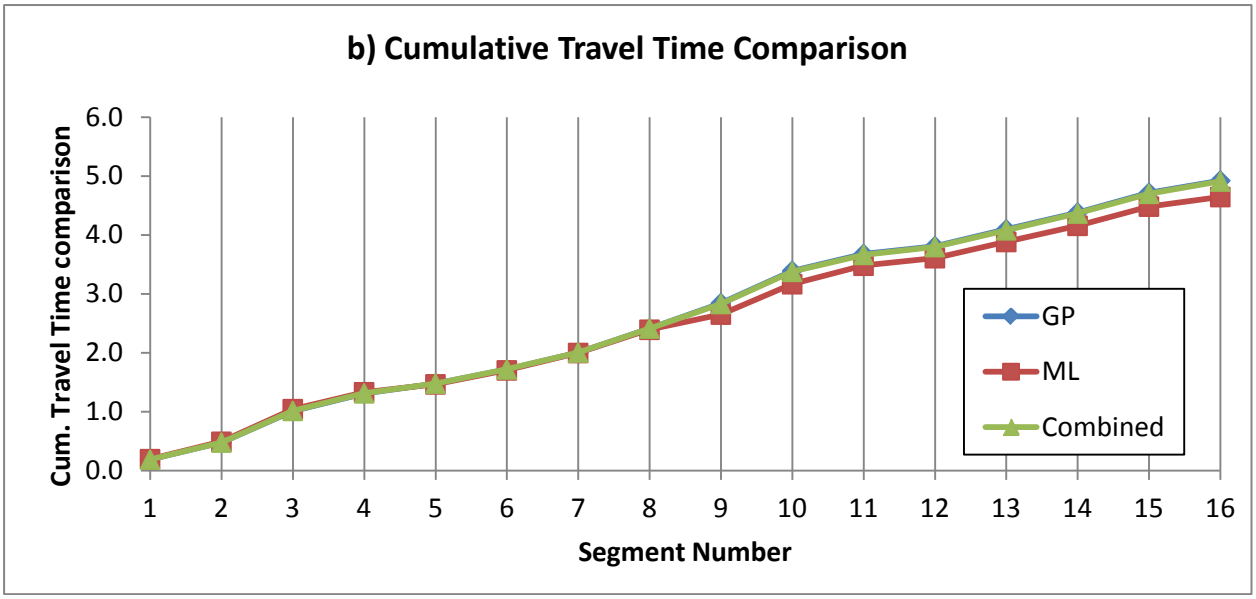

Exhibit 35 Cumulative Speed and Travel Time Comparison for ML and GP lanes

EXAMPLE PROBLEM 2

The Facility

The second sample facility has a northbound ML of 11.3 miles. In total, 38 segments are defined for this case study. Again, this example is based upon an actual ML facility in the U.S. to demonstrate the capability of the methodology in replicating the geometry of actual facilities. The separation type in this facility is *buffer-separation*, where the frictional effect will be modeled when the GP density exceeds 35 pcpmpl. There are a total of five access segments between ML and GP lanes. Exhibit 36 shows all lane groups for this facility based on the developed methodology.

Without MLs, the GP facility would have only had 29 segments. However, nine additional segments are added to preserve the parallel lane group assumption. For example Segments 22, 23, and 24 would have been coded as one basic GP segment in the absence of ML, but are now modeled as Basic, GP-Access, and Basic. The GP-Access segment is coded in parallel to a ML-Access segment.

Example Problem 2 – Section 1 of 3

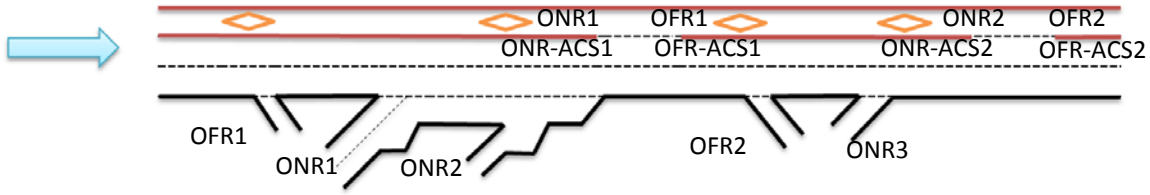

Segment Number	1	2	3	4	5	6	7	8	9	10	11	12
GP Segment Type	B	OFR	B	ONR	ONR	GP-ACS	OFR	B	ONR	B	GP-ACS	B
ML Segment Type	ML-B	ML-B	ML-B	ML-B	ML-B	ML-ACS	ML-B	ML-B	ML-B	ML-B	ML-ACS	ML-B
Length (feet)	10	740	3274	1450	1050	2300	720	2500	1500	700	1500	2900

Example Problem 2 – Section 2 of 3

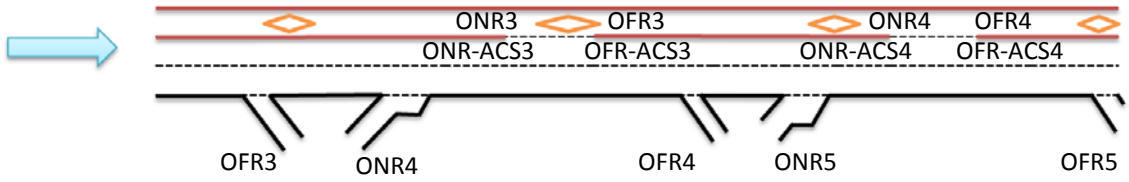

Segment Number	12	13	14	15	16	17	18	19	20	21	22	23	24	25
GP Segment Type	B	OFR	B	ONR	B	GP-ACS	B	OFR	B	ONR	B	GP-ACS	B	OFR
ML Segment Type	ML-B	ML-B	ML-B	ML-B	ML-B	ML-ACS	ML-B	ML-B	ML-B	ML-B	ML-B	ML-ACS	ML-B	ML-B
Length (feet)	2900	1500	2587	1500	802	1500	932'	1500	2800	1500	750	1500	1300	1500

Example Problem 2 – Section 3 of 3

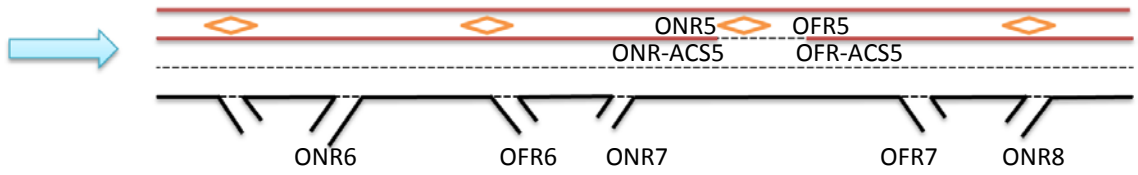

Segment Number	25	26	27	28	29	30	31	32	33	34	35	36	37	38
GP Segment Type	OFR	B	ONR	R	OFR	B	ONR	B	GP-ACS	B	OFR	B	ONR	B
ML Segment Type	ML-B	ML-B	ML-B	ML-B	ML-B	ML-B	ML-B	ML-B	ML-ACS	ML-B	ML-B	ML-B	ML-B	ML-B
Length (feet)	1500	2640	1200	82	1200	1848	1500	974	1500	3314	1500	3300	1500	200

Exhibit 36 Lane Group Segmentation for Example Problem 2

The Facts

In addition to the information contained in Exhibit 36, the following characteristics of the facility are known:

GP Lane Group:

FFS= 60 mi/h (all mainline segments)

Heavy vehicles= 0%

ML Lane Group:

FFS= 70 mi/h

Heavy vehicles= 0%

Analysis duration= 60 min (divided into four 15-min intervals)

Fifteen-minute demand flow rates are given in vehicles per hour under prevailing conditions. These demands must be converted to passenger cars per hour under equivalent ideal conditions for use in the parts of the methodology rated to segment LOS estimation.

Step 1: Input Data

The demand input data for this facility are shown in Exhibit 37 for GP lanes and Exhibit 38 for the ML portion of the facility.

Exhibit 37 GP Lane Group Demand Inputs for Example Problem 2

Time Interval (15 min)	Entering Flow Rate (veh/h)	Ramp Flow Rate by Time Period (veh/h)							
		ONR1	ONR2	ONR3	ONR4	ONR5	ONR6	ONR7	ONR8
1	2000	325	400	300	1000	200	1400	10	250
2	2900	325	400	300	1000	200	1400	10	250
3	2800	325	400	300	1000	200	1400	10	250
4	2700	325	400	300	1000	200	1400	10	250

Time Interval (15 min)	OFR1	OFR2	OFR3	OFR4	OFR5	OFR6	OFR7	ONR-ACS1	OFR-ACS1
1	326	400	1000	350	10	1600	240	300	250
2	326	400	1000	350	10	1600	240	350	250
3	326	400	1000	350	10	1600	240	164	258
4	326	400	1000	350	10	1600	240	358	320

Time Interval (15 min)	ONR-ACS2	OFR-ACS2	ONR-ACS3	OFR-ACS3	ONR-ACS4	OFR-ACS4	ONR-ACS5	OFR-ACS5	Exiting Flow Rate (veh/h)
1	400	300	700	350	350	400	400	350	2459
2	387	250	358	478	329	324	258	500	2859
3	369	258	168	145	358	147	300	450	2759
4	247	258	180	138	358	145	258	350	2659

Exhibit 38 ML Lane Group Demand Inputs for Example Problem 2

Time Interval (15 min)	Entering Flow Rate (veh/h)	Ramp Flow Rate by Time Period (veh/h)										Exiting Flow Rate (veh/h)
		ONR1	ONR2	ONR3	ONR4	ONR5	OFR1	OFR2	OFR3	OFR4	OFR5	
1	1400	250	300	350	400	350	300	400	700	350	400	900
2	1450	250	250	478	324	500	350	387	358	329	258	1570
3	1500	258	258	145	147	450	164	369	168	358	300	1399
4	1450	320	258	138	145	350	358	247	180	358	258	1260

Step 2: Demand Adjustments

The traffic flows in Exhibit 37 and Exhibit 38 are already given in the form of actual demands. Therefore no additional demand adjustment is necessary, since the flows represent true demand. Note that the FREEVAL-ML 2010 computational engine assumes that the user inputs true demand flows.

Step 3: Compute Segment Capacities

Segment capacities are determined using the methodologies of HCM 2010 Chapter 11 for basic GP segments, Chapter 12 for weaving segments, and Chapter 13 for merge and diverge segments and Section 2 of this chapter for Basic ML segments. The resulting capacities are shown in Exhibit 39 and Exhibit 40.

The computed GP segment capacities are shown in Exhibit 39. Since there are no weaving segments (on-ramp followed by off-ramp connected by an auxiliary lane) on this facility, the segment capacity for each segment is constant over all time periods. Variation of capacity across segments is related to the presence of ramps and GP access segments. For the ML segment, the capacities for all segments are the same, since the segments have the same cross-section.

Exhibit 39 GP Segment Capacities for Example Problem 2

Time Interval (15 min)	Capacities (veh/h) by Segment													
	1	**2**	**3**	**4**	**5**	**6**	**7**	**8**	**9**	**10**	**11**	**12**	**13**	**14**
1														
2	4,488	4,488	4,488	6,732	6,669	4,488	4,369	4,488	4,382	4,382	4,488	4,488	4,488	4,488
3														
4														

Time Interval (15 min)	Capacities (veh/h) by Segment													
	15	**16**	**17**	**18**	**19**	**20**	**21**	**22**	**23**	**24**	**25**	**26**	**27**	**28**
1														
2	4,368	4,368	4,488	4,382	4,382	4,488	4,419	4,419	4,488	4,488	4,488	4,488	4,488	4,488
3														
4														

Time Interval (15 min)	Capacities (veh/h) by Segment								
	29	**31**	**32**	**33**	**34**	**35**	**36**	**37**	**38**
1									
2	4,488	4,488	4,488	4,488	4,488	4,488	4,488	4,488	4,488
3									
4									

Exhibit 40 ML Segment Capacities for Example Problem 2

Time Interval (15 min)	Capacities (veh/h) by Segment													
	1	**2**	**3**	**4**	**5**	**6**	**7**	**8**	**9**	**10**	**11**	**12**	**13**	**14**
1														
2	2,341	2,341	2,341	2,341	2,341	2,341	2,341	2,341	2,341	2,341	2,341	2,341	2,341	2,341
3														
4														

Time Interval (15 min)	Capacities (veh/h) by Segment													
	15	**16**	**17**	**18**	**19**	**20**	**21**	**22**	**23**	**24**	**25**	**26**	**27**	**28**
1														
2	2,341	2,341	2,341	2,341	2,341	2,341	2,341	2,341	2,341	2,341	2,341	2,341	2,341	2,341
3														
4														

Time Interval (15 min)	Capacities (veh/h) by Segment								
	29	**31**	**32**	**33**	**34**	**35**	**36**	**37**	**38**
1									
2	2,341	2,341	2,341	2,341	2,341	2,341	2,341	2,341	2,341
3									
4									

Step 4: Adjust Segment Capacities

This step typically allows the user to adjust capacities of specific segments or time periods to model the effects of work zones and inclement weather, or incidents and such. It also allows for the capacity adjustment due to the cross-weave effect between a GP on-ramp to ML access point or the ML access point to a GP off-ramp. Exhibit 41 summarizes the cross-weave effects for all (potentially applicable) GP segments along the facility. The values in the table correspond to the percentage reduction in segment capacity due to cross-weave.

Exhibit 41: Summary of Estimated Cross-Weave Capacity Reduction Factors

	Cross Weave Capacity Reduction Factors												
	4	5	7	9	10	12	13	15	16	18	19	21	22
t=1	0.00	0.01	0.03	0.02	0.02	0.00	0.00	0.03	0.03	0.02	0.02	0.02	0.02
t=2	0.00	0.01	0.03	0.02	0.02	0.00	0.00	0.03	0.03	0.02	0.02	0.02	0.02
t=3	0.00	0.01	0.03	0.02	0.02	0.00	0.00	0.03	0.03	0.02	0.02	0.02	0.02
t=4	0.00	0.01	0.03	0.02	0.02	0.00	0.00	0.03	0.03	0.02	0.02	0.02	0.02

	24	25	31	32	34	35
t=1	0.00	0.00	0.00	0.00	0.00	0.00
t=2	0.00	0.00	0.00	0.00	0.00	0.00
t=3	0.00	0.00	0.00	0.00	0.00	0.00
t=4	0.00	0.00	0.00	0.00	0.00	0.00

Step 5: Compute Demand-to-Capacity Ratios

The demand-to-capacity ratios are calculated based on the demand flows and segment capacities in Exhibit 37 through Exhibit 40 for the GP and ML lane groups, separately, and with consideration of the cross-weave adjustments in Exhibit 41.

Exhibit 42 GP Segment Demand-to-Capacity Ratios for Example Problem 2

Time Interval (15 min)	Demand-to-Capacity Ratios by Segment													
	1	**2**	**3**	**4**	**5**	**6**	**7**	**8**	**9**	**10**	**11**	**12**	**13**	**14**
1	0.45	0.45	0.37	0.30	0.36	0.60	0.56	0.46	0.54	0.54	0.61	0.55	0.55	0.32
2	0.65	0.65	0.57	0.43	0.49	0.74	0.76	0.65	0.73	0.73	0.71	0.71	0.71	0.49
3	0.62	0.62	0.55	0.42	0.48	0.71	0.73	0.62	0.71	0.71	0.69	0.69	0.69	0.47
4	0.60	0.60	0.53	0.40	0.46	0.69	0.71	0.60	0.68	0.68	0.67	0.67	0.67	0.45

Time Interval (15 min)	Demand-to-Capacity Ratios by Segment													
	15	**16**	**17**	**18**	**19**	**20**	**21**	**22**	**23**	**24**	**25**	**26**	**27**	**28**
1	0.56	0.56	0.70	0.64	0.64	0.55	0.60	0.60	0.67	0.58	0.58	0.58	0.89	0.89
2	0.73	0.73	0.71	0.73	0.73	0.63	0.69	0.69	0.68	0.68	0.68	0.68	0.99	0.99
3	0.71	0.71	0.69	0.71	0.71	0.61	0.67	0.67	0.66	0.66	0.66	0.65	0.97	0.97
4	0.69	0.69	0.67	0.68	0.68	0.59	0.64	0.64	0.63	0.63	0.63	0.63	0.94	0.94

Time Interval (15 min)	Demand-to-Capacity Ratios by Segment								
	29	**31**	**32**	**33**	**34**	**35**	**36**	**37**	**38**
1	0.89	0.53	0.53	0.53	0.62	0.55	0.55	0.49	0.55
2	0.99	0.63	0.63	0.63	0.63	0.63	0.63	0.58	0.64
3	0.97	0.61	0.61	0.61	0.61	0.61	0.61	0.56	0.61
4	0.94	0.59	0.59	0.59	0.59	0.59	0.59	0.54	0.59

Exhibit 43 ML Segment Demand-to-Capacity Ratios for Example Problem 2

Time Interval (15 min)	Demand-to-Capacity Ratios by Segment													
	1	**2**	**3**	**4**	**5**	**6**	**7**	**8**	**9**	**10**	**11**	**12**	**13**	**14**
1	0.60	0.60	0.60	0.60	0.60	0.70	0.58	0.58	0.58	0.58	0.70	0.53	0.53	0.53
2	0.62	0.62	0.62	0.62	0.62	0.73	0.58	0.58	0.58	0.58	0.68	0.52	0.52	0.52
3	0.64	0.64	0.64	0.64	0.64	0.75	0.68	0.68	0.68	0.68	0.79	0.63	0.63	0.63
4	0.62	0.62	0.62	0.62	0.62	0.76	0.60	0.60	0.60	0.60	0.71	0.61	0.61	0.61

Time Interval (15 min)	Demand-to-Capacity Ratios by Segment													
	15	**16**	**17**	**18**	**19**	**20**	**21**	**22**	**23**	**24**	**25**	**26**	**27**	**28**
1	0.53	0.53	0.68	0.38	0.38	0.38	0.38	0.38	0.56	0.41	0.41	0.41	0.41	0.41
2	0.52	0.52	0.72	0.57	0.57	0.57	0.57	0.57	0.71	0.57	0.57	0.57	0.57	0.57
3	0.63	0.63	0.70	0.62	0.62	0.62	0.62	0.62	0.69	0.53	0.53	0.53	0.53	0.53
4	0.61	0.61	0.67	0.59	0.59	0.59	0.59	0.59	0.65	0.50	0.50	0.50	0.50	0.50

Time Interval (15 min)	Demand-to-Capacity Ratios by Segment								
	29	**31**	**32**	**33**	**34**	**35**	**36**	**37**	**38**
1	0.41	0.41	0.41	0.41	0.56	0.38	0.38	0.38	0.38
2	0.57	0.57	0.57	0.57	0.78	0.67	0.67	0.67	0.67
3	0.53	0.53	0.53	0.53	0.73	0.60	0.60	0.60	0.60
4	0.50	0.50	0.50	0.50	0.65	0.54	0.54	0.54	0.54

The computed demand-to-capacity ratio matrixes for GP and ML segments show that the GP lane group is operated at a demand level very close to capacity with d/c ratios of 0.99 in Segments 27 through 29. However, since no segment has a d/c ratio of more than 1.0, the facility is considered as globally under-saturated. Similarly, for the ML lane group, no segment has a d/c ratio greater than 1.0 in any time interval. Exhibits 44 and 45 show the volume-to-capacity ratios by segment and time interval for the two lane groups, respectively. Without any queuing impacts, the resulting v/c ratios are identical with the d/c ratios of the same segment and time period presented earlier.

Exhibit 44 Volume-to-Capacity Ratio for GP Lane Group by Segment and Time Interval

Time Interval (15 min)	Volume-to-Capacity Ratios by Segment													
	1	**2**	**3**	**4**	**5**	**6**	**7**	**8**	**9**	**10**	**11**	**12**	**13**	**14**
1	0.45	0.45	0.37	0.30	0.36	0.60	0.56	0.46	0.54	0.54	0.61	0.55	0.55	0.32
2	0.65	0.65	0.57	0.43	0.49	0.74	0.76	0.65	0.73	0.73	0.71	0.71	0.71	0.49
3	0.62	0.62	0.55	0.42	0.48	0.71	0.73	0.62	0.71	0.71	0.69	0.69	0.69	0.47
4	0.60	0.60	0.53	0.40	0.46	0.69	0.71	0.60	0.68	0.68	0.67	0.67	0.67	0.45

Time Interval (15 min)	Volume-to-Capacity Ratios by Segment													
	15	**16**	**17**	**18**	**19**	**20**	**21**	**22**	**23**	**24**	**25**	**26**	**27**	**28**
1	0.56	0.56	0.70	0.64	0.64	0.55	0.60	0.60	0.67	0.58	0.58	0.58	0.89	0.89
2	0.73	0.73	0.71	0.73	0.73	0.63	0.69	0.69	0.68	0.68	0.68	0.68	0.99	0.99
3	0.71	0.71	0.69	0.71	0.71	0.61	0.67	0.67	0.66	0.66	0.66	0.65	0.97	0.97
4	0.69	0.69	0.67	0.68	0.68	0.59	0.64	0.64	0.63	0.63	0.63	0.63	0.94	0.94

Time Interval (15 min)	Volume-to-Capacity Ratios by Segment								
	29	**31**	**32**	**33**	**34**	**35**	**36**	**37**	**38**
1	0.89	0.53	0.53	0.53	0.62	0.55	0.55	0.49	0.55
2	0.99	0.63	0.63	0.63	0.63	0.63	0.63	0.58	0.64
3	0.97	0.61	0.61	0.61	0.61	0.61	0.61	0.56	0.61
4	0.94	0.59	0.59	0.59	0.59	0.59	0.59	0.54	0.59

Exhibit 45 Volume-to-Capacity Ratio for ML Lane Group by Segment and Time Interval

Time Interval (15 min)	Volume-to-Capacity Ratios by Segment													
	1	**2**	**3**	**4**	**5**	**6**	**7**	**8**	**9**	**10**	**11**	**12**	**13**	**14**
1	0.60	0.60	0.60	0.60	0.60	0.70	0.58	0.58	0.58	0.58	0.70	0.53	0.53	0.53
2	0.62	0.62	0.62	0.62	0.62	0.73	0.58	0.58	0.58	0.58	0.68	0.52	0.52	0.52
3	0.64	0.64	0.64	0.64	0.64	0.75	0.68	0.68	0.68	0.68	0.79	0.63	0.63	0.63
4	0.62	0.62	0.62	0.62	0.62	0.76	0.60	0.60	0.60	0.60	0.71	0.61	0.61	0.61

Time Interval (15 min)	Volume-to-Capacity Ratios by Segment													
	15	**16**	**17**	**18**	**19**	**20**	**21**	**22**	**23**	**24**	**25**	**26**	**27**	**28**
1	0.53	0.53	0.68	0.38	0.38	0.38	0.38	0.38	0.56	0.41	0.41	0.41	0.41	0.41
2	0.52	0.52	0.72	0.57	0.57	0.57	0.57	0.57	0.71	0.57	0.57	0.57	0.57	0.57
3	0.63	0.63	0.70	0.62	0.62	0.62	0.62	0.62	0.69	0.53	0.53	0.53	0.53	0.53
4	0.61	0.61	0.67	0.59	0.59	0.59	0.59	0.59	0.65	0.50	0.50	0.50	0.50	0.50

Time Interval (15 min)	Volume-to-Capacity Ratios by Segment								
	29	**31**	**32**	**33**	**34**	**35**	**36**	**37**	**38**
1	0.41	0.41	0.41	0.41	0.56	0.38	0.38	0.38	0.38
2	0.57	0.57	0.57	0.57	0.78	0.67	0.67	0.67	0.67
3	0.53	0.53	0.53	0.53	0.73	0.60	0.60	0.60	0.60
4	0.50	0.50	0.50	0.50	0.65	0.54	0.54	0.54	0.54

Step 6: Compute Segment Service Measures

The methodology proceeds to calculate service measures for each segment and each time period starting with the first segment in time step 1. The computational details for each segment type are exactly as described in HCM 2010 Chapters 11–13 for GP segments and this chapter for ML segments.

The basic performance measures computed for each segment and each time step are the segment speed (Exhibits 46 and 47) and density (Exhibits 48 and 49). Other performance measures for comparing the two facilities are available as well.

Exhibit 46 GP Speed Matrix for Example Problem 2

Time Interval (15 min)	Space Mean Speed (mph)													
	1	**2**	**3**	**4**	**5**	**6**	**7**	**8**	**9**	**10**	**11**	**12**	**13**	**14**
1	60.00	54.09	59.77	60.00	55.79	43.88	53.97	59.56	53.93	58.98	41.79	59.48	52.98	59.74
2	60.00	54.09	59.77	60.00	55.25	42.95	53.97	59.56	52.84	58.80	42.76	59.51	52.98	59.74
3	60.00	54.09	59.77	60.00	55.32	44.54	53.97	59.56	53.03	58.83	42.79	59.51	52.98	59.74
4	60.00	54.09	59.77	60.00	55.39	41.59	53.97	59.56	53.19	58.85	44.02	59.55	52.98	59.74

Time Interval (15 min)	Space Mean Speed (mph)													
	15	**16**	**17**	**18**	**19**	**20**	**21**	**22**	**23**	**24**	**25**	**26**	**27**	**28**
1	53.84	59.05	37.73	56.89	54.05	59.82	53.65	58.97	39.92	57.92	54.62	59.81	50.52	56.41
2	52.84	58.89	38.49	57.00	54.05	59.82	53.11	58.89	41.89	58.13	54.62	59.81	48.06	51.73
3	53.03	58.92	47.18	58.21	54.05	59.82	53.27	58.91	45.59	58.51	54.62	59.81	48.71	52.93
4	53.19	58.94	47.40	58.24	54.05	59.82	53.41	58.93	45.80	58.53	54.62	59.81	49.30	54.05

Time Interval (15 min)	Space Mean Speed (mph)								
	29	**31**	**32**	**33**	**34**	**35**	**36**	**37**	**38**
1	51.98	59.19	53.89	59.18	40.65	59.61	54.24	59.88	53.84
2	51.98	59.19	53.41	59.11	39.03	59.58	54.24	59.88	53.39
3	51.98	59.19	53.53	59.13	39.64	59.59	54.24	59.88	53.52
4	51.98	59.19	53.65	59.14	42.15	59.64	54.24	59.88	53.64

Exhibit 47 ML Speed Matrix for Example Problem 2

Time Interval (15 min)	Space Mean Speed (mph)													
	1	**2**	**3**	**4**	**5**	**6**	**7**	**8**	**9**	**10**	**11**	**12**	**13**	**14**
1	64.87	64.87	64.87	64.87	64.87	46.96	65.55	65.55	65.55	65.55	45.88	66.75	66.75	66.75
2	64.12	64.12	64.12	64.12	64.12	45.88	65.55	65.55	65.55	65.55	45.78	67.13	67.13	67.13
3	63.32	63.32	63.32	63.32	63.32	47.18	61.64	61.64	61.64	61.64	45.92	63.60	63.60	63.60
4	64.12	64.12	64.12	64.12	64.12	45.61	64.69	64.69	64.69	64.69	46.88	64.53	64.53	64.53

Time Interval (15 min)	Space Mean Speed (mph)													
	15	**16**	**17**	**18**	**19**	**20**	**21**	**22**	**23**	**24**	**25**	**26**	**27**	**28**
1	66.75	66.75	43.41	69.32	69.32	69.32	69.32	69.32	45.24	69.09	69.09	69.09	69.09	66.58
2	67.13	67.13	44.62	65.77	65.77	65.77	65.77	65.77	45.88	65.83	65.83	65.83	57.33	57.33
3	63.60	63.60	48.14	63.97	63.97	63.97	63.97	63.97	46.93	66.76	66.76	66.76	59.80	59.80
4	64.53	64.53	48.26	65.13	65.13	65.13	65.13	65.13	47.10	67.56	67.56	67.56	62.03	62.03

Time Interval (15 min)	Space Mean Speed (mph)								
	29	**31**	**32**	**33**	**34**	**35**	**36**	**37**	**38**
1	66.58	69.09	69.09	69.09	45.50	69.32	69.32	69.32	69.32
2	57.33	65.83	65.83	65.83	45.50	62.09	62.09	62.09	62.09
3	59.80	66.76	66.76	66.76	45.63	64.88	64.88	64.88	64.88
4	62.03	67.56	67.56	67.56	46.68	66.64	66.64	66.64	66.64

Exhibit 48 GP Density Matrix for Example Problem 2

Time Interval (15 min)	Average Segment Density (veh/mi/ln)													
	1	**2**	**3**	**4**	**5**	**6**	**7**	**8**	**9**	**10**	**11**	**12**	**13**	**14**
1	16.67	18.71	14.00	11.11	14.33	30.41	22.58	17.20	21.69	19.91	32.50	20.59	22.58	12.13
2	24.17	26.45	21.53	16.11	19.90	37.96	29.89	24.34	28.32	27.20	36.98	26.88	29.03	18.40
3	23.33	25.59	20.70	15.55	19.28	35.52	29.03	23.50	27.54	26.34	35.79	26.04	28.17	17.57
4	22.50	24.73	19.86	15.00	18.65	36.81	28.17	22.66	26.76	25.48	33.68	25.18	27.31	16.73

Time Interval (15 min)	Average Segment Density (veh/mi/ln)													
	15	**16**	**17**	**18**	**19**	**20**	**21**	**22**	**23**	**24**	**25**	**26**	**27**	**28**
1	22.15	20.74	41.19	24.60	25.59	20.47	24.08	22.46	37.10	22.44	23.87	21.64	33.98	35.35
2	28.00	27.16	41.02	28.06	29.03	23.81	27.20	25.89	35.97	26.23	27.74	25.40	37.49	42.91
3	27.22	26.30	32.50	26.62	28.17	22.98	26.42	25.03	31.99	25.20	26.88	24.57	36.71	40.98
4	26.44	25.44	31.31	25.75	27.31	22.14	25.64	24.17	30.77	24.34	26.02	23.73	35.93	39.21

Time Interval (15 min)	Average Segment Density (veh/mi/ln)								
	29	**31**	**32**	**33**	**34**	**35**	**36**	**37**	**38**
1	35.82	20.18	22.21	20.27	34.01	20.54	22.58	18.44	22.57
2	39.69	23.98	25.72	24.10	36.03	23.91	26.02	21.78	25.69
3	38.83	23.14	24.94	23.25	34.25	23.07	25.16	20.95	24.91
4	37.97	22.29	24.16	22.39	31.05	22.21	24.30	20.11	24.13

Exhibit 49 ML Density Matrix for Example Problem 2

Time Interval (15 min)	Average Segment Density (veh/mi/ln)													
	1	2	3	4	5	6	7	8	9	10	11	12	13	14
1	21.58	21.58	21.58	21.58	21.58	35.14	20.59	20.59	20.59	20.59	35.97	18.73	18.73	18.73
2	22.61	22.61	22.61	22.61	22.61	37.05	20.59	20.59	20.59	20.59	34.95	18.07	18.07	18.07
3	23.69	23.69	23.69	23.69	23.69	37.26	25.86	25.86	25.86	25.86	40.33	23.32	23.32	23.32
4	22.61	22.61	22.61	22.61	22.61	38.81	21.83	21.83	21.83	21.83	35.62	22.05	22.05	22.05

Time Interval (15 min)	Average Segment Density (veh/mi/ln)													
	15	16	17	18	19	20	21	22	23	24	25	26	27	28
1	18.73	18.73	36.86	12.98	12.98	12.98	12.98	12.98	28.73	13.75	13.75	13.75	13.75	14.27
2	18.07	18.07	37.90	20.27	20.27	20.27	20.27	20.27	36.11	20.17	20.17	20.17	23.16	23.16
3	23.32	23.32	33.82	22.82	22.82	22.82	22.82	22.82	34.24	18.71	18.71	18.71	20.89	20.89
4	22.05	22.05	32.35	21.20	21.20	21.20	21.20	21.20	32.40	17.29	17.29	17.29	18.83	18.83

Time Interval (15 min)	Average Segment Density (veh/mi/ln)								
	29	31	32	33	34	35	36	37	38
1	14.27	13.75	13.75	13.75	28.57	12.98	12.98	12.98	12.98
2	23.16	20.17	20.17	20.17	40.18	25.29	25.29	25.29	25.29
3	20.89	18.71	18.71	18.71	37.24	21.56	21.56	21.56	21.56
4	18.83	17.29	17.29	17.29	32.52	18.91	18.91	18.91	18.91

Step 7: Adjacent Friction Effects

This facility does not have an active bottleneck, but still has several GP segments operating at a density above 35 pcpmpl. For these segments, the methodology invokes the friction effect module, resulting in a reduction in operating speed on the adjacent ML lane group. The corresponding ML speed drops by up to 8.5 mph in Segments 27 through 29 due to the frictional effect imposed onto ML. Note that if the facility had been designed with barrier separation, then no frictional effect would have been experienced by the ML traffic. The speeds shown in Exhibit 47 have already reflected this adjustment.

Step 8: Lane Group LOS

Upon the completion of the frictional effect adjustments, the LOS assignment for each segment within each 15-min time interval is performed. Exhibit 50 and Exhibit 51 show the distribution of LOS across all segments and time periods for both GP lanes and MLs.

Exhibit 50 GP LOS Matrixes for Example Problem 2

Time (15 min)	Segment 1	2	3	4	5	6	7	8	9	10	11	12	13	14
1	B	B	B	B	B	D	C	B	C	C	D	C	C	B
2	C	C	C	B	C	E	D	C	D	D	E	D	D	C
3	C	C	C	B	B	E	D	C	D	D	E	D	D	B
4	C	C	C	B	B	E	D	C	C	D	D	C	C	B

Time (15 min)	Segment 15	16	17	18	19	20	21	22	23	24	25	26	27	28
1	C	C	E	C	C	C	C	C	E	C	C	C	D	E
2	D	D	E	D	D	C	C	D	E	D	D	C	E	E
3	C	D	D	D	D	C	C	C	D	C	C	C	E	E
4	C	D	D	D	C	C	C	C	D	C	C	C	E	E

Time (15 min)	Segment 29	30	31	32	33	34	35	36	FACILITY LOS
1	E	C	C	C	D	C	C	C	C
2	E	C	C	C	E	C	C	C	C
3	E	C	C	C	E	C	C	C	C
4	E	C	C	C	D	C	C	C	C

Exhibit 51 ML LOS Matrixes for Example Problem 2

Time (15 min)	Segment 1	2	3	4	5	6	7	8	9	10	11	12	13	14
1	C	C	C	C	C	E	C	C	C	C	E	C	C	C
2	C	C	C	C	C	E	C	C	C	C	E	C	C	C
3	C	C	C	C	C	E	D	D	D	D	E	C	C	C
4	C	C	C	C	C	E	C	C	C	C	E	C	C	C

Time (15 min)	Segment 15	16	17	18	19	20	21	22	23	24	25	26	27	28
1	C	C	E	B	B	B	B	B	D	B	B	B	B	B
2	C	C	E	C	C	C	C	C	E	C	C	C	C	C
3	C	C	D	C	C	C	C	C	E	C	C	C	C	C
4	C	C	D	C	C	C	C	C	D	B	B	B	C	C

Time (15 min)	Segment 29	30	31	32	33	34	35	36	FACILITY LOS
1	B	B	B	B	D	B	B	B	B
2	C	C	C	C	E	C	C	C	C
3	C	C	C	C	E	C	C	C	C
4	C	B	B	B	D	C	C	C	C

Step 9: Compute Facility MOEs

The speed comparison is shown graphically in Exhibit 52a for the entire facility. The figure also highlights speed drops in both ML and GP lanes in the five ML/GP Access segments along the facility (Segments 6, 11, 17, 23, and 33). The speed-drop is the result of lane-change turbulence in those access segments. The effect of the adjacent frictional effect is evident in Segments 27 through 29, where the GP lanes operate at LOS E and thus result in a speed drop on the ML.

The cumulative travel time comparison is shown in Exhibit 52b, which again highlights (slightly) superior performance on the ML, as opposed to the GP lanes, which operate at demand levels close to capacity at LOS E.

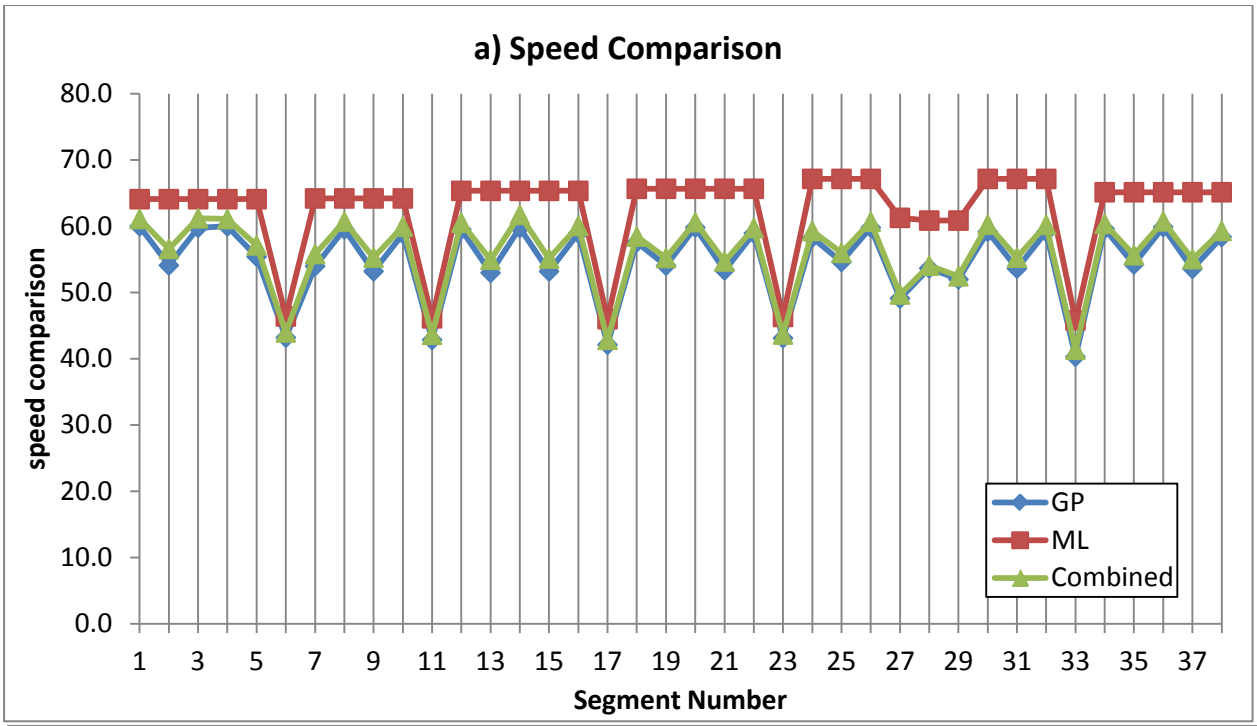

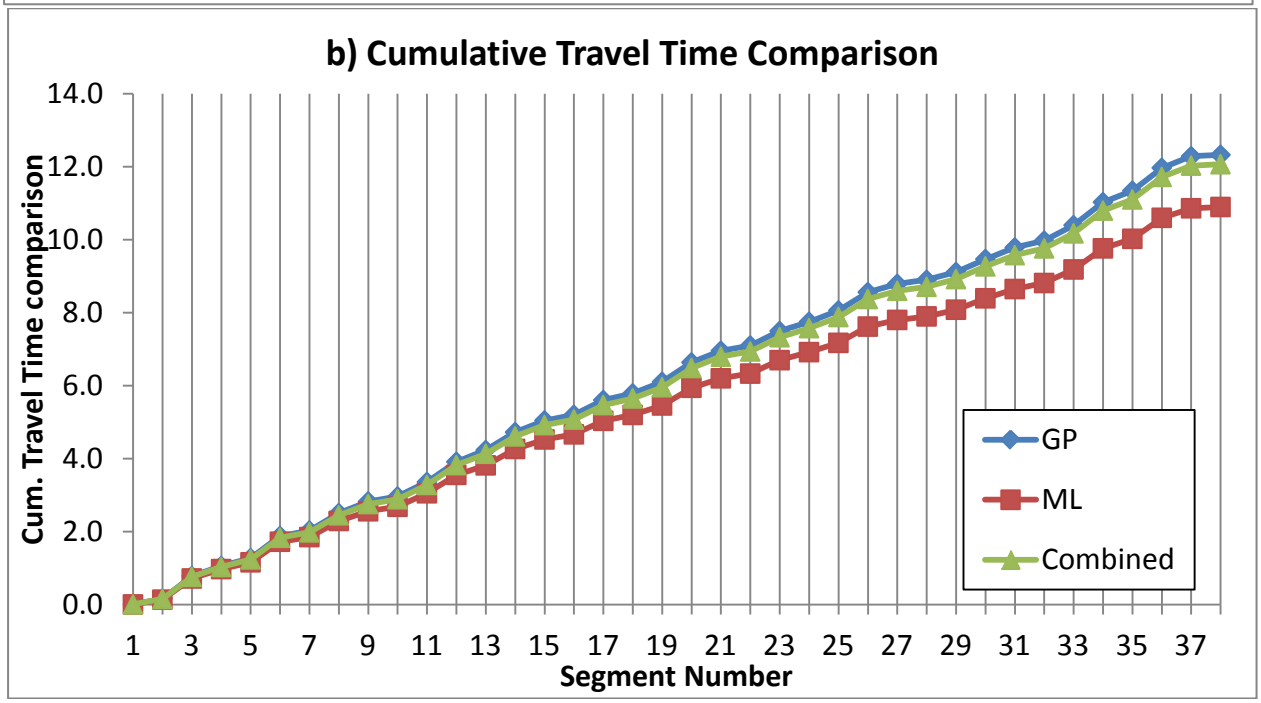

Exhibit 52 Speed and Travel Time Comparison for ML and GP Lanes

6. REFERENCES

1. Wang, Y., Liu, X., Rouphail, N., Schroeder, B., Yin, Y., Bloomberg, L. NCHRP Project 3-96. *Analysis of Managed Lanes on Freeway Facilities*, Final Report. The University of Washington, August, 2012.

2. *Highway Capacity Manual.* Chapter 3: Basic Freeway Sections, TRB, National Research Council, Washington, D.C., 1994.

3. Liu, X., Schroeder, B., Thomson, T., Wang, Y., Rouphail, N., and Yin, Y., Analysis on Operational Interactions between Freeway Managed Lanes and Parallel General Purpose Lanes, *Transportation Research Record*: *Journal of Transportation Research Board,* In Press, 2011.

4. Schroeder B., S. Aghdashi, N. Rouphail, X. Liu and Y. Wang. Deterministic Approach to Modeling Managed Lanes on Extended HCM Freeway Facilities, Transportation Research Board 91st Annual Meeting, 2012.